

Editorial Board

Editor-in-Chief:

Suleimanov Bagir A.
«OilGasScientificResearchProject» Institute, SOCAR, Baku, Azerbaijan

Founding Editor:

Veliyev Elchin F.
«OilGasScientificResearchProject» Institute, SOCAR, Baku, Azerbaijan

Members of Editorial Board:

Abdullayev Vugar J.
«OilGasScientificResearchProject» Institute, SOCAR, Baku, Azerbaijan

Aliev Fikret A.
Scientific Research Institute of Applied Mathematics, Baku, Azerbaijan

Aliyev Chingiz S.
Institute of Geology and Geophysics, Ministry of Science and Education, of the Republic of Azerbaijan, Baku, Azerbaijan

Hamzayev Khanlar M.
Azerbaijan State Oil and Industry University, Baku, Azerbaijan

Imamverdiyev Nazim A.
Baku State University, Baku, Azerbaijan

Ismailov Fakhreddin S.
«OilGasScientificResearchProject» Institute, SOCAR, Baku, Azerbaijan

Ismayilov Rayyat H.
Institute of Catalysis and Inorganic Chemistry named after academician Murtuza Naghiyev, Ministry of Science and Education of the Republic of Azerbaijan, Baku, Azerbaijan

Jamalbayov Mahammad A.
«OilGasScientificResearchProject» Institute, SOCAR, Baku, Azerbaijan

Jafarov Yasin I.
Baku State University, Baku, Azerbaijan

Kazimov Elchin A.
«OilGasScientificResearchProject» Institute, SOCAR, Baku, Azerbaijan

Tapdigov Shamo Z.
«OilGasScientificResearchProject» Institute, SOCAR, Baku, Azerbaijan

Salmanov Ahmed M.
«OilGasScientificResearchProject» Institute, SOCAR, Baku, Azerbaijan

Bahtizin Ramil N.
Ufa State Petroleum Technological University, Ufa, Russia

Chudyk Igor I.
Ivano-Frankivsk National Technical University of Oil and Gas, Ivano-Frankivsk, Ukraine

Gasumov Ramiz A.
«SevCavNIPGas» JSC, Stavropol, Russia

Peng Shie-Ming
National Taiwan University, Taipei, Taiwan, China

Shakhverdiev Azizaga Kh.
Russian Academy of Natural Sciences, Section of Oil and Gas, Moscow, Russia,
Sergo Ordzhonikidze Russian State University for Geological Prospecting, Moscow, Russia

Vishnyakov Vladimir M.
University of Huddersfield, Huddersfield, United Kingdom

Vityaz Oleg Yu.
Educational and Scientific Institute of Oil and Gas Engineering, IFNTUOGas, Ivano-Frankivsk, Ukraine

GUIDE FOR AUTHORS

«Scientific Petroleum» is intended for oil and gas industry specialists, post-graduate (students and scientific workers. Journal covers the fields of petroleum (and natural gas) exploration, production and flow in its broadest possible sense. Topics include:

- Oil and gas fields geology, geophysics and exploration
- Well drilling
- Reservoir and petroleum engineering
- Oil and gas transportation and storage
- Oil and gas refining. Petrochemistry
- Oil and gas field structures (including sea structures, corrosion protection and so on)
- Oil and gas industry economics
- Environment protection in oil and gas industry
- Fundamental scientific investigations having applied sense for oil and gas industry

Articles are published on three languages: Azeri, English and Russian.

To simplify procedure of interaction between author (co-authors) and publisher we encourage you to send us your article in electronic form so it can be refereed without postal delays and be published more quickly.

When submitting a manuscript, authors need to provide following information about them: surname, first name, academic degree, affiliation, position, e-mail address, full postal address and phone number.

The electronic version of article must include the following files: 1) File (*.doc, *.docx) containing the text of article, short abstract (no longer than 100 words), keywords, tables, references and captions of figures; 2) Files containing all illustrations. Every figure and photograph should be given by separate file in the following format: *.jpg, *.tiff, *.psd, *.cdr). Graphs and diagrams should be presented as *.xls, *.xlsx.

Send your article's single compressed archive (*.rar) through the manuscript submission window «Submit your Paper».

Editorial staff:

Editor-in-Chief

B. A. Suleimanov

Founding Editor

E. F. Veliyev

Managing

Editor

O. A. Zeynalova

Design/Graphics

T. Y. Abdullayeva

Web-Editor

E. E. Mamedov

Since 28.12.2023 the Journal is in the list of editions that are recommended for publication of main conclusions of DS and PhD dissertations by decision of Supreme Attestation Commission attached to the President of Azerbaijan Republic

*Journal is indexed by
Russian Scientific
Citation Index*

**An Official Publication of
«Scientific Petroleum»**

Frequency:

4 issues per year

Tel.: (+994 12 408 67 15)
Fax: (+994 12 408 67 15)
E-mail:
scientificpetroleum@gmail.com

Address: AZ1025,
Azerbaijan Republic, Baku,
N. Rafiyev st. 78

CONTENTS

GEOLOGY, GEOPHYSICS & FORMATION EVALUATION

*H. I. Shakarov, M. A. Bakirov, N. H. Mehdiyeva,
A. Q. Bakirova, A. E. Abdullayeva*

New directions in the analysis of well geophysical survey data in seismoactive zones.....

2

S. H. Jafarov

Petrogeochemical characteristics of Jurassic volcanic rocks of the Chovdar ore field (Lesser Caucasus).....

9

M. F. Tagiyev, O. V. Rajabli

Application of statistical techniques on study of sedimentary organic matter distribution.....

18

RESERVOIR ENGINEERING

Fariz F. Ahmed, Arzu H. Gayibova, Maharat A. Huseynov

Stabilization of unstable reservoirs in oil fields of Azerbaijan: potential and prospects of copolymer-based methods.....

23

PRODUCTION & OPERATIONS

*Sh. P. Kazimov, L. G. Hajikarimova, E. S. Abdullayeva,
E. Sh. Azimova*

On the efficient operation of submersible pumps with low liquid levels.....

28

S. A. Isayeva

Sand risk in weakly consolidated rocks and the application of chemical consolidation technologies: a research review on Garadagh and Kalmas underground gas storages.....

34

F. F. Ahmed, S. İ. Mansurova, M. A. Rzayeva

Enhancing oil recovery in the late stage of field development through behind-the-casing flow isolation.....

40

J. M. Eyvazov, T. A. Aslanov

The effect of different hydraulic fracture lengths on well production.....

45

K. F. Aliyev

An integrated data-driven intelligent automation framework for predicting and controlling liquid loading in gas-condensate wells.....

50

NEW DIRECTIONS IN THE ANALYSIS OF WELL GEOPHYSICAL SURVEY DATA IN SEISMOACTIVE ZONES

H. I. Shakarov^{*1}, M. A. Bakirov¹, N. H. Mehdiyeva²,
A. Q. Bakirova¹, A. E. Abdullayeva¹

¹«OilGasScientificResearchProject» Institute, SOCAR, Baku, Azerbaijan

²Geophysics and Geology Department, SOCAR, Baku, Azerbaijan

ABSTRACT

The article substantiates the necessity of taking into account the variations of geophysical and geochemical fields under the influence of geodynamic processes during the analysis of well geophysical survey (WGS) data. Studies conducted at numerous research polygons around the world have thoroughly examined the variations in the Earth's natural electric and geomagnetic fields prior to earthquakes. Analysis of the obtained results has shown that changes in the Earth's geomagnetic and natural electric fields, as well as in the electrical resistivity of rocks, are observed both before and after earthquakes. Considering these indicators, during the reanalysis of well geophysical survey data from certain fields located on the Absheron Peninsula, the influence of geodynamic processes and variations in geophysical and geochemical fields on the evaluation of reservoir oil and gas content has been determined. In order to identify the impact of geodynamic processes on well geophysical survey data, a catalog of earthquakes felt on the Absheron Peninsula and adjacent areas was compiled. Based on this catalog, an epicenter map of earthquakes expected to be observed within the studied fields was created. The WGS materials from wells drilled during «active» and «quiet» seismic periods were comparatively analyzed, the main layer parameters were recalculated, and the influence of geodynamic activity was substantiated. The research results have shown that the proper consideration of geodynamic processes ensures high accuracy and reliability in the exploration and exploitation of oil and gas fields. At the same time, the obtained results indicate that the assessment of geodynamic processes directly affects not only geophysical parameters but also geochemical indicators to the closure of the Tethys Ocean at the end of the Cretaceous and beginning of the Paleogene.

KEY WORDS:

geodynamic processes; seismic activity; earthquake–production relationship; hydrocarbon-bearing reservoirs; geochemical fields; geophysical field variations; borehole geophysical investigations; well log analysis; electrical resistivity.

*e-mail: hafiz.shekerov@socar.az

<https://doi.org/10.53404/Sci.Petro.20250200075>

Date submitted: 14.10.2025

Date accepted: 06.11.2025

One of the main tasks of current oilfield geophysical research is the identification of layers possessing filtration-capacity properties within the well section and the accurate calculation of their oil and gas saturation coefficients. The analyses performed show that, in some cases, the conclusions drawn from well geophysical survey (WGS) data do not coincide with the results of perforation and testing operations. For instance, in some cases, layers previously evaluated as oil-bearing have yielded only water during testing, whereas layers classified as water-bearing have produced commercially significant oil. Our analyses indicate that such discrepancies are more frequently encountered in wells where logging operations were carried out during periods of geodynamic activation. The review of scientific research in the field of geodynamic events shows that, during such activation periods, geophysical and geochemical fields may

vary by 25–35 %, and in some cases even more. These unexpected anomalies cause changes in the values of geophysical parameters measured during the studies, leading to distortions in the evaluation of reservoir saturation – that is, the actual conditions are not correctly reflected. All these factors negatively affect the assessment and exploitation of the reserves of the studied field, resulting in certain oil-bearing layers not being included in production, and consequently, large quantities of oil remaining unextracted within the subsurface. Comprehensive and comparative analysis of well logging diagrams has made it possible to determine that the main layer parameters observed in front of oil- and gas-bearing reservoirs differ from the established field-specific criteria.

Analysis of the depth distribution of earthquake hypocenters within the territory of Azerbaijan has shown that the main stress accumulation zone – that

is, the earthquake focus – is often located at depths of up to 30 km [1]. It is known that the thickness of the sedimentary cover within the boundaries of our country also varies approximately between 3 and 23 km. The formation, development, and distribution characteristics of oil and gas fields are closely related to this sedimentary cover.

In several fields located within the Lower Kura depression (LKD), which is considered one of the oil- and gas-bearing regions of our republic, the temporal and spatial variations of the seismogeodynamic conditions were studied and evaluated, taking into account the features mentioned above. Using various sources, the main parameters of earthquakes were first determined, and based on these data, corresponding catalogs were compiled. According to the obtained information, the well geophysical survey (WGS) materials from wells drilled in the studied field were reanalyzed by considering the anomalous variations in the geodynamic conditions. As a result, the main layer parameters were recalculated, and the oil and gas content of the section was accurately evaluated [2].

Accurate determination of the parameters characterizing earthquakes plays an important role in identifying the extent of stress zones generated by geodynamic processes and in assessing their influence on the physical and mechanical properties of the sedimentary complex. When the physical and mechanical properties of the sedimentary complex change within the Earth's crust, whether in local or regional areas, additional stress is generated and spreads intensively to the surrounding zones. Depending on the distance from the source, the physical and mechanical properties of the sedimentary complexes forming the geological section in adjacent zones also undergo varying degrees of alteration. Therefore, when analyzing earthquake parameters, the first step is to thoroughly examine the geological-tectonic and geodynamic characteristics of the medium in which the hypocenter (depth) is located, followed by an investigation of the preparatory stage, as well as the pattern and intensity of stress propagation [3].

Analysis of seismic activity recorded in various regions of Azerbaijan shows that stress variations occurring in earthquake foci correspond to anomalous changes observed across wide areas. The results of these studies indicate that seismic events should be regarded not only as local phenomena but also as the consequences of deformation processes occurring on a regional scale. Although the subsurface stresses—whether compressional or extensional—differ from one region to another, the anomalous geophysical variations observed in these areas reflect both the state and evolution of the prevailing geodynamic con-

ditions. This, in turn, demonstrates the existence of a close and reciprocal relationship between the changes recorded in geophysical fields and the geodynamic processes taking place within earthquake foci [4, 5].

In many cases, abrupt variations in the parameters of geophysical and geochemical fields have been observed in polygons located at a certain distance from the epicenter prior to an earthquake. Notably, after the occurrence of the earthquake, both geochemical and geophysical field parameters returned to their normal values characteristic of the area. These observations indicate that the noticeable anomalies in the parameters of geophysical fields recorded at polygons remote from the epicenter, as well as the earthquakes themselves, originate from a single natural phenomenon—the influence of geodynamic processes occurring within the massive tectonic blocks of the Earth's interior.

For a long time, in many developed countries of the world, including Azerbaijan, the variations observed in the parameters characterizing both geochemical and geophysical fields, caused by geodynamic and tectonic processes occurring in earthquake focal zones, have been extensively analyzed [4]. At the same time, large-scale studies are being carried out to determine the reasons why anomalies arising from sudden geodynamic events are recorded at observation stations located far (sometimes 100–500 km) from the earthquake-affected area. In various polygons, measurement operations are conducted using modern instruments and equipment that meet current scientific standards. At these observation sites, parameters such as seismic wave velocity, magnetic field intensity, electrical resistivity, thermal energy, temperature, and other physical quantities are monitored, along with the variations in different components of geochemical fields. The analyses have revealed that during periods of geodynamic activation, the indicators of geophysical field parameters exhibit anomalous variations ranging between 10–25 %, 35–65 %, and in some cases even 70–200 %, in both spatial and temporal domains [6, 7]. These anomalies do not occur suddenly; rather, they are observed over time spans of 7–15 to 350–500 days—or even longer—depending on the energy level of the potential stress source, and they encompass vast areas, including large tectonic blocks.

Figure 1 illustrates the variation graph of seismic wave velocity measured prior to earthquakes, as well as the ratio of longitudinal to transverse wave velocities (V_p/V_s). As seen, the V_p/V_s ratio generally fluctuates around its normal value of approximately 1.73. However, some time before an earthquake occurs, this ratio decreases by about 15–20 %, and then, shortly before the event, it abruptly returns to values close to normal (around 1.73). The earthquake typically occurs

at this moment. The described patterns are observed not only in the V_p/V_s ratio but also in the propagation velocity of longitudinal waves. Furthermore, the analysis of the presented graphs shows that the magni-

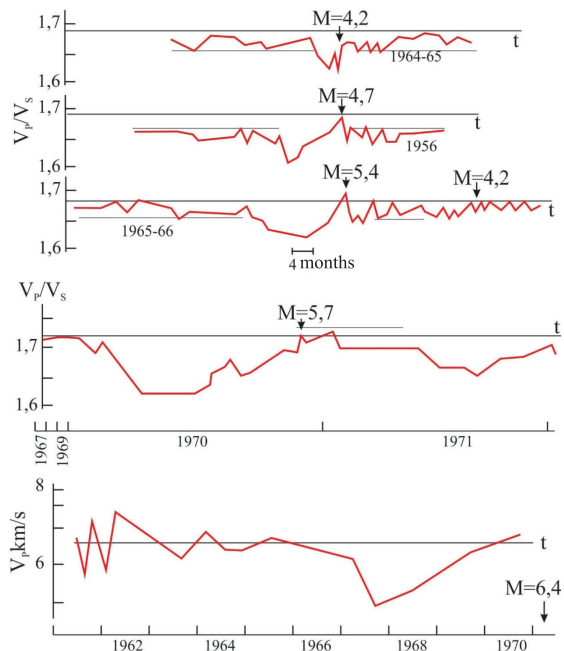


Fig. 1. Variation graphs of seismic wave velocity prior to the earthquake

tude and duration of the anomalous variations in both the V_p/V_s ratio and the longitudinal wave velocity depend on the energy class (magnitude) of the occurring earthquake. It should be noted that the graphs described above were constructed based on research conducted in the Garm region of the Republic of Uzbekistan.

It has been confirmed by numerous studies conducted at various observation polygons that anomalous variations in the Earth's natural electric and geomagnetic fields occur in relation to seismic activity. Analysis of the results has shown that, prior to earthquakes, more pronounced changes are observed in the measured values of the apparent electrical resistivity of the sedimentary complex. Experiments carried out in the Garm region and in the city of Sizi, China, investigated the variations in the apparent resistivity of rocks. The results demonstrated that, before earthquakes, the resistivity of rocks decreases by approximately 15–20 %. It is clearly evident that both the magnitude and duration of this decrease are directly proportional to the earthquake's magnitude (fig. 2).

Extensive research has also been carried out at geodynamic polygons in Azerbaijan to study variations in the parameters of electric, magnetic, and gravitational fields, as well as in the components of geochemical fields, yielding significant and noteworthy data [8, 9].

The analyses indicate that the quantitative and qualitative variation criteria of geochemical and geophysical field parameters under the influence of geodynamic processes have not yet been unambiguously assessed. The analysis of observational data obtained from various geodynamic polygons has made it possible to classify the observed anomalies and their causes into two main groups [10, 11].

The first type of activation has a regional character and is accompanied by slow, long-term variations within different tectonic blocks over geological time scales. The study of this phenomenon is possible through long-term observations using specialized instruments and by analyzing the geological evolution history. In research aimed at forecasting the generation, migration, and accumulation of hydrocarbons, an adequate assessment of the influence of this factor is one of the most important issues.

The second type of activation, by its nature, manifests suddenly within a localized area inside an individual tectonic block over a very short geological period. Such sudden processes can be measured using various specialized instruments, allowing for monitoring of their development dynamics and determination of the affected area depending on their energy class [12, 13]. Analyses have shown that during this type of activity, the anomalies observed in physical

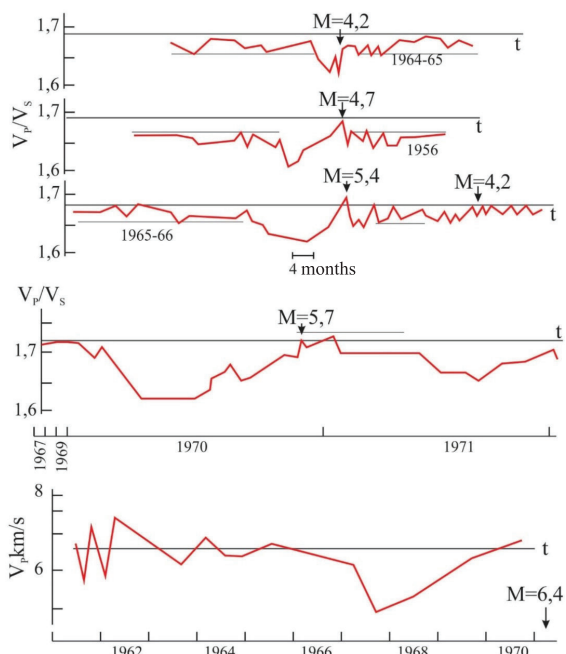


Fig. 2. Variation graphs of the apparent resistivity of rocks prior to the earthquake

field parameters exert a stronger influence on the geochemical measurements carried out for hydrocarbon exploration and prospecting. This can be explained by the fact that, under the influence of geodynamic processes occurring in small local areas, the physical and mechanical properties of rocks undergo changes, which in turn are reflected in the measured geophysical parameters [14–20].

Based on observations conducted at geodynamic polygons, the anomalous variations identified in geochemical and geophysical fields have been comparatively analyzed, and their variation tendencies (either negative or positive) have been examined. The analyses show that the anomalous changes observed in the monitored parameters at geodynamic polygons are sometimes characterized by negative, and in other cases by positive values — that is, they may deviate either above or below the general background level. In our view, this variability is related to the fact that the geodynamic processes causing these anomalies occur at different times and in areas that differ significantly from one another in terms of their geological and tectonic characteristics. It is well known that the occurrence of both strong and weak earthquakes is regionally associated with variations in the stress-strain conditions. Therefore, when analyzing the influence of geodynamic processes on the parameters measured during geophysical surveys, it is essential to take this feature into account as one of the critical factors.

Analyses show that earthquakes occurring within the territory of our country, in the Caspian Sea, and in neighboring states (Russia, Turkey, Iran, and Georgia) also contribute to the spatio-temporal variations of the geodynamic conditions in the Absheron Peninsula [5, 12, 17, 21, 22]. Most of the oil and gas fields currently under exploitation in the Absheron Peninsula are affected by various types of disjunctive faults and dislocations and are surrounded by periodically active mud volcanoes. Therefore, the impact of geodynamic processes is more distinctly observed in these fields. It has been clearly substantiated through the conducted analyses that geodynamic processes play a significant role in the formation, migration, and exploitation of oil and gas deposits. This influence extends to the parameters measured during geophysical and well logging investigations. The analysis of monitoring data shows that, under the influence of geodynamic processes, the values of geophysical field parameters in some cases decrease, while in others they increase (fig. 3). This phenomenon can be explained by the formation of zones subjected to structural extension or compression on local and regional scales due to geodynamic processes. Moreover, the parameter (K), which characterizes the variation of the stress-strain state of structures experiencing expansion or com-

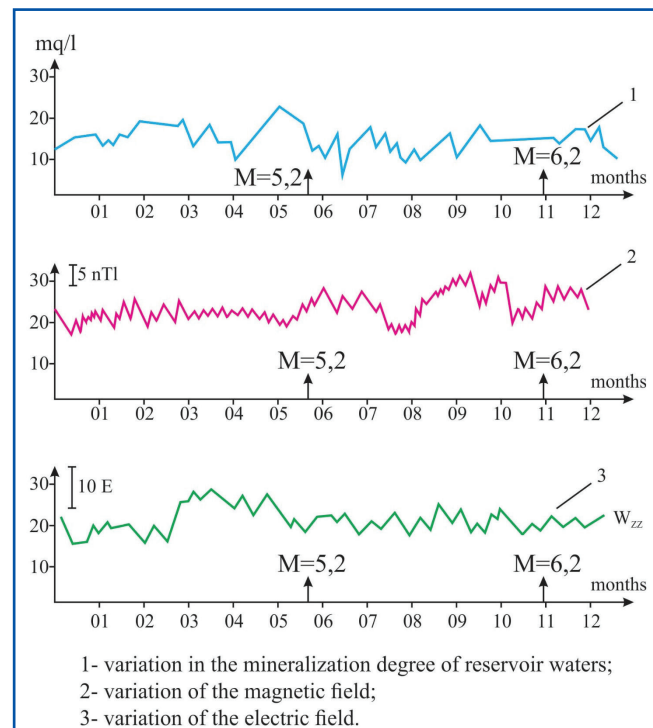


Fig. 3. Temporal variations of physical fields

pression in proportion to the energy released from the earthquake focus, also varies. In geodynamically stable areas, the value of K is taken as unity. Values of $K < 1$ correspond to compression zones, while $K > 1$ indicates extension zones. Taking these factors into account, reanalysis of well geophysical data from the Hovsan and Lokbatan–Puta–Qushkhana fields, located in the Absheron Peninsula, was carried out to study the variations in geochemical and geophysical field parameters under the influence of geodynamic processes.

To determine the influence of geodynamic processes on well geophysical data, earthquakes with potential impact on the Absheron Peninsula were first identified, and a corresponding catalog was compiled. Based on this catalog, an epicenter map of earthquakes—whose effects could be observed in the Hovsan and Lokbatan–Puta–Qushkhana fields depending on their energy class—was prepared (fig. 4). Using this map, along with a comparative analysis of the activation periods of mud volcanoes affecting the study area, geodynamically «active» and «quiet» time intervals were defined for the investigated regions.

During the reanalysis of well geophysical survey materials, several parameters were determined to identify reservoir layers and assess their oil and gas saturation. These include the true resistivity (ρ_{stone}),

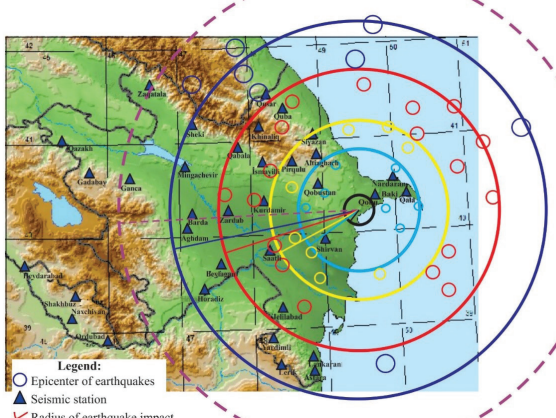


Fig. 4. Spatial distribution scheme of earthquakes

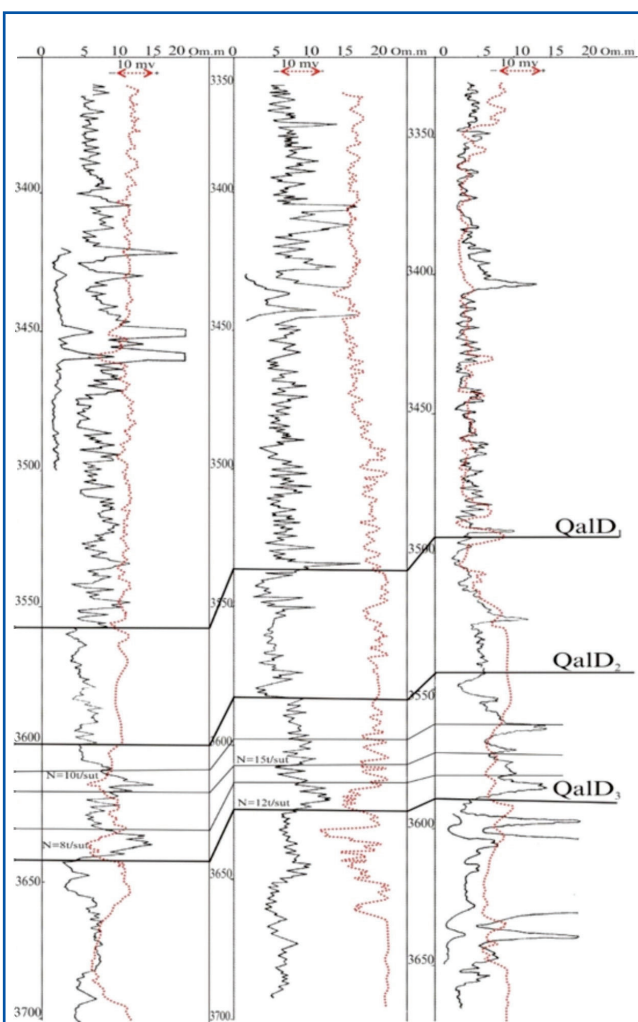


Fig. 5. Comparative analysis of well logging diagrams

relative resistivity (P), resistivity ratio ($\rho_{stone}/\rho_{shale}$), clay content coefficient (C_{shale}), porosity coefficient (K_{por}), and oil saturation coefficient (K_{sat}). Based on these parameters, the oil and gas saturation of the section was evaluated using new methodological approaches [23-25]. To identify new productive layers in wells drilled during geodynamically active periods, the above-mentioned parameters were calculated using the updated methodology, and the obtained results were comparatively analyzed with perforation and testing data. As a result, the presence of previously unidentified oil- and gas-bearing layers was confirmed in several well sections. In some cases, to perform a comparative analysis of the measured parameters, correlation between well data obtained during seismically «quiet» and «active» periods was also conducted (fig. 5).

During the re-interpretation of well logging (WGS) data in the study area, the research was carried out in the following sequence:

- First, seismically active and calm time intervals were determined for the area.
- To identify wells drilled during active and calm periods, the chronology (year, month, day) of the performed WGS studies was compared with the earthquake catalog.
- During the period when WGS operations were conducted, the criteria of variation in geochemical and geophysical field parameters were determined for the study area and its adjacent zones.
- Within the same tectonic block, the correlation of reservoir layers corresponding to the same stratigraphic unit was performed based on the comparative analysis of logging diagrams of wells drilled during seismically calm and active periods.
- Based on the well data, reservoir layers were identified, necessary corrections were applied to the measured parameters considering the influence of geodynamic stress, and the layer parameters — specific resistivity (ρ_{stone}), relative resistivity (P), resistivity ratio ($\rho_{stone}/\rho_{shale}$), shaliness coefficient (C_{shale}), porosity coefficient (K_{por}), and oil saturation coefficient (K_{sat}) — were recalculated.
- Using the developed software package and algorithms, mathematical-statistical analyses were carried out, and for wells drilled during seismically active and calm periods, the boundary values and variation intervals of the calculated parameters were determined.
- Dependency graphs were constructed between parameters characterizing the filtration-capacity properties of the reservoirs.

Thus, well data from several wells drilled in different years within the study areas were reinterpreted, and the presence of new oil- and gas-bearing intervals was predicted in some wells. It should be noted that subsequent perforation testing confirmed these predictions.

To verify the accuracy of the data obtained from the repeated reinterpretation works conducted in the study areas, as well as to determine the boundary values and distribution intervals of the calculated parameters, mathematical-statistical analyses were performed. Based on these operations, the interdependence among the layer parameters — specific resistivity (ρ_{stone}), relative resistivity (P), resistivity ratio ($\rho_{stone}/\rho_{shale}$), shaliness coefficient (C_{shale}), porosity coefficient (K_{por}), and oil saturation coefficient (K_{sat})

— was analyzed; corresponding regression equations were derived, and correlation coefficients were determined. As a result, equations describing the relationships between parameters characterizing the filtration-capacity properties of the layers were established. Based on the conducted analyses, both qualitative and quantitative variations in geochemical and geophysical field parameters under the influence of geodynamic processes were assessed, and the impact criteria on logging parameters were determined. Comparative correlation of oil- and gas-bearing layers was carried out across the study areas. Correlation of well-logging data showed that in well sections where logging was conducted during calm and active periods, the measured parameters in the same stratigraphic unit and at equivalent depths differed significantly.

Conclusions

1. The conducted studies show that geodynamic processes significantly affect the geochemical and geophysical field parameters, and these effects are clearly reflected in the parameters measured during well geophysical surveys.
2. Analysis of the variations observed before and after earthquakes in parameters such as geomagnetic intensity, natural electric fields, and rock resistivity has shown that these changes are strongly correlated with seismic activity.
3. As a result of geodynamic monitoring and re-interpretation of WGS data carried out in the Absheron Peninsula and other study areas, it became possible to predict previously unnoticed oil- and gas-bearing reservoirs.
4. The main stages of the research included: identification of active and calm seismic periods, selection of wells drilled during these intervals, comparative analysis of well logging diagrams, and recalculation of key formation parameters. Consequently, the variation ranges of rock electrical resistivity, porosity, saturation coefficient, and other indicators, as well as their relation to seismic activity, were substantiated using statistical and graphical methods.
5. It has been demonstrated that considering geodynamic processes in oil and gas exploration, prospecting, and field development significantly improves the accuracy and efficiency of the obtained data.

References

1. Ahmadbayli, F. S., Hasanov, A. G., Kadirov, F. A., et al. (2001). Spatial-temporal distribution of seismic events on the territory of Azerbaijan. In: *The Proceedings of the Third Geophysical Readings named after V.V. Fedynsky. Moscow, Russia*.
2. Valiyev, H. O. (2001). Methodology for identifying oil-gas-bearing objects overlooked due to geodynamic-tectonic stress in oil fields. *Baku*.
3. Barsukov, O. M., & Sorokin, O. N. (1973). Change in apparent resistivity of rocks in the Garm seismoactive region. *Physics of the Earth*, 10, 101–103.
4. Yetirmishli, G. J., Rzaev, A. G., Kazimov, I. E., & Kazimova, S. E. (2018). Modeling of the geodynamic

situation of the Kura depression based on the latest seismological, geodetic and magnetometric data. *Bulletin of the Orenburg Scientific Center of the Russian Academy of Sciences*, 2, 1–11.

5. Yetirmishli, G. J., Ismailova, S. S., Kazimova, S. E., & Islamova, Sh. K. (2024). Assessment of seismicity in Azerbaijan and adjacent regions in 2022 based on data from "Kinematics" seismic stations. *Seismoprognozis Observations in the Territory of Azerbaijan*, 26(2), 3–14.
6. Ogadjanov, V. A. (1998). The concept of geophysical research based on the phenomenon of rock dilation. *Scientific-Technical Journal Geophysics*, 4, 10.
7. Morkunov, V. A. (2001). Rock creep at the final stage of earthquake preparation. *Physics of the Earth*, 4, 3–11.
8. Hasanov, A. H., Rzayev, A. Q., & Karamova, R. A. (2000). Investigation of the conditions for earthquake prediction in the geophysical and geochemical fields of Azerbaijan's seismopredictive polygons. *AGY Journal*, 1, 37–41.
9. Nurmammadov, F. A. (2002). Study of the impact of an occurred earthquake on oil and gas fields. *Azerbaijani Geologist. Bulletin of the ANGC*, 7, 55–61.
10. Vorobyev, V. Ya., Ogadzhanov, V. A., Solomin, S. V.. (1999). The relationship between geodynamics and the stress state of the Earth's crust of the East European platform with hydrocarbon potential. *Scientific-Technical Journal Geophysics*, 4, 52–55.
11. Popov, E. A. (2001). Earthquake forecasting – a delicate matter. In: *The Proceedings of the Third Geophysical Readings named after V. V. Fedynsky* (pp. 136–140). Moscow, Russia.
12. Lapenna, V. (2024). Detecting DC electrical resistivity changes in seismic active areas: State-of-the-art and future directions. *Geosciences*, 14(5), 118.
13. Saraev, A. K. (2025). Magnetotelluric monitoring of earthquake precursors. *Geohazards*, 6(4), 61.
14. Dobrovolskiy, I. P. (1980). On the model of earthquake preparation. *Physics of the Earth*, 1, 23–31.
15. Kaledin, V. O., Lastoveckiy, V. P. (1999). Mathematical modeling of stress-strain state of rocks in application to oil and gas exploration problems. *Scientific-Technical Journal Geophysics*, 3, 63–68.
16. Wang, Y., Yu, C., Yu, H., et al. (2021). Stress-induced apparent resistivity variations at the Kalpin Observatory and the correlation with the 2020 Mw 6.0 Jiashi earthquake. *Atmosphere*, 12(11), 1420.
17. Gokhberg, M. B., Morgounov, V. A., Pokhtelov, O. A. (1995). Earthquake prediction – seismo-electromagnetic phenomena. Amsterdam: Gordon & Breach.
18. Cicerone, R. D., Ebel, J. E., Britton, J. A. (2009). A systematic compilation of earthquake precursors. *Tectonophysics*, 476, 371–396.
19. Li, A., Parsekian, A. D., Grana, D., Carr, B. J. (2025). Quantification of measurement uncertainty in electrical resistivity tomography data and its effect on the inverted resistivity model. *Geophysics*, 90(3).
20. Zhang, J., Du, W., Yue, M., Liu, C., Liang, X., & Yang, J. (2025). Observational evidence of anisotropic changes in apparent resistivity before strong earthquakes. *arXiv Preprint*.
21. Yetirmishli, G. J., Kazimova, S. E., & Kazimov, I. E. (2023). Oil and gas potential and modern seismicity of the Azerbaijan sector of the Caspian Sea. *Geofizicheskiy Zhurnal*, 45(1).
22. Abdullayeva, R. R., Kazimova, S. E., Ismayilova, S. S., & Akbarov, E. A. (2016). Geodynamics of Azerbaijan part of the Caspian Sea. *Seismoprognozis Observations in the Territory of Azerbaijan*, 13(1).
23. Shakarov, H. I. (2008). The impact of geodynamic processes on the electrical properties of the environment. In: *The Catalogue of seismopredictive observations in Azerbaijan in 2007*, Baku, Azerbaijan.
24. Shakarov, H. I., Abuzarova, A. H., Kerimova, Y. H. (2025). A comprehensive analysis of geophysical well logging data in the study of low-resistivity thin beds. *Scientific Petroleum*, 1, 2–8.
25. Shakarov, H. I., et al. (2007). On some causes of low resistance in productive reservoirs. *Karotazhnik*, 12(165), 47–48.

PETROGEOCHEMICAL CHARACTERISTICS OF JURASSIC VOLCANIC ROCKS OF THE CHOVDAR ORE FIELD (LESSER CAUCASUS)

S. H. Jafarov

¹Baku State University, Baku, Azerbaijan

²AzerGold, Baku, Azerbaijan

ABSTRACT

The article is devoted to the petrogeochemical features of Jurassic volcanic rocks of the Chovdar ore field of the Lesser Caucasus based on 94 silicate and 36 trace element analyses from various volcanic rock samples within the ore field. The data reveal a diverse range of lithologies; including basaltic; andesitic; dacitic; and rhyolitic compositions; predominantly of calc-alkaline and tholeiitic affinity. Diagrams such as TAS; AFM; and tectonic discrimination plots confirm the subduction-related magmatic setting and suggest a mature island arc environment with complex magmatic differentiation. The interpretation of the spider diagram shows that the studied samples were formed from magma formed under subduction conditions; enriched with volatile-transported elements; and formed under conditions that underwent a significant period of crustal development; which; as mentioned earlier; is consistent with the formation of the Lesser Caucasus metallogenic province; Lok-Karabakh structural formation zone under the conditions of island arc volcanism. The presence of both low-K mafic and calc-alkaline felsic rocks reflects multi-stage magmatism linked to extensional tectonics and mantle metasomatism. The trace element data further corroborates subduction-derived magma evolution; characterized by HFSE depletion and LILE enrichment. These findings collectively indicate that the Chovdar ore field evolved under sustained arc volcanism; with implications for regional metallogenies in the Lesser Caucasus. Geochemical differences between the Lower and Upper Bajocian units reveal a transition from early tholeiitic to later calc-alkaline magmatism; indicative of changing mantle source characteristics and increasing crustal interaction. The coexistence of low-K basaltic and high-silica dacitic-rhyolitic rocks implies polyphase magmatism and mantle-crust mixing. Overall; the results point to an island arc regime with active subduction; mantle wedge metasomatism; and multi-stage magmatic evolution contributing to the mineralization and alteration processes within the Chovdar ore field.

e-mail: ceferovsoltan@gmail.com

<https://doi.org/10.53404/Sci.Petro.20250200076>

Date submitted: 22.08.2025

Date accepted: 10.12.2025

KEYWORDS:

Chovdar ore field;
Lesser Caucasus;
petrogeochemical
characteristics;
TAS diagram;
spider diagram;
geochemical analyses;
rare earth and trace
elements; tectonic
discrimination and
spyder diagram.

1. Introduction

The Lesser Caucasus represents a significant segment of the Alpine-Himalayan orogenic belt, encompassing a tectonically active region influenced by the complex interaction of lithospheric plates. Within this domain, the Chovdar ore field occupies a strategic position in the Lok-Karabakh structural zone and serves as a geologically critical site for evaluating the interplay of magmatism, tectonics, and ore formation during the Mesozoic to Cenozoic periods. The geodynamic evolution of this region is marked by multiple stages of oceanic subduction, continental collision, and post-collisional extension, which collectively shaped the magmatic architecture and metallogenic potential of the area.

The Chovdar ore field exhibits a wide variety of volcanic and subvolcanic rocks, which range in composition from basalts to rhyolites. These rocks have been subjected to varying degrees of hydrothermal alteration, particularly silicification and metasomatism, which have important implications for interpreting geochemical data. This study seeks to characterize the petrochemical and geodynamic framework of the Chovdar area by examining whole-rock silicate and trace element compositions, supported by classification and tectonic discrimination diagrams. Through this, we aim to establish the magmatic affinity, tectonic setting, and evolution of the volcanic units, and to elucidate their relationship to the broader metallogenic context of the Lesser Caucasus.

2. Geological setting and formation of Chovdar ore field

The Lesser Caucasus is one of the interesting segments of the extensive Alpine-Himalayan orogenic system. The Lesser Caucasus tectonic development is strictly linked to broader lithospheric processes; also, geodynamic evolution is commonly analyzed within the context of the central Mediterranean tectonic domain [1, 5, 10].

As noted by M. I. Rustamov [14], after the final stages of oceanic evolutionary processes and the complete subduction of oceanic basins of the Meso-Tethys, there was a noticeable reduction in compressive tectonic movements. During the mentioned period, diminishing regional compression and volcanic activities associated with supra-subduction settings persisted, manifesting as island arcs and rift-related volcanic systems within arc-related basins. Subsequently, during the Late Senonian period, widespread carbonate sedimentation developed within the region, including in residual troughs along ophiolitic sutures, and reflecting a phase of relative tectonic immobility [7].

According to Y. V. Koryakin [8] and M. I. Rustamov [14], the mentioned tectonic conditions marked the beginning of the collisional stage of the Late Alpine orogenic period, ranging from the Maastrichtian–Paleocene boundary through to the Quaternary. This major tectonic transitioning period reflects the final stage of closure of the Tethys Ocean and highlights the ongoing evolution of the Alpine-Himalayan system as a continental collisional belt. The region's structural-tectonic framework and associated magmatism played a vital role in understanding active tectono-magmatic systems within such convergent plate boundaries.

Regional-wise, the Chovdar ore area is situated within the Lok-Karabakh structural zone, as part of the Shamkir uplift, adjacent to the junction with the Dashkesan caldera. A key geological specification of the Chovdar mineralization area is the persistence and inheritance of Alpine-age structural elements that influenced the formation of both descending and uplifting tectonic blocks during orogenic, post-orogenic, and neotectonic periods. Chovdar ore area is structurally bounded to the east and west by major fault zones—the Khosbulag–Khanlar–Alazan and Shamkircay–Aliabad faults—that form a system of parallel, morphogenetically bounded structures trending indirectly to the major Caucasus orientation [10].

Magmatic activity within the Chovdar area is mostly associated with Alpine orogenesis and can be classed into distinct stages—Bajosian, Bathonian, and Late Jurassic. These stages are defined by their lithofacies assemblages and are typically separated by transitions involving volcanogenic-sedimentary interlayers. While effusive volcanic rocks are dominant across the region,

occurrences of subvolcanic and intrusive bodies are also observed. The magmatism of the Lower Bajosian is characterized by basalt-andesites basalt sequences, whereas the Upper Bajosian is distinguished by dacitic to rhyolitic volcanic complexes.

3. Methodology

Petrogeochemical investigations were conducted using whole-rock geochemical analyses of 94 rock samples for major elements via X-ray fluorescence (XRF), and 36 selected samples were further analyzed for trace and rare earth elements. Sampling was performed with careful consideration to minimize the effects of hydrothermal alteration; where possible, fresh or slightly altered rocks were selected.

The classification of volcanic rocks was conducted using established geochemical diagrams, including the Total Alkali-Silica (TAS) diagram [9], AFM ternary plots [6], FeO^*/MgO - SiO_2 plots, and tectonic discrimination diagrams [11, 12]. In addition, MORB-normalized spider diagrams [15] and element ratio plots were utilized to assess magmatic evolution, crustal assimilation, and tectonic setting. All geochemical data were interpreted in the context of subduction-related processes and volcanic arc regimes.

4. Petrogeochemical characteristics of Chovdar ore area

Petrochemical studies were conducted using X-ray fluorescence (XRF) analysis on 94 samples taken from the ore field from rocks reflecting different lithological and petrological characteristics. Also, it must be considered that rock types that have undergone intensive metasomatic changes were not used during the studies. One of the characteristic specifications of the Chovdar ore area is the metasomatic alteration of rock types at different intensities. Therefore, when comparing the petrographic thin sections of the rocks with their geochemical compounds, it is possible to observe that samples that correspond to basaltic rocks in terms of petrographic composition (composed of olivine, labrador (plagioclase), augite, and biotite) are confused with andesite-dacite or dacite-containing rocks in terms of silicate analysis. The above-mentioned case is that they have been altered to some extent by hydrothermal processes through silicification. While collecting the samples for analysis, either alteration-free rock types or slightly altered specimens are selected if unaltered ones cannot be found successfully (table 1).

The SiO_2 content of the analyzed rocks varied from 42.5 to 78.9 percent (table 1). When studying the TAS diagram, it is possible to see that the samples taken and analyzed from the ore region vary from basalt to rhyolite. The TAS diagram (fig. 1) [9] illustrates that the analyzed rocks mainly belong to the subalkaline series.

Table 1

Results of silicate analysis of the Jurassic volcanic rocks of the Chovdar ore field

Sample ID	Al ₂ O ₃	SiO ₂	Na ₂ O	MgO	Fe ₂ O ₃	CaO	TiO ₂	P ₂ O ₅	MnO	K ₂ O	Cr ₂ O ₃	Loss	Σ	Σ+Loss
CHPSMPL-0001	17.2	59.1	3.497	3.099	7.198	4.701	0.505	0.096	0.204	2.099	0.029	3	97.73	100.73
CHPSMPL-0002	17.795	46.995	1.5	3.103	11.203	11.098	0.704	0.103	0.197	0.103	0.024	7.3	92.82	100.12
CHPSMPL-0003	14.404	62.296	3.804	2.799	7.498	3.005	0.501	0.096	0.105	0.598	0.007	5.1	95.11	100.21
CHPSMPL-0004	11.399	69.5	2.004	0.996	4.998	3.104	0.398	0.104	0.1	1.501	0.008	6	94.11	100.11
CHPSMPL-0005	17.702	48.005	2.198	3.601	11.999	9.896	0.804	0.103	0.3	0.102	0.014	5.3	94.72	100.02
CHPSMPL-0006	18.602	49.095	4.203	3.999	9.904	7.997	0.598	0.103	0.205	0.201	0.009	6.5	94.92	101.42
CHPSMPL-0007	16.396	60.905	3.297	2.696	7.705	4.9	0.498	0.096	0.104	1.203	0.014	3	97.81	100.81
CHPSMPL-0008	19.701	51.503	3.002	4.198	8.202	6.996	0.702	0.098	0.1	0.402	0.005	6.5	94.91	101.41
CHPSMPL-0009	20	51.102	7.297	4.004	9.701	1.603	0.7	0.099	0.203	0.598	0.01	4.3	95.32	99.62
CHPSMPL-0010	8.297	78.898	3.401	1.699	3.804	0.704	0.202	0.001	0.103	0.102	0.011	2.8	97.22	100.02
CHPSMPL-0011	17.202	42.798	0.705	3.402	10.699	7.903	0.701	0.101	0.103	0.404	0.007	15.9	84.02	99.92
CHPSMPL-0012	18.7	47.702	1.703	3.198	10.803	11.901	0.799	0.101	0.201	0.001	0.007	5.8	95.12	100.92
CHPSMPL-0013	17.502	47.999	1.903	3.904	11.7	8.297	0.797	0.097	0.198	0.1	0.01	7.2	92.51	99.71
CHPSMPL-0014	18.902	47.002	4.304	3.499	11.497	6.701	0.596	0.104	0.199	0.197	0.008	7	93.01	100.01
CHPSMPL-0015	19.203	49.404	2.102	4.099	9.804	8.699	0.602	0.103	0.295	0.105	0.014	5.5	94.43	99.93
CHPSMPL-0016	18.1	50.796	2.104	3.202	10.6	8.699	0.598	0.098	0.201	0.096	0.007	5.2	94.5	99.7
CHPSMPL-0017	13.897	69.801	3.305	1.502	4.604	0.899	0.499	0.103	0.103	1.501	0.007	3.5	96.22	99.72
CHPSMPL-0018	10.796	75.596	4.905	0.497	3.095	1.295	0.397	0.096	0.003	0.204	0.011	1.7	96.9	98.6
CHPSMPL-0019	16.697	61.601	5.205	1.699	6.898	0.798	0.705	0.1	0.104	1.203	0.012	5	95.02	100.02
CHPSMPL-0020	14.896	63.295	5.904	1.897	7.102	1.896	0.596	0.203	0.105	0.599	0.01	3.2	96.5	99.7
CHPSMPL-0021	19.097	47.201	2.105	2.398	9.799	13.903	0.7	0.103	0.204	0.201	0.014	5.3	95.72	101.02
CHPSMPL-0022	16.803	52.697	4.105	4.396	9.4	3.005	0.599	0.102	0.104	0.297	0.006	8.6	91.51	100.11
CHPSMPL-0023	16.8	51.404	4.096	3.597	10.397	5.896	0.702	0.099	0.203	0.498	0.006	6.8	93.7	100.5
CHPSMPL-0024	16.499	53.2	7.398	3.499	9.701	3.103	0.804	0.101	0.105	0.003	0.013	5.4	94.43	99.83
CHPSMPL-0025	18.798	52.298	7	4.205	9.096	1.705	0.6	0.099	0.098	0.396	0.011	4.9	94.31	99.21
CHPSMPL-0026	17.703	61.102	4.003	2.698	7.099	3.302	0.504	0.1	0.096	1.198	0.011	3.4	97.82	101.22
CHPSMPL-0027	15.196	56.598	5.704	5	10.496	1.102	0.595	0.096	0.101	0.396	0.011	4.4	95.29	99.69
CHPSMPL-0028	16.696	51.598	1.697	3.402	11.205	10.503	0.802	0.096	0.097	0.103	0.014	3.6	96.21	99.81
CHPSMPL-0029	19.295	46.304	2.6	6.904	13.004	4.302	0.797	0.099	0.102	0.698	0.014	7.3	94.12	101.42
CHPSMPL-0030	15.497	53.502	2.5	3.997	9.498	6.104	0.598	0.102	0.102	0.396	0.009	7.5	92.3	99.8
CHPSMPL-0031	17.196	48.498	1.702	3.499	14.203	11	0.598	0.098	0.197	0.099	0.014	2.6	97.1	99.7
CHPSMPL-0032	11.802	64.502	2.495	1.101	6.8	6.201	0.5	0.098	0.103	0.3	0.011	6.1	93.91	100.01
CHPSMPL-0033	18.396	50.705	2.001	4.002	12.703	7.799	0.798	0.104	0.102	0.099	0.015	4.2	96.72	100.92
CHPSMPL-0034	17.499	48.698	1.698	2.698	11.297	12.897	0.696	0.105	0.199	0.003	0.009	5.3	95.8	101.1
CHPSMPL-0035	15.704	48.195	1.597	3.602	11.401	8.798	0.601	0.095	0.198	0.201	0.015	9.2	90.41	99.61
CHPSMPL-0036	14.703	52.803	1.696	3.803	12.905	4.501	0.701	0.103	0.102	0.2	0.011	8.2	91.53	99.73
CHPSMPL-0037	9.505	76.298	2.405	1.701	4.403	0.396	0.3	0.103	0.102	1.099	0.01	3.2	96.32	99.52
CHPSMPL-0038	18.897	50.103	3.595	5.295	10.997	5.699	0.599	0.104	0.202	0.099	0.007	5.5	95.6	101.1
CHPSMPL-0039	14.802	63.503	6.203	1.401	8.196	2.097	0.601	0.202	0.102	0.195	0.013	3.7	97.32	101.02
CHPSMPL-0040	18.998	49.599	6.604	4.098	12.297	2.103	0.8	0.102	0.203	0.297	0.006	5.3	95.11	100.41
CHPSMPL-0041	18.902	58.501	3.502	1.9	7.603	2.097	0.603	0.103	0.102	0.699	0.007	6.8	94.02	100.82
CHPSMPL-0042	14.304	58.196	0.103	3.498	14.596	1.099	0.605	0.097	0.204	1.504	0.014	7.3	94.22	101.52
CHPSMPL-0043	18.201	58.603	4.097	3.201	7.902	4.397	0.5	0.103	0.102	2.398	0.012	2.3	99.52	101.82
CHPSMPL-0044	17.803	58.704	3.199	3.402	7.798	5.796	0.502	0.096	0.098	1.596	0.013	2.6	99.01	101.61
CHPSMPL-0045	9.797	77.704	2.9	1.405	2.998	2.305	0.305	0.101	0.098	0.101	0.011	3.8	97.72	101.52
CHPSMPL-0046	16.396	63.4	4.299	3.202	7.301	3.099	0.5	0.1	0.197	0.395	0.007	2.8	98.9	101.7
CHPSMPL-0047	14.303	61.104	3.897	3.496	7.399	3.701	0.499	0.101	0.096	0.105	0.01	7	94.71	101.71

Table 1 (continued)

Sample ID	Al ₂ O ₃	SiO ₂	Na ₂ O	MgO	Fe ₂ O ₃	CaO	TiO ₂	P ₂ O ₅	MnO	K ₂ O	Cr ₂ O ₃	Loss	Σ	Σ+Loss
CHPSMPL-0048	11.803	66.104	2.299	2.301	6.703	4.397	0.501	0.099	0.104	0.003	0.013	6.7	94.32	101.02
CHPSMPL-0049	18.601	50.603	5.205	6.1	11.899	2.103	0.805	0.099	0.296	0.096	0.011	5.4	95.82	101.22
CHPSMPL-0050	16.298	60.597	2.305	3.001	7.496	7.101	0.499	0.097	0.197	0.102	0.009	3.8	97.7	101.5
CHPSMPL-0051	16.702	58.7	4.796	3.002	8.396	2.196	0.598	0.098	0.2	0.195	0.005	5.2	94.89	100.09
CHPSMPL-0052	16.405	61.598	2.397	2.599	7.198	6.598	0.502	0.095	0.103	0.297	0.008	3.3	97.8	101.1
CHPSMPL-0053	17.096	59.4	5.497	2.2	6.896	4.503	0.803	0.104	0.302	0.201	0.015	4.1	97.02	101.12
CHPSMPL-0054	16.297	61.104	4.202	3.296	7.604	3.399	0.501	0.104	0.099	0.401	0.007	3.5	97.01	100.51
CHPSMPL-0055	16.204	63.395	0.001	2.5	7.098	2.301	0.601	0.1	0.203	0.197	0.005	4.7	92.6	97.3
CHPSMPL-0056	13.397	77.704	4.902	0.1	2.296	0.399	0.497	0.096	0	0.104	0.014	6	99.51	105.51
CHPSMPL-0057	18.198	55.1	4.202	3.802	9.503	2.6	0.497	0.102	0.095	0.2	0.012	6.2	94.31	100.51
CHPSMPL-0058	16.702	61.595	2.096	3.4	7.796	3.296	0.497	0.103	0.198	0.401	0.011	3.4	96.1	99.5
CHPSMPL-0059	15.899	60.902	3.701	2.696	7.296	6.497	0.5	0.098	0.198	0.201	0.008	3.9	98	101.9
CHPSMPL-0060	16.304	62.205	4.696	2.301	7.996	5.304	0.499	0.102	0.096	0.396	0.007	2.3	99.91	102.21
CHPSMPL-0061	14.801	66.903	4.498	2.695	5.496	1.903	0.4	0.002	0.102	0.002	0.014	4.3	96.81	101.11
CHPSMPL-0062	15.902	62.396	3.602	3.502	7.699	2.998	0.5	0.096	0.198	0.398	0.01	3.3	97.3	100.6
CHPSMPL-0063	16.498	63.195	9.302	2.7	7.597	3.998	0.5	0.104	0.095	0.399	0.008	3.4	104.4	107.8
CHPSMPL-0064	15.796	62.502	5.701	2.5	7.096	3.199	0.505	0.102	0.097	0.304	0.011	4.4	97.81	102.21
CHPSMPL-0065	17.204	60.702	5.802	1.198	2.304	3.604	0.802	0.197	0.201	0.101	0.001	3.2	92.12	95.32
CHPSMPL-0066	16.403	59.805	4.398	2.304	9.5	2.8	0.599	0.096	0.104	0.299	0.004	4.4	96.3	100.7
CHPSMPL-0067	15.902	62.999	0.001	3.399	7.803	1.995	0.505	0.1	0.098	0.497	0.001	2.7	93.3	96
CHPSMPL-0068	16.703	60.796	2.496	3.201	7.297	3.302	0.498	0.101	0.196	0.598	0.002	2.5	95.19	97.69
CHPSMPL-0069	14.104	68.899	1.595	0.103	7.995	4.299	0.497	0.096	0.199	0.096	0.004	8.4	97.88	106.28
CHPSMPL-0070	17.296	48.302	3.996	3.696	5.496	7.1	0.603	0.096	0.2	0.1	0.001	10.2	86.89	97.09
CHPSMPL-0071	17.397	51.101	4.003	4.197	7.701	9.696	0.795	0.1	0.198	0.003	0.001	6	95.18	101.18
CHPSMPL-0072	14.997	64.002	3.798	2.905	6.895	3.503	0.501	0.098	0.099	0.4	0.005	3.9	97.19	101.09
CHPSMPL-0073	15.296	65.401	4.499	2.797	6.699	2.704	0.498	0.097	0.096	0.398	0.003	3	98.48	101.48
CHPSMPL-0074	15.6	64.197	1.5	2.297	6.698	4.1	0.499	0.099	0.099	0.296	0.004	2.8	95.39	98.19
CHPSMPL-0075	15.901	61.998	5.702	2.004	7.601	5	0.498	0.101	0.097	0.401	0.005	2.6	99.31	101.91
CHPSMPL-0076	15.596	64.1	3.101	2.196	7.099	2.598	0.502	0.102	0.101	0.496	0.002	3.4	95.89	99.29
CHPSMPL-0077	18.403	50.796	1.498	2.604	10.5	12.302	0.7	0.096	0.197	0.003	0.005	4	97.09	101.09
CHPSMPL-0078	14.602	63.397	4.601	1.301	7.205	3.305	0.502	0.1	0.095	0.104	0	4.2	95.21	99.41
CHPSMPL-0079	16.097	63.501	0.005	2.697	7.003	5.096	0.502	0.1	0.096	0.399	0.004	2.2	95.49	97.69
CHPSMPL-0080	17.403	49.703	2.099	2.098	10.3	13.099	0.802	0.103	0.195	0.001	0.004	6.2	95.8	102
CHPSMPL-0081	18.297	51.199	2.803	3.904	10.996	7.895	0.796	0.105	0.196	0.104	0.003	3.4	96.29	99.69
CHPSMPL-0082	18.6	42.598	4.096	0.399	9.003	11.797	0.8	0.098	0.2	0.095	0.003	16.3	87.68	103.98
CHPSMPL-0083	15.802	60.895	3.598	4.098	7.503	4.999	0.501	0.1	0.101	0.2	0.004	4.5	97.79	102.29
CHPSMPL-0084	15.102	60.098	5.298	0.999	6	9.502	0.502	0.103	0.098	0.304	0.004	5.5	98	103.5
CHPSMPL-0085	15.597	62.304	5.3	3.497	7.103	3.499	0.504	0.098	0.205	0.504	0.003	3.1	98.61	101.71
CHPSMPL-0086	15.401	62.498	4.5	2.796	7.102	3.197	0.502	0.095	0.103	0.703	0.005	3.9	96.9	100.8
CHPSMPL-0087	15.502	61.998	4.797	2.696	6.596	2.697	0.5	0.095	0.098	0.595	0.004	4	95.57	99.57
CHPSMPL-0088	16.304	61.803	6.001	3.297	7.402	2.305	0.501	0.098	0.104	0.502	0.004	3.1	98.31	101.41
CHPSMPL-0089	18.898	56.402	1.7	3.502	8.905	4.701	0.595	0.101	0.199	0.5	0.004	3.2	95.51	98.71
CHPSMPL-0090	16.902	57.104	3.698	4.903	9.403	1.396	0.703	0.096	0.098	0.096	0.002	6	94.4	100.4
CHPSMPL-0091	13.404	68.399	3.002	1.299	6.498	0.597	0.505	0.098	0.101	0.199	0	3.8	94.1	97.9
CHPSMPL-0092	18.399	46.603	3	3.702	9.803	11.395	0.802	0.1	0.196	0.105	0.001	7.6	94.1	101.7
CHPSMPL-0093	16.502	44.102	5.296	7.902	9.097	7.698	1.304	0.297	0.203	0.004	0.003	11	92.4	103.4
CHPSMPL-0094	16.9	60.096	2.704	3.802	8.096	5	0.603	0.103	0.199	0.495	0.002	3.3	98	101.3
Average	16.302	58.102	3.501	2.995	8.4	4.999	0.602	0.098	0.102	0.4	0.001	5.1	95.5	100.6

It is possible to say that the majority of the analyzed tests, especially containing $\text{SiO}_2 > 54\%$, correspond to the low-medium K-alkaline series, and a small part to the K-calc-alkaline series [13]. It is obvious that during the Bajosian period, contrasting, bi-modal basalt-rhyolite volcanism was observed. Two complexes of Lower Bajosian and Upper Bajosian age are distinguished in the composition, which form basalt-andesite and dacite-rhyolite complexes, respectively. The volcanic complexes of the Bat period are represented by successive basalt-andesite-dacite containing facies. The volcanic formations of this period are also characterized mainly by normal alkaline complexes, among which, in some cases, calc-alkaline members are noticeable. The mentioned geochemical features correspond to the products of volcanic arcs of active plate margins or island arc volcanism, where the mantle plume that has been subjected to further metasomatism and the melting of the shuttered fragment of the subducting plate formed as a result of volcanic processes that produced mantle-derived melt which contaminated with volatiles and lithophile elements [9, 13].

Based on the analysis results of the rock samples taken, they are considered to belong to the magnesium rich, calc-alkaline series in the AFM diagram [6] (fig. 2). In accordance with the requirements of the subduction, the rocks illustrate a typical island arc regime with a decrease in the amount of Fe in the system, medium-high alkaline content, where, under the influence of vapor released from the melted subducting lithospheric wedge, while the upper mantle material is transformed into a hydrated magma [3, 17]. It is obvious that the increase in SiO_2 content through the basalt to rhyolite within the ore field clearly reflects the presence of magmatic differentiation and assimilation processes within the lithosphere and magmatic com-

pounds, especially medium-high silica types.

The observed geochemical characteristics allow us to consider that the products of calc-alkaline magmatism within the region were involved in differentiation processes. The observation of gradual transitions towards members with medium-acid composition and the absence of transitions between dacite, rhyolite-dacite, and rhyolite in some cases are factors indicating a higher intensity of volcanism processes during the formation of the mentioned rocks.

The position of the analyzed rocks in the FeO^*/MgO - SiO_2 diagram varies depending on the amount of SiO_2 in the rocks. It is no coincidence that the Bajocian andesites fall into the calc-alkaline zone in the diagram, while the Bathonian basalts and andesite-basalt rocks of the andesite-bearing part fall into the zone where the rocks of the tholeiitic series are located (fig. 3). Thus, Lower Bajocian volcanism with tholeiitic composition of the Middle Jurassic period was replaced by calc-alkaline volcanism in the Upper Bajocian stage, and in the Bathonian period, volcanism of the tholeiitic series was firstly replaced by calc-alkaline volcanism, which underwent differentiation, which is considered a characteristic feature of the volcanism of the geodynamic conditions of the island arc [5].

It should be noted that, in addition to the island arc conditions mentioned, one of the most important factors that can be considered, reflecting the reactivation of tectonic processes at different times, is the presence of both low-K basalts and calc-alkaline andesite-dacites within the area, which can be evaluated as multi-stage magmatic differentiation, mixing of mantle-derived melts, and even reloading of the existing magma chamber, reflecting the reactivation of tectonic processes at different times, which can be considered as a geodynamic interpretation. The absence of intensive alkaline rocks within

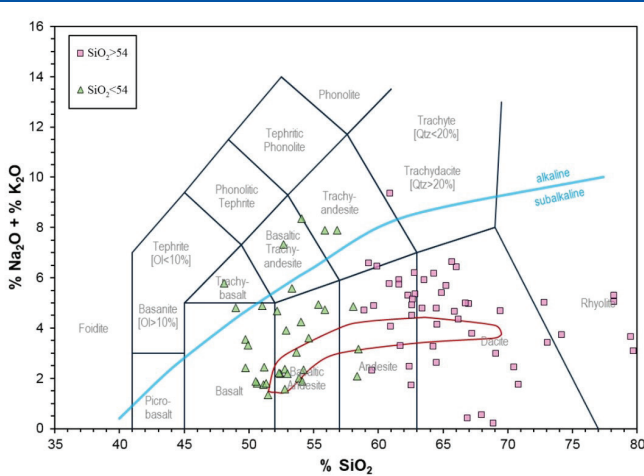


Fig. 1. Position of the analyzed rocks in the TAS classification diagram [9]

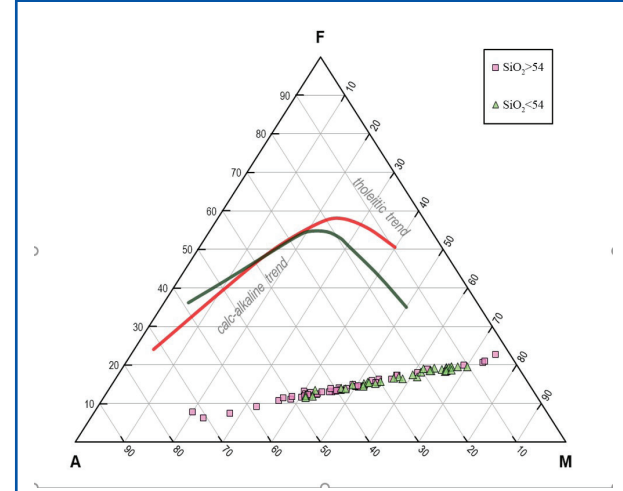


Fig. 2. Position of the analyzed rocks in the AFM diagram [6]

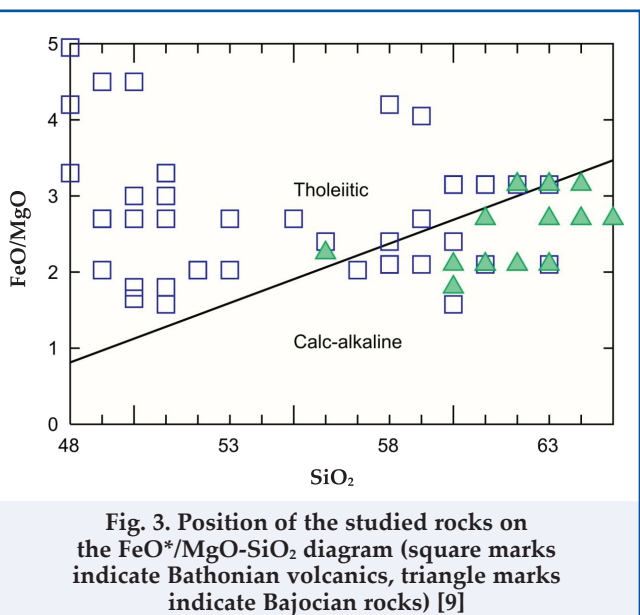


Fig. 3. Position of the studied rocks on the FeO^*/MgO - SiO_2 diagram (square marks indicate Bathonian volcanics, triangle marks indicate Bajocian rocks) [9]

the ore field indicates that the ore-forming processes were not formed by a post-collisional or intracontinental regime, but by an extensional type, plate crust thinning, and transformation into mature island arc conditions.

As a result of the above, it can be noted that the petrochemical characteristics of the analyzed samples indicate mature island arc conditions in the Lesser Caucasus metallogenic province, Lok-Karabakh structural formation zone [1, 7]. The occurrence of hydrothermal alteration in the silicate analysis samples taken within the Chovdar ore field created the possibility that silicate analysis may show inaccurate results in some cases, which created the need for the analysis of elements that are more resistant to hydrothermal alteration processes. The analysis of rare earth elements and other minor elements that are resistant to low-temperature hydrothermal alteration processes, the analysis of

the obtained results should provide reasonable results to determine the correctness of the interpretation of the results of silicate analyses, as well as to give an idea of the conditions of formation and geodynamic regime of the ore field. For this reason, when collecting the samples to be analyzed, both partially altered and as far as possible metasomatic alteration-free rock types were used, as in the silicate analyses. As a result, 22 different elements, including Nb and Ta, were analyzed in 36 different samples (table 2).

Volcanic rocks as can be seen from the N-MORB (normalized to MORB) Spider diagram (fig. 4), the rhyolite-bearing rocks of the Chovdar ore field reflect the characteristics of typical felsic-bearing volcanic rocks associated with subduction. The above idea can be proven by the following statements [2, 13]:

1. High content of lithophile elements with high ionic radius, such as Rb, Ba, Th, U, and Cs in the rocks;
2. Partial enrichment in rare earth elements, especially La and Ce;
3. Negative trends in the relative Nb and Ta anomalies, with a milder trend in Sr and Ti, as well as intraplate conditions indicated by Zr-Hf-Y values.

These features reflect intraplate volcanic arc conditions, where magma rising to the surface has been partially melted or metamorphosed with the participation of the lower part of the crust, and has been mixed with volatiles released from the subducting slab. In the diagram prepared based on Nb and Ta, which are considered to high field strength elements to external processes (HFSE), the anomaly areas of these elements (fig. 4) are involved as a diagnostic factor for subduction zones, since they indicate the presence of Ti phases within the metamorphism process due to the influence of rutile-bearing eclogite remnants or slabs within the mantle [11].

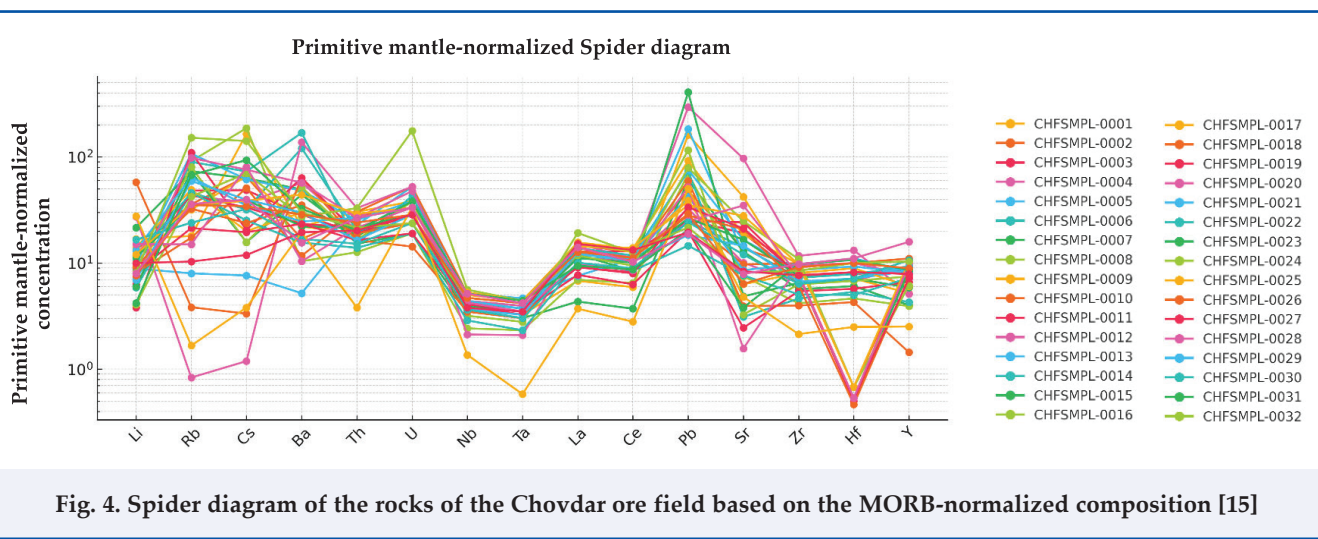


Fig. 4. Spider diagram of the rocks of the Chovdar ore field based on the MORB-normalized composition [15]

Table 2

Results of analyses of rare earth elements and other minor elements conducted at the Chovdar ore field

Samples	Li	Rb	Cs	Sr	Ba	Cr	Co	Ni	V	Sc	Cu	Zn	Pb	La	Ce	Y	Zr	Ta	Hf	Nb	Th	U
CHFSMPL-0001	25.3	10.8	3.5	277.0	170.0	2.0	15.3	3.2	135.0	22.2	72.7	62.0	29.9	4.4	9.9	13.0	63.0	0.1	2.0	2.5	1.5	0.5
CHFSMPL-0002	20.0	21.5	1.4	90.6	130.0	13.0	2.3	2.0	23.0	11.9	2.6	28.0	8.8	8.4	18.9	27.6	91.2	0.2	2.8	3.1	2.2	0.7
CHFSMPL-0003	9.4	28.9	1.0	126.5	220.0	3.0	5.5	1.0	34.0	15.6	15.9	77.0	4.7	5.9	13.7	21.4	74.6	0.2	2.2	2.7	1.5	0.6
CHFSMPL-0004	18.2	25.9	0.8	66.4	440.0	16.0	7.0	7.2	24.0	13.0	5.5	64.0	6.0	9.1	18.8	23.3	65.2	0.1	1.9	2.5	1.6	0.5
CHFSMPL-0005	13.3	4.8	0.2	81.2	40.0	10.0	1.8	1.5	12.0	11.3	2.5	14.0	33.9	7.1	18.6	21.0	65.1	0.2	2.0	2.9	1.8	1.1
CHFSMPL-0006	8.8	27.7	0.7	92.8	930.0	9.0	4.6	1.3	27.0	14.5	8.3	71.0	4.6	7.8	17.9	23.3	72.7	0.2	2.2	2.6	1.6	0.5
CHFSMPL-0007	9.0	44.0	1.3	84.6	380.0	8.0	1.3	3.0	20.0	12.9	6.9	8.0	11.1	2.8	6.2	10.0	56.5	0.1	1.7	2.3	1.2	0.4
CHFSMPL-0008	10.4	54.7	3.9	49.6	80.0	24.0	0.8	1.5	9.0	10.3	3.8	4.0	12.8	4.5	10.9	9.8	41.7	0.1	1.3	1.6	1.0	0.4
CHFSMPL-0009	15.6	19.1	1.4	122.0	170.0	29.0	2.4	3.0	11.0	11.3	7.0	43.0	17.0	10.1	22.8	22.5	97.7	0.2	0.2	3.3	2.4	0.8
CHFSMPL-0010	12.1	10.4	1.1	64.1	90.0	11.0	3.9	1.5	18.0	10.4	10.7	36.0	4.7	9.5	21.3	23.7	99.7	0.2	0.2	3.4	2.4	1.1
CHFSMPL-0011	17.7	26.1	0.7	160.0	180.0	9.0	4.5	1.2	30.0	15.0	41.5	68.0	4.6	8.3	21.6	22.5	75.5	0.1	0.1	2.6	1.7	0.6
CHFSMPL-0012	40.9	0.5	0.0	638.0	170	14.0	0.8	1.8	66.0	10.1	29.6	1.0	54.6	9.9	18.2	12.8	117.0	0.1	3.7	1.4	2.6	1.1
CHFSMPL-0013	14.7	64.4	1.3	56.5	370.0	24.0	9.2	12.4	51.0	15.0	33.3	77.0	7.8	4.9	18.4	20.6	97.9	0.2	3.1	3.4	2.0	0.8
CHFSMPL-0014	13.0	53.9	1.5	20.5	360	3.0	2.5	1.5	22.0	12.0	173.0	553.0	13.6	8.9	19.8	10.7	46.2	0.2	1.5	2.8	1.2	0.9
CHFSMPL-0015	32.3	43.5	0.3	32.0	340.0	7.0	6.0	3.3	42.0	13.1	23.0	428.0	75.4	7.8	14.1	14.7	64.9	0.1	2.0	2.4	1.4	0.8
CHFSMPL-0016	11.3	48.3	0.3	21.6	400.0	4.0	9.0	1.8	52.0	15.8	20.8	323.0	21.5	12.4	21.0	18.7	62.9	0.1	1.9	2.1	1.3	0.8
CHFSMPL-0017	21.1	29.4	0.4	41.7	230.0	7.0	5.3	2.6	38.0	14.7	13.7	140.0	7.2	9.9	21.2	15.1	80.5	0.2	2.5	2.8	1.7	0.6
CHFSMPL-0018	87.0	2.3	0.1	26.0	490.0	15.0	0.2	0.2	22.0	5.7	4.6	3.0	11.0	8.1	18.1	3.6	39.7	0.1	1.2	2.3	1.3	0.3
CHFSMPL-0019	5.7	66.1	0.4	16.2	490.0	8.0	5.9	0.9	22.0	13.9	12.9	36.0	3.7	5.0	10.6	16.6	54.2	0.2	1.6	2.7	1.5	0.6
CHFSMPL-0020	10.9	58.8	1.6	10.3	440.0	8.0	4.0	1.2	24.0	16.2	26.0	428.0	9.6	7.3	17.2	19.1	94.6	0.2	2.8	2.9	2.1	1.0
CHFSMPL-0021	19.8	38.6	0.7	109.0	190.0	22.0	4.6	1.5	30.0	12.2	15.5	94.0	14.0	7.7	18.6	20.2	85.9	0.2	2.6	2.9	2.1	0.7
CHFSMPL-0022	27.6	0.5	50.5	120.0	25.0	6.7	1.4	24.0	11.6	5.9	92.0	2.7	6.5	14.2	18.1	50.6	0.1	1.4	1.9	1.1	0.4	
CHFSMPL-0023	17.1	21.0	0.8	109.5	170.0	29.0	3.8	2.8	13.0	9.8	12.9	44.0	4.9	7.2	16.9	21.2	75.7	0.2	0.2	2.6	1.7	0.6
CHFSMPL-0024	6.1	25.4	1.5	163.5	210.0	32.0	1.1	1.2	53.0	10.1	17.2	15.0	14.6	7.6	15.8	15.4	109.0	0.2	0.2	3.7	2.6	3.7
CHFSMPL-0025	18.1	21.1	0.8	184.0	340.0	6.0	6.4	3.7	33.0	17.7	8.1	94.0	6.5	9.2	23.3	26.0	97.6	0.2	0.2	3.5	2.3	0.7
CHFSMPL-0026	13.8	19.5	0.5	137.5	270.0	26.0	2.3	1.9	11.0	9.6	12.4	51.0	5.2	8.4	18.8	18.3	62.0	0.1	0.1	2.3	1.5	0.5
CHFSMPL-0027	12.4	12.8	0.4	140.0	180.0	18.0	2.4	0.8	24.0	12.8	6.9	60.0	6.2	5.9	13.4	17.9	78.3	0.2	0.2	2.7	1.3	0.4
CHFSMPL-0028	22.6	9.0	1.7	230.0	80.0	11.0	5.4	0.9	40.0	16.4	5.8	85.0	4.6	6.3	14.3	24.6	76.0	0.2	0.2	2.8	1.7	0.7
CHFSMPL-0029	10.4	35.6	0.8	95.9	230.0	4.0	5.1	0.7	31.0	12.7	10.3	66.0	3.4	8.1	17.3	23.2	66.9	0.1	2.0	2.4	1.3	0.6
CHFSMPL-0030	24.9	14.4	0.7	79.2	130.0	7.0	5.6	0.7	33.0	12.6	7.8	55.0	4.5	6.5	15.0	26.6	63.7	0.1	2.0	2.4	1.2	0.5
CHFSMPL-0031	6.3	40.5	2.0	25.1	250.0	8.0	1.9	0.2	16.0	9.8	10.8	89.0	3.8	6.1	14.6	21.5	97.6	0.2	3.0	3.4	1.6	0.8
CHFSMPL-0032	12.2	91.0	3.0	53.7	230.0	3.0	5.4	0.7	34.0	16.9	15.7	63.0	4.0	9.8	21.8	25.9	84.5	0.2	2.8	3.1	1.7	0.5
CHFSMPL-0033	41.6	1.0	31.6	150.0	25.0	1.4	3.3	320.0	24.6	48.9	4.0	9.3	2.4	4.7	6.3	21.4	0.0	0.7	0.9	0.3	0.7	
CHFSMPL-0034	11.4	21.1	0.7	41.9	220.0	10.0	1.9	0.4	12.0	9.2	2.0	45.0	5.4	8.2	18.7	22.3	91.5	0.2	2.8	3.1	1.9	0.6
CHFSMPL-0035	15.0	6.2	0.3	55.2	150.0	13.0	4.4	1.2	14.0	8.5	4.8	88.0	3.6	9.8	22.2	19.7	76.8	0.2	2.3	2.5	1.6	0.6
CHFSMPL-0036	12.0	21.6	0.8	52.0	120.0	20.0	1.3	2.4	20.0	9.8	7.9	30.0	3.5	9.1	17.2	39.6	97.8	0.2	3.1	3.4	2.1	0.7

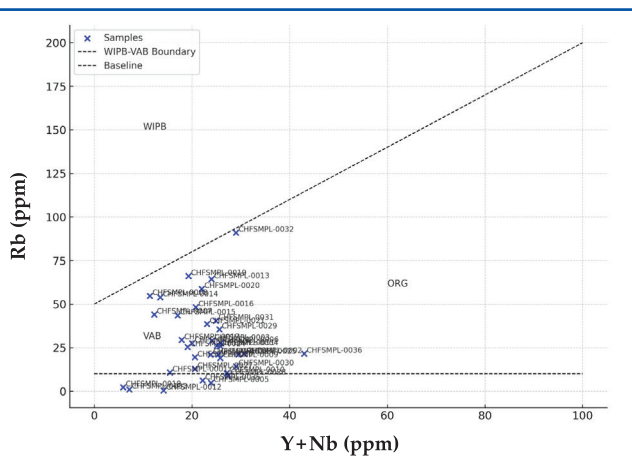


Fig. 5. Tectonic discrimination diagram (Pearce et al., 1984) of the rocks of the Chovdar ore field: WIPB – Intraplate basalts; VAB – Volcanic arc basalts; ORG – Oceanic ridge granites [12]

The sharp decrease in the Sr content in some samples reflects the formation of plagioclase fractionation in the magma ascending to the surface, as well as the relative stability of rare earth elements in terms of quantity in the low-to-medium pressure fractionation regime [16, 17].

In general, the interpretation of the Spider [15] diagram shows that the studied samples were formed from magma formed under subduction conditions, enriched with volatile-transported elements, and formed under conditions that underwent a significant period of crustal development, which, as mentioned earlier, is

consistent with the formation of the Lesser Caucasus metallogenic province, Lok-Karabakh structural formation zone under the conditions of island arc volcanism.

The tectonic discrimination diagram allows us to form an opinion about the origin based on the amounts of Rb/Y+Nb elements (fig. 5). Thus, the relative change of Rb as a highly incompatible element in the direction of increasing the amount of Y+Nb indicates the presence of crustal melting during the development of the magma.

The studied rocks are considered to be depleted in Hf, Nb elements, and enriched in Rb, Ba, Pb, U, Th, and Y elements, which can be considered characteristic of island arc volcanism. Nb here, as an accessory element in the composition of the magma, indicates the tectonic formation environment and the origin of the magma. The low amount of Y+Nb elements may indicate the formation of the magma in arc conditions, and the low amount of Nb may indicate subduction-related infiltration or partial accumulation, as well as differentiation processes.

As can be seen from the results and the diagram, it is possible to say that the analysis results are in the cluster of volcanic arc basalts (VAB) and oceanic ridge granites (ORG), as well as some of them are located close to the trend line separating intraplate basalts (WIPB), which indicates that they were formed in the regime of island arc tectonic structure reflecting intraplate island arc characteristics, and some of them are located below the lower limit of Rb ($Rb=10$ ppm) indicating that they were formed in conditions suitable for mid-ocean ridge basalts (MORB) or intrabasin volcanic arcs [11].

Conclusions

- Conclusions**

 1. The analyzed rocks from the Chovdar ore field exhibit a broad compositional range from basalt to rhyolite, with SiO_2 contents varying between 42.5 and 78.9 %. The TAS diagram indicates a subalkaline affinity for most samples, with a predominance of calc-alkaline rocks, particularly in the upper stratigraphic levels. AFM and FeO^*/MgO - SiO_2 plots confirm that the volcanic series follows a typical island arc calc-alkaline trend, evolving through fractional crystallization and limited crustal contamination.
 2. Trace element analyses reveal enrichments in large ion lithophile elements (LILEs) such as Rb, Ba, and Pb, and depletions in high field strength elements (HFSEs) such as Nb, Ta, and Ti – patterns consistent with subduction zone magmatism. The presence of negative Nb and Ta anomalies, along with La-Ce enrichment and subdued Sr and Ti values, suggests derivation from a metasomatized mantle source influenced by slab-derived fluids. MORB-normalized spider diagrams show typical arc signatures, and tectonic discrimination diagrams place most samples within the volcanic arc basalt (VAB) and oceanic ridge granite (ORG) fields, supporting a mature island arc setting.
 3. Geochemical differences between the Lower and Upper Bajocian units reveal a transition from early tholeiitic to later calc-alkaline magmatism, indicative of changing mantle source characteristics and increasing crustal interaction. The coexistence of low-K basaltic and high-silica dacitic-rhyolitic rocks implies polyphase magmatism and mantle-crust mixing. Overall, the results point to an island arc regime with active subduction, mantle wedge metasomatism, and multi-stage magmatic evolution contributing to the mineralization and alteration processes within the Chovdar ore field.

References

1. Adamia, Sh., Sosson, M., Stephenson, R. (2010). Tectonic evolution of the Eastern Black Sea and Lesser Caucasus regions. *Geological Society, London, Special Publications*, 340, 261–280.
2. Adamia, Sh., Zakariadze, G., Chkhhotua, T., et al. (2011). Geology of Caucasus: A review. *Turkish Journal of Earth Sciences*, 20, 489–544.
3. Gill, J. B. (1981). Orogenic andesites and plate tectonics. *Springer-Verlag*.
4. Imamverdiev, N. A., Salmanly, R. M., Musaev, Sh. D., et al. (2015). Middle Jurassic island arc volcanism and related gold mineralization, Chovdar area (Lesser Caucasus, Azerbaijan). *Otechestvennaya Geologiya*, 2, 43–57.
5. Imamverdiyev, N. A., Jafarov, S. H. (2025). Geodynamic evolution of the Lesser Caucasus as a metallogenetic province. *Scientific Petroleum*, 1, 2–9.
6. Irvine, T. N., Baragar, W. R. A. (1971). A guide to the chemical classification of the common volcanic rocks. *Canadian Journal of Earth Sciences*, 8, 525–548.
7. Keskin, M. (2003). Magma generation by slab steepening and breakoff beneath a subduction–accretion complex: A model for collision-related volcanism in Eastern Anatolia, Turkey. *Geological Society, London, Special Publications*, 219(1), 363–366.
8. Koryakin, Yu. V. (1989). Geodynamics of the formation of volcanic complexes of the Lesser Caucasus. *Moskva: Nauka*.
9. Le Bas, M. J., Le Maitre, R. W., Streckeisen, A., et al. (1986). A chemical classification of volcanic rocks based on the total alkali–silica (TAS) diagram. *Journal of Petrology*, 27, 745–750.
10. Musayev, Sh., Baretti, M., Isayev, E. (2011). Report on the results of geological prospecting works carried out in the Chovdar ore field in 2008–2010. *Unpublished geological report*, 80–87.
11. Pearce, J. A. (1982). Trace element characteristics of lavas from destructive plate boundaries. *Journal of the Geological Society, London*, 139, 531–548.
12. Pearce, J. A., Harris, N. B. W., Tindle, A. G. (1984). Trace element discrimination diagrams for the tectonic interpretation of granitic rocks. *Journal of Petrology*, 25, 956–983.
13. Peccerillo, A., Taylor, S. R. (1976). Geochemistry of Eocene calc-alkaline volcanic rocks from the Kastamonu area, Northern Turkey. *Contributions to Mineralogy and Petrology*, 58, 63–80.
14. Rustamov, M. I. (2016). Geodynamics and magmatism of the Zagros–Caucasian segment in the Phanerozoic. *Palmarium Academic Publishing*.
15. Sun, S. S. (1980). Lead isotopic study of young volcanic rocks from mid-ocean ridges, ocean islands and island arcs. *Philosophical Transactions of the Royal Society of London. Series A*, 297(1431), 411–428.
16. Wilson, M. (1991). Igneous petrogenesis: A global tectonic approach. *Netherlands: Springer*.
17. Wyman, D. A. (1997). Trace element geochemistry of volcanic rocks: Applications for massive sulfide exploration (Short course notes). *Geological Association of Canada*, 12, 79–113.

APPLICATION OF STATISTICAL TECHNIQUES ON STUDY OF SEDIMENTARY ORGANIC MATTER DISTRIBUTION

M. F. Tagiyev, O. V. Rajabli*

«OilGasScientificResearchProject» Institute, SOCAR, Baku, Azerbaijan

ABSTRACT

The amount of organic carbon in sediments within the Ganja petroliferous region has been investigated based on various sources of data. The Ganja region is located at the southwestern-most margin of the Yevlakh-Aghjabedi Basin and occupies the southeastern part of the Lesser Caucasus monocline. The Mesozoic-Cenozoic sedimentary pile has an average thickness of approximately 8 km. The Mesozoic surface dips northeastward to depths of approximately 4-5 km. The region exhibits interformational and intraformational unconformities, along with structural discordances between the Mesozoic, Paleogene-Miocene, and Pliocene stratigraphic complexes. Throughout most of the Ganja region drilling reported predominantly shaly Paleogene-Miocene strata with infrequent sandy-silty and carbonate interlayers. These units are proven to be commercially productive in the Gazanbulag, Ajidara, Naftalan, and Terter fields, where oil accumulations occur within sandy reservoirs of Eocene and Oligocene-Miocene age. Among different age sedimentary units, the Maykop and Eocene formations are distinguished by their relatively higher organic carbon contents. In the study reports of earlier years distribution of the Corg in the Eocene sediments is represented by minimum, mean and maximum values. To maximize the value of these borehole core based analytical evidences we turned to statistical study techniques. Taking into consideration available min-average-max values synthetic random datasets were generated, their conformity to logarithmic theoretical distribution evaluated, and statistical tests performed. Using the nonparametric Kruskal-Wallis test a hypothesis on affiliation of the studied localities to a common geochemical population was examined, and the differences revealed interpreted. The organic-geochemical variability trend was determined, thereby providing the input structure for further basin analysis.

KEYWORDS:

organic carbon in sediments; Eocene; the Ganja petroliferous region; logarithmic distribution; statistical test.

*e-mail: orkhan.rajabli@socar.az

<https://doi.org/10.53404/Sci.Petro.20250200077>

Date submitted: 27.11.2025

Date accepted: 12.12.2025

Introduction

Paleogene sediments in onshore and offshore areas of Azerbaijan are of particular importance as source rocks [1-3]. In different years, the study of organic matter in these sediments has been carried out by several scientific research organizations using various methods. In the second half of the last century source rock studies were based on chemical-bituminological methods [4]. Beginning in the 1990s, geochemical studies started using pyrolysis and other modern laboratory methods, leading to the publication of the first results. [1, 5-7].

In the 1940s and 1950s, petroleum exploration work in the Ganja oil and gas bearing region covered vast areas and detailed geochemical studies were conducted based on core data obtained from wells [4]. The numeric material reported in these studies remains a significant and relevant source for analysis today. Recognizing the importance of these data for

studying Paleogene sediments, and aiming to derive the fullest possible insights, we employed statistical techniques widely used in the Earth sciences.

The Ganja monocline oil and gas bearing region encompasses the southwestern flank of the Yevlakh-Aghjabedi depression extending along the eastern slope of the Lesser Caucasus Mountains. Structural noses and hemisynclines formed in the Mesozoic era and then erosional zones emerged in places in Paleogene have complicated tectonic structure of the region. Stratigraphically the region is composed of the Mesozoic-Quaternary age sediments. In the northwestern part, Cretaceous sediments crop out, while in the southwest and south Jurassic sediments are exposed. Mesozoic sediments have also been studied through drilled wells. The Jurassic sediments were uncovered in wells No. 30 and 31 drilled in the southeastern Beylagan area. The Middle Jurassic is volcanic, while the Upper Jurassic is composed of

terrigenous, volcanic, and carbonate sediments. The Lower Cretaceous sediments consist of terrigenous and volcanoclastic sediments accumulated in shallow marine conditions. The Upper Cretaceous strata are carbonate dominated with effusive-tuffaceous and sandstone sediment input [8].

Paleocene sediments are made of marl and calcareous sandstone layers interbedding with clays. Starting from Paleocene and continuing through Eocene marine transgression intensifies, resulting in increased clastic deposition [9]. The total thickness of the Eocene in the Sovetler area is 820 m; it consists of clayey-marly sediments with limestone, sandstone and siltstone layers. Although thickness of the Upper Eocene is more than 500 m in this area, it is not present in the section northwesterly in the Gazanbulag area. Maykop sediments are up to 2300 m thick in the Middle Kura Depression [10]. Lithologically Ajidara and Gazanbulag sections are characterized by clays that are interbedded with conglomerate and coarse-grained sandstones. In the southeastern Naftalan and Terter areas sandstones become less abundant in the section and towards the Gulluja area they become finer grained. Tarkhan, Chokrak, Karagan and Konk sediments were studied through wells drilled in Borsunlu, Duzdag, Godekboz, Shirvanly, Aghjabedi, Sovetler and Beylagan areas of the region. These sediments have a total thickness of 550 meters. The thickness of Sarmatian sediments rises from 250 m to 800 m from the flank of the basin towards its center. This stratigraphic unit is mostly shaly, with sand and marl interlayers in the lower part [8, 11].

Economically significant hydrocarbon deposits in the Ganja monocline were revealed in Maykop and Eocene sediments in Naftalan, Gazanbulag, Terter and Ajidara areas. Jurassic and Cretaceous sediments considered prospective for oil were studied through exploration wells, but no positive results were obtained [12, 13].

Geochemical studies conducted in the Ganja monocline oil and gas bearing region indicate high organic carbon content in Maykop and Eocene sediments (fig. 1). Within the Eocene itself organic matter percentage is higher in the middle division than in the lower and upper ones [14, 15, 10].

Geochemical studies conducted in the Yevlakh-Aghjabedi depression in later years revealed that TOC (total organic carbon) content of the Meso-Cenozoic sedimentary cover varied from 0.08 to 2.74%. Using pyrolysis data catagenetic maturity of potential source rocks was assessed. It was determined that Eocene sediments in the Sovetler area are in the initial stage of oil formation [5].

Measurements from wells within the Yevlakh-Aghjabedi depression show that formation tempera-

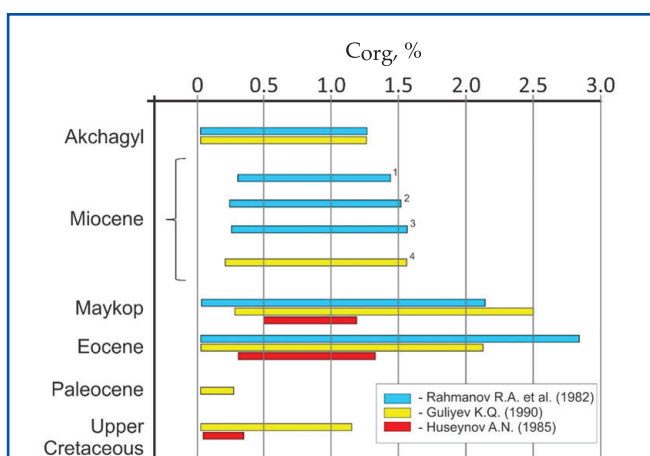


Fig. 1. Range of Corg variation in sediments of different age: 1 – Sarmatian, 2 – Konk-Karagan, 3 – Chokrak, 4 – Middle-Upper Miocene (Sarmatian, Konk-Karagan, Chokrak)

ture increases from the basin center toward its flanks at a given depth horizon. This pattern is attributed to the fact that the ancient Jurassic basement rises closer to the Earth's surface along the margins. However, coeval sediments in the deeper central part of the basin still experience higher thermobaric conditions than those on the flanks [16].

The above analysis indicates that the Eocene sediments of the Ganja monocline oil and gas bearing region contain both reservoir and oil and gas generative layers. Geochemical studies conducted in the last century documented the organic matter content of these sediments, including minimum, maximum and average values, along with sample counts. In conditions of data scarcity this type of values was effectively utilized through statistical methods grounded in theoretical quantitative principles.

Methodological approach

During the data preparation stage, statistical information on the amount of organic carbon expressed as a mass fraction (minimum, average, and maximum values) was used to generate a random data set (an array of statistically random values). To check whether the obtained random data set fits the theoretical logarithmic distribution curve, criteria such as the χ^2 test (Chi-square), df degree of freedom, and p -value are used [17]. The p -value determined by special calculations indicates the probability that the test result obtained was not random. If the p -value is too small, the null hypothesis is rejected. The χ^2 statistic is calculated to test the fit to a theoretical distribution based on the sample mean and standard deviation. Finally, the values obtained were checked against a table that also takes the degrees of freedom into account [18].

The theoretical lognormal curve (red line) provides a close fit to the histograms reflecting the empirical distribution of observations (fig. 2). The results of the corresponding χ^2 test also confirm this correspondence.

To reveal differences between empirical observations various statistical techniques are utilized (ANOVA, Mann-Whitney, Kruskal-Wallis, etc.). The Kruskal-Wallis method is a non-parametric statistical test used to evaluate differences in a parameter of interest between two or more observation sources. Unlike the ANOVA method, this approach does not require the assumption that the studied variable follows a normal distribution. When testing the null hypothesis, the groups are summarized, and the statistical parameter H is calculated based on the number of samples and the sum of the rank orders for each group. This parameter reflects the differences in rank order among the groups. To check the critical value of the parameter H , a table reflecting the critical values of the χ^2 distribution in the case of $df=n-1$ can be used. The fact that the H parameter is greater than the critical χ^2 value indicates that the field observations do not belong to the same population [19].

If there are no ties (two identical observations) in the data, the H parameter can be calculated based on the following formula:

$$H = \frac{12}{N(N+1)} \sum_{i=1}^C \frac{R_i^2}{n_i} - 3(N+1)$$

where C = the number of samples; n_i = the number of observations in the i -th sample; $N = \sum n_i$ the number of observations in all samples combined, R_i = the sum of the ranks in the i -th sample.

If there are ties, the calculation is based on the following formula:

$$H = \frac{\frac{12}{N(N+1)} \sum_{i=1}^C \frac{R_i^2}{n_i} - 3(N+1)}{1 - \sum T / (N^3 - N)}$$

where t = the number of tied observations in the group; $T = \sum (t^3 - t)$, the summation is over all groups of ties.

According to these formulas, a high H value means rejection of the null hypothesis [20].

The results of the Kruskal-Wallis test indicate that samples from different localities do not belong to the same population, and the median values differ sharply from each other. When all areas were tested simultaneously, the H value was high, and the p -value was close to zero. This result indicates a significant difference between the sites in terms of their observed organic carbon values. Then, samples (sites) were taken pairwise and tested. In this case as well, differences were observed in the statistical indicators, and the results rejected the null hypothesis (i.e., the hypothesis of a common source/origin).

Discussion and interpretation

Based on the results of the non-parametric statistical test, it was found that the distribution of Corg in the Yevlakh-Aghjabedi depression is spatially variable (fig. 3). This variation in the parameter can be attributed to the fact that organic richness of geochemical facies increases to southeast.

In the natural sciences, the results of observations often depend on the information we obtain from random experiments. In the observations, the geochemical parameter exhibits not only anomalously low values but also occasionally anomalously high values. The Beylagan and Mil sample sets, differing in peak values as illustrated in figure 3, provide another example of this. The Beylagan and Mil sites, represented solely by their minimum, average, and maximum values, were calculated from 2 samples and 39 samples, respectively. One of the key aspects of this analysis is the ability to compare the Beylagan area, represented by a small sample, with the Mil site, which has many observations, using a statistical «reconstruction» method. As a result, it was determined that they possess different geochemical characteristics [18].

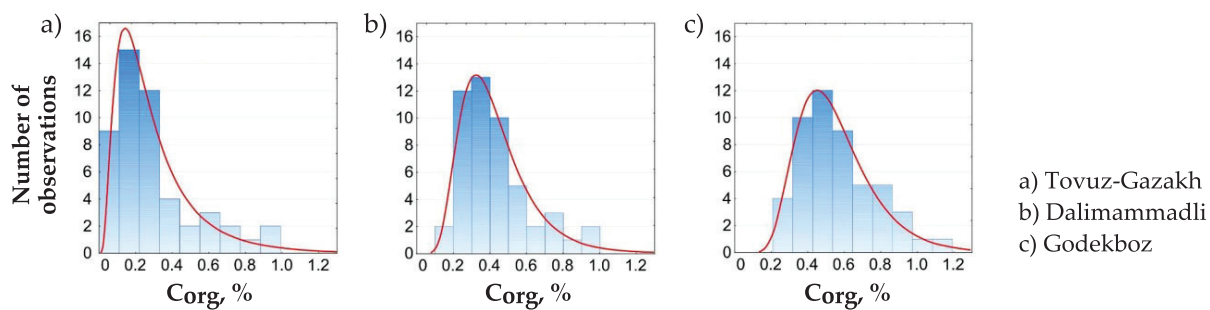


Fig. 2. Histograms showing distribution of random values for the areas

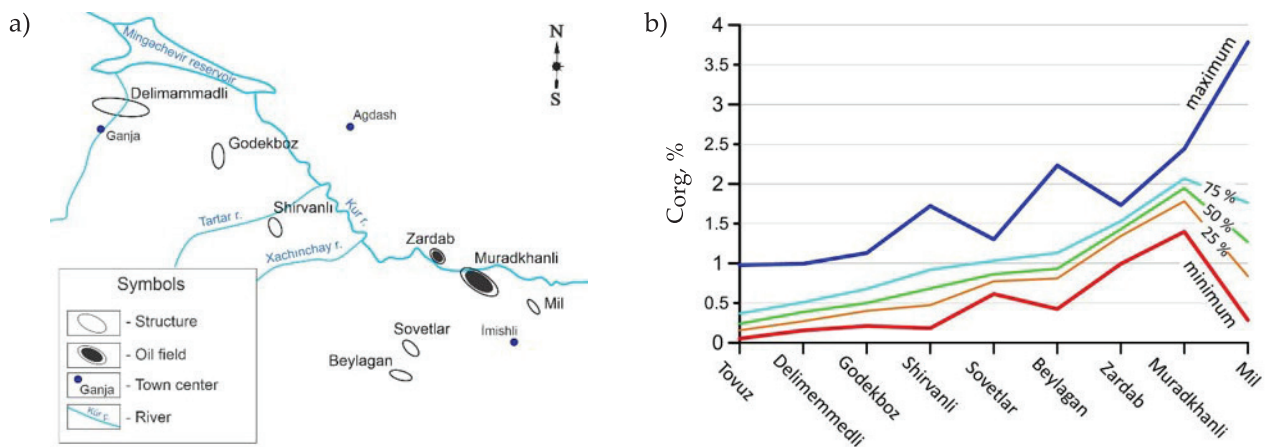


Fig. 3. Reconstruction of the statistical distribution of the organic matter: a) location scheme of the observation points, b) diagrammatic representation of minimum, quartile and maximum values

Conclusions

- Using the min-average-max data of organic carbon, a theoretical logarithmic normal distribution was reconstructed, and a data set was prepared for hypothesis testing.
- The Corg data from the different observation sites were analyzed using the non-parametric Kruskal-Wallis test for a common source, and significant differences were observed.
- The regional variation in Corg content can also be considered as evidence of differing depositional characteristics of the ancient Eocene basin along its various directions.

References

1. Abrams, M. A., Narimanov, A. A. (1997). Geochemical evaluation of hydrocarbons and their potential sources in the western South Caspian depression, Republic of Azerbaijan. *Marine and Petroleum Geology*, 14(4), 451–468.
2. Guliyev, I. S., Tagiyev, M. F., & Feyzullaev, A. A. (2001). Geochemical characteristics of OM of the Maikop deposits of Eastern Azerbaijan. *Lithology and Mineral Resources*, 3, 324–329.
3. Feyzullayev, A. A., Tagiyev, M. F., Lerche, I. (2015). On the origin of hydrocarbons in the main Lower Pliocene reservoirs of the South Caspian Basin, Azerbaijan. *Energy, Exploration & Exploitation*, 33(1), 1–14.
4. Ali-zade, A. A., Akhmedov, G. A., Aliyev, G.-M., et al. (1975). Assessment of oil and gas producing properties of Mesozoic-Cenozoic deposits of Azerbaijan. *Baku: Elm*.
5. Klosterman, M. J., Abrams, M. A., Aleskerov, E. A., et al. (1997). Hydrocarbon system of the Evlakh- Agdzhabedi depression. *Azərbaycan Geoloqu elmi bülleteni*, 1, 90–120.
6. Katz, K. J., Richards, D., Long, D., Lawrence, W. (2000). A new look at the components of the petroleum system of the South Caspian Basin. *Journal of Petroleum Science and Engineering*, 28, 161–182.
7. Feyzullayev, A. A., Guliyev, I. S., Tagiyev, M. F. (2001). Source potential of the Mesozoic-Cenozoic rocks in the South Caspian Basin and their role in forming the oil accumulations in the Lower Pliocene reservoirs. *Petroleum Geoscience*, 7(4), 409–417.
8. Guseynov, A. N., Akhmedov, A. M., Kocharli, Sh. S., et al. (1977). Review information: Oil and gas potential of the Middle Kura depression and prospects for further exploration work. *Baku: AzNIINTI*.
9. Mamedov, A. V. (1977). History of geological development and paleogeography of the Middle Kura depression in connection with its oil and gas potential. *Baku: Elm*.
10. Guliyev, K. G. (1990). Maykop series of the Middle Kura depression and prospects for oil and gas deposits (Doctoral dissertation). *Baku: IGANA*.

11. Salayev, S. G., Averbukh, B. M., Mamedov, S. B., et al. (1982). Prospects for oil and gas potential of Paleogene-Miocene deposits of Western Azerbaijan and the direction of further exploration work. In: *Oil and gas potential of Western Azerbaijan*, Baku: Elm.
12. Ismayilov, F. S., Salmanov, A. M., Maharramov, B. I. (2024). Oil-gas fields and prospective structures of Azerbaijan: Lesser Caucasus–Talysh oil and gas province. Baku: MSV MMC Press.
13. Salayev, S. G., Kastrulyin, N. S., Rizayev, N. K., et al. (1988). Conditions of oil and gas formation and accumulation in the Paleogene-Miocene deposits of Azerbaijan. In: *Problems of oil and gas potential of the Caucasus*, Moscow: Nauka.
14. Rakhmanov, R. A., Efendiiev, D. I., Mamedov, S. B., et al. (1982). Geochemical criteria for assessing the oil and gas potential of Paleogene-Miocene deposits of Western Azerbaijan. In: *Oil and gas potential of Western Azerbaijan*, Baku: Elm.
15. Guseynov, A. N. (1985). Features of the geological structure and oil and gas potential of the Yevlakh-Aghjabedi trough (Doctoral dissertation). Moscow: IGIRGI.
16. Nadirov, S. G., Gadzhiev, F. M., Khalilov, et al. (1985). Geothermal characteristics of the Yevlakh-Aghjabedi trough. *Azerbaijan Oil Industry*, 7, 4–9.
17. Wang, S., Gui, W. (2020). Corrected maximum likelihood estimations of the lognormal distribution parameters. *Symmetry*, 12(6), 968.
18. Davis, J. C. (2002). Statistics and data analysis in geology (3rd ed.). New York: John Wiley & Sons.
19. McKnight, P. E., Najab, J. (2010). Kruskal-Wallis test. In: I. B. Weiner & W. E. Craighead (Eds.), *The Corsini Encyclopedia of Psychology* (4th ed., Vol. 2, pp. 903–905), Wiley.
20. Kruskal, W. H., Wallis, W. A. (1952). Use of ranks in one-criterion variance analysis. *Journal of the American Statistical Association*, 47(260), 583–621.

STABILIZATION OF UNSTABLE RESERVOIRS IN OIL FIELDS OF AZERBAIJAN: POTENTIAL AND PROSPECTS OF COPOLYMER-BASED METHODS

F. F. Ahmed^{*1}, A. H. Gayibova¹, M. A. Huseynov²

¹«OilGasScientificResearchProject» Institute, SOCAR, Baku, Azerbaijan

²Scientific Research Institute «Geotechnological Problems of Oil, Gas, and Chemistry»

ABSTRACT

This research focuses on the application of copolymer technologies for stabilizing unstable oil reservoirs, with particular attention to the oil fields in Azerbaijan. Unstable reservoirs, characterized by weakly consolidated sandstone formations, often experience sand production and formation damage, which significantly reduce well productivity and complicate extraction processes. The study explores how copolymers-synthetic polymers composed of two or more different monomers—can be used to enhance the mechanical stability of reservoir rocks by forming flexible, durable films within the porous matrix. These films help to bind loose particles and reduce sand influx while maintaining sufficient permeability for oil flow. A comprehensive SWOT analysis is presented to assess the advantages and limitations of copolymer stabilization in oil reservoirs. Strengths include the polymers' resistance to thermal degradation and chemical attack in harsh reservoir environments, the ability to tailor polymer properties to specific geological conditions, and the potential for increased oil recovery through improved reservoir conformance. However, challenges such as the complexity of polymer formulations, potential injectivity issues, environmental concerns related to polymer degradation products, and higher initial costs are also discussed. Recommendations for pilot-scale testing and gradual field deployment in Azerbaijan's oil sector are outlined, highlighting the need for rigorous laboratory characterization, reservoir simulation, and real-time monitoring to optimize copolymer treatment design. The research concludes that copolymer technologies represent a promising and sustainable approach to mitigating sand production, improving well integrity, and boosting overall oil recovery, thereby contributing to the efficient development of Azerbaijan's hydrocarbon resources.

KEYWORDS:

copolymer technologies; reservoir stabilization; unstable oil reservoirs; enhanced oil recovery; polymer flooding; sand control; Azerbaijan oil fields; gel formation; nanostructured polymers; stimuli-responsive polymers; oil production optimization; reservoir permeability.

*e-mail: fariz.ehmed@socar.az

<https://doi.org/10.53404/Sci.Petro.20250200078>

Date submitted: 14.10.2025

Date accepted: 10.12.2025

Introduction

The problem of unstable reservoirs in Azerbaijan's oil fields represents a significant obstacle to the efficient and safe extraction of hydrocarbons. The stability of reservoir rocks is critical for maintaining pressure within the reservoir and preventing undesirable phenomena such as formation collapse and excessive sand production in wells.

The main causes of reservoir instability are the geological features of Azerbaijan's fields, especially in the Absheron Peninsula and the Caspian Sea, which are characterized by complex geological structures, including fractured and poorly consolidated layers. These features increase the risk of reservoir degradation. Improper production management, including excessive pressure depletion, can lead to the collapse of porous layers and a decline in reservoir permeability. The use of inadequate development methods, such as over-drilling or improper well operation, may cause

mechanical damage to the reservoir.

Reservoir instability ultimately leads to reduced hydrocarbon recovery efficiency, resulting in lower recovery factors and increased production costs. Collapse of the reservoir can cause hydrocarbon blowouts to the surface, posing a threat of environmental pollution.

Inefficient reservoir operation due to unstable formations leads to higher restoration costs and reduced project profitability [1-4].

To address these issues, technologies aimed at strengthening the reservoir must be applied, such as the injection of cement slurries or special chemical compositions to improve rock strength. Innovative modeling and monitoring methods should be used to predict reservoir behavior and take timely stabilization measures. More effective and safer production methods should be developed and implemented, taking into account the geological structure and reservoir conditions.

Solving the problem of unstable reservoirs requires a comprehensive approach that includes geological studies, the use of modern technologies, and advanced production management methods. Only with effective monitoring of reservoir conditions can sustainable and safe development of Azerbaijan's oil industry be ensured.

Theoretical foundations and principles of copolymer application

The use of copolymer technologies is a relevant and promising direction in the oil and gas industry, enabling the effective solution of unstable reservoir problems through physico-chemical impact on rock, enhancing stability and selective regulation of filtration flows. This results in increased productivity, reduced accident risks, and optimized costs, which is especially important under conditions of depleting easily accessible reserves.

Copolymer molecules consist of various monomer units, imparting combined properties to the materials that can be tailored to specific reservoir conditions. In oil production, copolymers are used for wellbore stabilization through the formation of flexible but durable films; for controlling particle migration (anti-flocculation, stabilization of pore structure); for reducing water cut and filtration through the formation of polymer screens; and for resistance to thermal and chemical effects, especially in highly mineralized formation water environments [5–8].

The mechanism of copolymer action in reservoir consolidation (commonly used in oil production) involves enhancing the structural stability of rocks (typically unconsolidated sandstones), stabilizing the formation, and preventing mechanical particle (sand) production along with well fluids. Copolymer solutions are injected into the reservoir and, due to their low viscosity and small molecular size, penetrate the

pore space of the rock. The polymer adsorbs onto the surface of rock grains (e.g., quartz sand), leading to adhesion of the polymer molecules to the mineral surface. After gelation, a thin cementing film forms between grains. Reservoir particles (such as sandstone) are bonded together, creating a solid structure. This reduces sand mobility and prevents it from being carried with production fluids. Thanks to controlled volume and viscosity, the treatment does not clog the pores, maintaining sufficient fluid flow [9–11].

Practical aspects of copolymer application in oil production

Chemical waterflooding method (enhanced oil recovery, EOR): Injection of aqueous copolymer solutions into the reservoir to increase the viscosity of the injected water. Water-soluble copolymers are used, such as copolymers of acrylamide with acrylic acid or their salts.

SWOT analysis of copolymer technologies for stabilizing unstable reservoirs

1. Strengths

- High selectivity and targeting capabilities. Copolymers enable selective treatment of problematic zones without affecting stable formations;
- Resistance to harsh conditions. Copolymer systems demonstrate excellent chemical and thermal stability, essential for high-temperature and highly mineralized reservoir environments;
- Economic efficiency. Reduction in well repair costs, fewer downtimes, and longer reservoir life contribute to long-term cost savings;
- Enhanced oil recovery (EOR). More uniform distribution of injected agents redirects flow into less permeable, oil-bearing zones, improving recovery factor;

Summary table for the classification of copolymer technologies

Table

Type of copolymer	Synthesis method	Main characteristics	Examples of application
Random (statistical)	Radical/Ionic polymerization	Random arrangement of monomers	Paints, plastics
Block	Sequential polymerization	Alternating blocks of monomers	Thermoplastics, adhesives
Gradient	Controlled monomer feed	Gradual variation in composition	Specialized coatings
Hydrogels	Crosslinking of hydrophilic monomers	High water absorption	Biomedicine, agriculture
Emulsion-based	Emulsion radical polymerization	Fine particles dispersed in water	Paints, glues
Micro/Nanoemulsions	Enhanced dispersion	Very fine particle size	Specialized coatings
Solution-based	Polymerization in solution	Used in liquid formulations	Varnishes, coatings

- Operational success stories:
- in Western Siberia, implementation of copolymer technology increased well lifespan by 25%, reduced downtime by 30%, and cut repair costs by 15%;
- at a field in Tatarstan, copolymer-based consolidation reduced water breakthrough, improving oil quality.

2. Weaknesses

- Limited scalability. Technologies may require customization based on geological and reservoir-specific conditions;
- Complex formulation design. Precise calculation of copolymer composition is required depending on pH, temperature, salinity, etc.;
- Need for skilled personnel. Successful implementation demands specialized knowledge, training, and technical expertise;
- High initial investment. Despite long-term savings, initial deployment of copolymer systems can be capital-intensive.

3. Opportunities:

- Expansion to complex and mature fields. Especially relevant for depleted or hard-to-recover reserves;
- Integration with other technologies. Combination with methods like hydraulic fracturing (HF) or waterflooding (WF) can yield synergistic results;
- Development of domestic technologies. Reduces dependency on imports—particularly important under sanctions and trade restrictions;
- Improved production sustainability. Helps extend the operational lifespan of oil fields and ensures more stable production rates.

4. Threats

- Technological risks. Unpredictable behavior of copolymers under real reservoir conditions may hinder performance;
- Environmental concerns. Potential for environmental damage if the technology is improperly applied or monitored. Oil price volatility. Falling global oil prices can reduce the economic feasibility of deploying advanced technologies;
- Logistical and supply chain challenges. Issues with delivery and availability of reagents, especially in remote areas or during trade disruptions.

Research trends:

- -Nanostructuring and architectural control of copolymers. Focus is shifting from simple composition to precise sequence and structure control (e.g., block vs. random copolymers).

In systems like P(NIPAM-co-AM), properties such as LCST/UCST depend on block arrangement and length, affecting swelling behavior, temperature responsiveness, and mechanical performance. Even in «single-stage» microgel syntheses, structures often tend toward block-like arrangements, influencing material behavior.

Prospects and recommendations for Azerbaijan

1. Pilot projects. Start with experimental and field pilot tests at one or two reservoirs characterized by weak consolidation and where problems of sand production and formation instability during expansion are already observed. For these sites, select several types of copolymers, including those containing ATBS or other thermally stable and ion-resistant components.
2. Laboratory studies on core samples. Determine the response of rock types typical for Azerbaijan to various polymeric agents: measurement of viscosity loss in saline/alkaline water, thermal stability (e.g., up to 60–100 °C), the effect of physical loads (flow velocities, pressure gradients), degree of adsorption, and the ability to «bind» grains or reduce sand production.
3. Use of modified gels. In fractured zones or formations with weak cementation, the application of polymer gels—possibly with small fillers (sand grains, fine cement/microcement slurry)—may be beneficial to create a stabilizing «shell».
4. Combinations (copolymer+nanoparticles, surfactant + polymer, gel + polymer, etc.). Examples from Kazakhstan and other countries show that combined formulations can deliver better performance, especially under complex reservoir conditions.
5. Monitoring and control. Methods for monitoring should be planned in advance: how the formation behaves after injection, whether undesirable pore blocking occurs, how permeability changes, the impact on oil and water production, and whether new flow paths appear. Simulation modeling may be required prior to actual field interventions.
6. Development of a regulatory framework and standards. For safe and environmentally responsible application of chemical agents, certification of substances should be carried out and quality standards for copolymers established, ensuring compatibility with local conditions [4, 10, 12, 13-15, 19].

Trends in scientific research

Nanostructuring and control of copolymer architecture. Research is increasingly focused not only on copolymer composition but also on monomer sequence—block, random segments, their length, and alternation. For example, in P(NIPAM-co-AM) systems it has been shown that LCST/UCST depend on block structure and block length. Studies indicate that even in «single-stage» syntheses of microgels, the apparent structure becomes closer to block-like

rather than fully random, which significantly affects swelling behavior, temperature responsiveness, and mechanical properties.

Smart, stimuli-responsive systems. New kinetic models have been developed for CO₂-sensitive copolymers, enabling their use in acid gas-rich reservoirs. These systems respond to changes in temperature, pH, gas composition, and more, making them promising for future downhole applications.

Conclusions

1. The application of copolymer technologies in the oil industry demonstrates significant potential for enhancing reservoir management and well performance. Copolymers effectively contribute to gel formation and thickening of formation fluids, enabling selective blockage of high-permeability channels and improving sweep efficiency by redirecting flow to oil-rich zones. Their use in well treatment processes provides corrosion inhibition, stabilization of solutions, and protection of equipment, ultimately extending well lifetimes.
2. Case studies from Western Siberia and Tatarstan highlight the practical benefits of copolymer technologies, including extended well service life, reduced downtime, decreased repair costs, and improved oil quality through better water control. The SWOT analysis confirms that despite challenges such as high initial costs, complex formulation requirements, and the need for skilled personnel, copolymer applications offer robust strengths and promising opportunities, particularly when integrated with other enhanced oil recovery methods.
3. Emerging research trends focused on nanostructuring and the architectural control of copolymers open new avenues for tailoring material properties to reservoir conditions. Stimuli-responsive systems sensitive to temperature, pH, and CO₂ represent a frontier in smart polymer design, enabling adaptive responses to harsh and variable downhole environments.
4. Overall, copolymer technologies represent a versatile and effective approach to addressing key challenges in oil extraction and reservoir management, with ongoing innovations poised to further increase their efficiency and applicability.

References

1. Seidov, V. M., Khalilova, L. N., Bayramova, I. I. (2024). Reservoir properties of effusive rocks of the Muradkhanli field (Azerbaijan). *Geofizicheskiy Zhurnal* 46(1).
2. Yusubov, N. P., Rajabli, J. B., Quliyeva, U. M. (2020). Sedimentation features of reservoir formation and leakage assessment of the Galmaz underground gas storage. *Geofizicheskiy Zhurnal* 42(6).
3. Ahmadov, T., Namazli, N. (2025). Unveiling sedimentation hiatuses: Key factors in hydrocarbon reservoir formation in Azerbaijan. *Anuário do Instituto de Geociências*.
4. Gurbanov, V. S., Sultanov, L. A., Gulueva, N. I. (2020). Analysis of petrophysical studies of deep-lying oil and gas reservoirs of onshore and offshore fields in Azerbaijan. *Perm Journal of Petroleum and Mining Engineering*, 20(2), 114–124.
5. Ambaliya, M., Bera, A., et al. (2023). Perspective review on the current status and development of polymer flooding in enhanced oil recovery using polymeric nanofluids. *Industrial & Engineering Chemistry Research* 62(4), 204–213.
6. Mirzaie Yegane, M., Boukany, P. E., Zitha, P. (2022). Fundamentals and recent progress in the flow of water-soluble polymers in porous media for enhanced oil recovery. *Energies* 15(22), 8575.

7. Kakati, A., Al-Yaseri, A. (2022). A review on advanced nanoparticle-induced polymer flooding for enhanced oil recovery. *Chemical Engineering Science* 262, 117994.
8. Gbadamosi, A., Patil, S., Kamal, M. S., et al. (2022). Application of polymers for chemical enhanced oil recovery: A review. *Polymers* 14(7), 1433.
9. Li, X., Su, L., Fu, M. (2023). Study on plugging mechanism of gel plugging agent in fractured carbonate oil reservoirs. *Innovative Technologies of Oil and Gas* 59, 507–516.
10. Wang, W., Guo, X., Duan, P. (2023). Investigation of plugging performance and enhanced oil recovery of multi-scale polymer microspheres in low-permeability reservoirs. *Natural Gas Industry* 10(3), 223–232.
11. Zhu, D.-Y., Zhang, J., Zhang, T., et al. (2025). Damage mechanism analysis of polymer gel to petroleum reservoirs and development of new protective methods based on NMR technique. *Petroleum Science* 22(3), 1225–1233.
12. Baig, A. R., Alarifi, S. A., Murtaza, M. (2024). Assessing the viability of different bio polymers and synthetic copolymers with modified enzyme induced carbonate precipitation solutions for sand consolidation applications. *Journal of Petroleum Exploration and Production Technology* 14, 3013–3029.
13. Saghandali, F., Baghban Salehi, M., Hosseinzadehsemanani, R., et al. (2022). A review on chemical sand production control techniques in oil reservoirs. *Energy & Fuels* 36, 5185–5208.
14. Hu, S., Ding, M., Hu, Y. (2023). Optimization of the methods to develop stable polymer gels for water management in medium- and ultra-high-salinity reservoirs. *Gels* 9(7), 540.

ON THE EFFICIENT OPERATION OF SUBMERSIBLE PUMPS WITH LOW LIQUID LEVELS

Sh. P. Kazimov¹, L. G. Hajikarimova², E. S. Abdullayeva^{*2}, E. Sh. Azimova²

¹Azerbaijan State Oil and Industry University, Baku, Azerbaijan

²«OilGasScientificResearchProject» Institute, SOCAR, Baku, Azerbaijan

ABSTRACT

The method of operating wells with rod-type deep well pumps is widely used in the final stage of oil field development. In a group of low-liquid-level wells operated with rod-type submersible pumps, delays occur in the operation of the intake valve and complete filling of the pump cylinder is not achieved. In wells with low liquid levels, since the pump cylinders are not completely filled with liquid, the plunger hits the lower part of the cylinder during the downward movement of the plunger, which causes premature pump failure. On the other hand, in wells with sand formations and low liquid levels, the pump intake is exposed to the active influence of mechanical impurities. A constructive solution has been developed to overcome the above problems. Based on the developed constructive solution, the pump intake valve is opened and closed and the pump cylinder is filled regardless of the dynamic level of the liquid in the well. The problem of the pump cylinder not being completely filled, the plunger hitting the cylinder, and the intensive wear of the pump intake part due to the influence of mechanical mixtures are prevented. As a result of the introduction of the new pump, it is possible to improve the filling of the pump with liquid in wells with low liquid levels. Delays in opening and closing valves are eliminated. The newly developed pump design prevents the pump's intake valves from quickly failing due to mechanical impurities. By eliminating pump idling, the application of the new pump design in wells with low liquid levels results in increased well production. As a result of the introduction of a new pump design, the service life of the pumps is increased and the TAM is increased.

*e-mail: elmira.s.abdullayeva@socar.az

<https://doi.org/10.53404/Sci.Petro.20250200079>

Date submitted: 08.10.2025

Date accepted: 05.12.2025

The oil industry of the Republic of Azerbaijan has entered a new stage of its development. At this stage of development, the main focus was on the development of oil production – the exploitation of rich oil and gas deposits located in the deep parts of the sea on the Caspian Sea shelf.

The full development of the oil industry cannot be achieved without paying due attention to the rational development of old oil fields, whose oil reserves have not been completely exhausted. It should be noted that these oil fields, which have been in operation for a long time, are mainly exploited with low-yield wells. This is mainly explained by the depletion of oil production in the layers due to the long-term inactivity of onshore oil fields. The vast majority of wells operated by mechanical exploitation methods belong to the category of low-production wells. A small part of the total oil produced in the republic is extracted from this fund of wells.

The large number of low-yielding wells and the relatively high cost of the wells that make up this fund

make the exploitation of these wells quite important, and in this regard, their rational exploitation is of great importance from an economic point of view.

As a result of long-term exploitation of oil fields, their reserves decrease and their depletion occurs, and production in the wells exploiting the fields also naturally decreases over time, and as a rule, due to the decrease in exploitation in the wells, they are switched to mechanized exploitation methods. The liquid column in the well exerts hydrostatic pressure on the wellbore:

$$P = \rho \cdot g \cdot h$$

where P is the hydrostatic pressure; ρ – the density of the fluid; g – the acceleration of free fall; h – the height of the liquid column.

For fluid to enter the well from the formation, the formation pressure must be greater than the hydrostatic pressure created by the fluid column in the wellbore. If the formation pressure is initially high and the formation pressure is greater than the pressure

KEYWORDS:

well; pump;
plunger; cylinder;
hydraulic shock;
dynamic liquid level;
mechanical mixtures;
intake valve.

created by the liquid column in the wellbore, then a natural flow occurs from the formation to the wellbore and the well is operated by the fountain method.

If the formation pressure does not provide the flow of oil into the well, then, as can be seen from the formula, it is necessary to either reduce the density of the fluid in the wellbore, or reduce the height of the fluid column. Free fall is an instantaneous constant quantity, it is impossible to change it by influencing it.

The method of operating wells using the gas lift method is based on ensuring the extraction of fluid by changing its density. In this method, compressed gas is injected into the well with the help of pump-compressor pipes. As gas bubbles rise to the wellhead, the density of the liquid column decreases, the hydrostatic pressure created by the liquid decreases, and favorable conditions are created for the natural flow of liquid from the formation to the wellbore.

If reducing the fluid density is not sufficient to ensure oil flow from the formation to the well, then another means of reducing the fluid column is considered. This is achieved by pumping the well. A pump is lowered into the well and the liquid is removed, the liquid level in the well is reduced until oil enters the well bottom from the formation. In the pumping operation method, a certain liquid level is set – the dynamic liquid level, the pump operates below that level. Thus, under appropriate conditions, three main methods of operation are used in the well – fountain, gas lift and pumping.

Among the mechanized exploitation methods, exploitation by deep pumping methods is very widespread in the world and in Azerbaijan. Most of the oil wells located on land in Azerbaijan are exploited by the deep pumping method. In these oil wells, which are mainly located on land, the volume of the product entering the well from the formation is reduced, it is mainly watered, and mechanical mixtures enter the well from the formation together with the liquid. At this stage of exploitation, the wells are exploited in complex conditions. Water formation, sand formation, decrease in formation pressure, and lowering of the liquid level create complications during the process of extracting oil from the wells.

Of the methods of operating wells with submersible pumps, the method of operating wells with submersible pumps with a rod is more widespread. The main advantages of rod-type submersible pumps are their relatively simple installation, the ability to change their parameters in accordance with changes in production, and a fairly high efficiency ratio (EFR). The disadvantages are the requirement for high-precision manufacturing of the plunger-cylinder pair and valves, their susceptibility to wear, high wear on

the pump-compressor pipes and pump rods, and the complexity of their repair.

The pump is lowered into the well via lifting pipelines, a discharge valve is installed above the plunger, and a suction valve is installed at the bottom of the cylinder. The plunger is suspended from the pump rods, and the plunger is moved back and forth by means of a crankcase.

A plunger pump is a positive displacement pump, and the plunger moves up and down with the help of a surface electric motor through a rod belt. In simple terms, a plunger pump consists of a plunger that moves up and down in a cylinder that is machined with special precision. A check valve is also used as a check valve installed on the plunger, which allows the liquid to flow up instead of down. The check valve, which plays the role of a discharge and check valve, consists of a ball and a saddle. The suction valve installed at the bottom of the cylinder also consists of a ball check valve and allows the well product to flow up and prevents it from flowing down.

The topmost, first rod is called the polished rod. It connects the crankcase with the balancer head at the wellhead. The working principle of a rod-type submersible pump is quite simple. As the plunger moves upward from the bottom of the pump, liquid is sucked in through the pump's intake valve, after which the plunger begins to move downward, the suction valve is closed by the pressure of the pumped liquid, and the liquid passing through the discharge valve enters the riser pipes. The rod-type submersible pump continuously works, filling the inside of the riser pipes with the liquid pumped, and finally the liquid is directed to the wellhead.

Depending on the geological and technical characteristics of the well and the composition of the extracted fluid, the operating conditions of pumping equipment during oil production can be conditionally divided into normal and complex types.

In normal wells, standard pumps operate at a high filling factor without special arrangements. In this case, the service life of the pumping equipment is quite long.

In wells of the second complexity category, oil exploitation with standard rod pumps is less efficient due to the low efficiency of the pump and the short period between repairs. The exploitation of wells with complex operating conditions should be divided into the following main groups:

- curved body;
- high viscosity;
- emulsion;
- gas;
- sandy;
- corrosive and low productivity.

Wells that are in the final stage of operation and operated in difficult conditions (water formation, sand formation, etc., corresponding rod-type deep pumping wells) and with low productivity are characterized by incomplete filling of the pump cylinder. There is a group of wells operated with rod-type deep well pumps, in which production is very low, pump cylinders are not filled and idle operation is observed. Due to waterlogging in these wells, oil production is significantly lower than water production. Waterlogging of wells also increases the intensity of sand occurrence. Sand plugs often form in the well, and the underground part of the pumping equipment is exposed to the intense influence of sand and loses its working capacity [1-13]. For this reason, wells of this nature are often repaired, and the operating time between repairs is reduced. Over time, the decrease in oil production and the increase in water production also increase the cost of oil extraction. The issue of increasing the operational efficiency of such wells is of a pressing nature.

The experience of using periodic operation method in such wells with low liquid level is known [14]. That is, the well is shut down for a certain period, and during this time, the liquid is allowed to accumulate at the bottom of the well, creating a certain level. However, there are certain disadvantages to using this method in sandy wells. During the period when the well is stopped, mechanical impurities in the liquid can settle both at the bottom of the well and in the pump compressor pipes. On the other hand, when rod-type deep well pumps start working after a certain interval, the probability of the plunger seizing in the cylinder increases. In this regard, there are limitations in applying the periodic operation method in wells with low fluid levels and sand content. For these cases, it is more appropriate to use the proposed pump design.

Compared to other wells, in low-yield wells with sand manifestations, the fluid extraction rate is lower, so the sand also settles more intensively. Sand entering the well with the fluid from the formation passes through the filter and enters the well bottom together with the fluid. When entering the production pipeline, the fluid flow sharply loses speed. Favorable conditions are created for sand to separate from the fluid flow moving at a low speed from the production pipeline towards the pump-compressor pipes and accumulate at the well bottom. The fluid passing through the intake valve of the deep well pump, inside the plunger, and then through the injection valve, is forced to change its speed several times. The parts through which the fluid passes through the pump nodes and cuts become slots for the sand to settle. The liquid leaving the pump enters the pump-com-

pressor pipes, and here, too, since the diameter of the pump plunger is always smaller than the diameter of the pump-compressor pipes (PCP), in accordance with the laws of hydrodynamics, a slowdown – loss of the velocity of the liquid and the velocities of the mechanical particles inside it occurs, ensuring their separation and sedimentation from the liquid. In almost all wells with sand formations operated with rod-type submersible pumps, sand deposition occurs in this manner.

In oil wells with low production and low liquid levels, the corresponding process occurs more prominently [15-17]. Since the liquid level in these wells is low, the immersion depth under the liquid level is increased in order to increase the pump filling coefficient. In this case, the distance between the pump intake and the filter zone of the well is reduced. That is, the mechanical impurities in the liquid entering the well from the area around the wellbore of the formation enter the wellbore either completely or in large part without the possibility of settling at the wellbore and are subjected to the intensive influence of sand particles in its intake section. As a result, the parts of the pump intake valve wear out in a short time, the hermeticity of the valve and the optimal operation of the downhole equipment are disrupted.

In these wells with low dynamic fluid levels, the main problem is the delay in the opening and closing of the intake valve (the ball rising from the saddle surface and seating on the saddle) during the up-down movement of the plunger. Since the immersion depth under the dynamic fluid level in these wells is within the possible limits, the pressure created by the corresponding fluid level is not enough to open the intake valve. In similar conditions, in these wells with low fluid levels, the pump cylinder is not completely filled. Since the cylinder is not completely filled and the suction valve closing process is not performed immediately, it is delayed, which creates conditions for the liquid in the cylinder to flow back into the well. When the appropriate situation arises, when the amount of liquid inside the cylinder is small, when the cylinder is not completely filled, it becomes necessary to create hydraulic shock conditions during the downward movement of the plunger. In the normal case – when the liquid level in the well is high enough, the pump cylinder is completely filled with liquid and during the downward movement of the plunger, the plunger encounters the liquid inside it, not the cylinder. In wells with a low liquid level, however, since the cylinder is not completely filled with liquid, and during the downward movement of the plunger, the volume of intermediate liquid between the plunger and the cylinder is small, the plunger hits the bottom of the cylinder, creating

a shock situation and accelerating the rapid failure of the lower part of the pump. A new pump design has been developed to achieve filling of the rod pump cylinder with well product, to exclude shock situations caused by the downward movement of the rods, to delay the opening and closing processes of the intake valve, and to prevent the wear and tear of its structural elements due to the active action of sand particles inside the product extracted from the well. In these wells with a low liquid level, it is more expedient to use the pump design described below. The essence of the pump design is that its intake part has been structurally modified. In the developed rod-type submersible pump design, unlike standard designs, the liquid enters the cylinder from the sides, not from the bottom. In order for the liquid to enter the cylinder, no additional energy is spent on lifting the ball of the intake valve above the saddle, as in existing pumps. In this pump design, hydraulic resistances are reduced, and conditions are created for the liquid to rotate in order to limit the entry of sand into the pump body with the liquid. In the developed pump design, the intake valve does not open due to the pressure created by the dynamic liquid level during the upward movement of the balancer, as in traditional rod-type submersible pumps. In this pump, the intake valve is constructively connected to the plunger, and during the upward (downward) movement of the balancer, the plunger moves, and the movement of the plunger leads to the upward (downward) movement of the intake valve stem and the opening (closing) of the valve. In the proposed design of a rod-type deep well pump [18], the up-and-down movement of the polished rod, caused by the oscillation of the rocker head, is transmitted to the plunger, which is freely connected to the intake valve groove by means of rods. The movement of the intake valve groove is achieved at the ends of the upward and downward movements of the plunger, which ensures the forced opening of the pump suction valve regardless of the pressure created by the dynamic liquid column in the well. The effect of the liquid column pressure on the opening (closing) of the suction valve, in other words, on the filling of the cylinder with liquid, is eliminated.

In the proposed design of a rod-type deep well pump [18], the up-and-down movement of the polished rod, caused by the oscillation of the rocker head, is transmitted to the plunger, which is freely connected to the intake valve groove by means of rods. The movement of the intake valve groove is achieved at the ends of the upward and downward movements of the plunger, which ensures the forced opening of the pump suction valve regardless of the pressure created by the dynamic liquid column in the well. The effect

of the liquid column pressure on the opening (closing) of the suction valve, in other words, on the filling of the cylinder with liquid, is eliminated.

The rod well pump (fig.) controlled by the movement of the balance head consists of a cylinder 1, a plunger 2 and a hollow suction valve 3. In the lower side of the cylinder 1, there are holes 4 replacing the suction valve and a cap 5 is attached to its lower end. The plunger 2 consists of a discharge valve 6, an annular restrictor 7 and a cap 8 with a hole in the middle. The intake valve consists of a hollow 3 and a hollow rod 9 with a protrusion at the top, rigidly connected to it.

The rod belt 11 is suspended from the suspension of the rocker head of the jacking machine installed at the wellhead. Depending on the movement of the rocker head, the plunger of the pump 2 is moved up and down by the rod belt 11.

At a certain stage of the downward movement of the rods 11, the end of the rod 9 of the bore 3 rests on the limiting ring 7 located below the impact valve 6 and, moving the bore 3 downward, opens the front of the cuts 4 opened on the pump cylinder 1. At a certain stage of the upward movement of the rod belt 11, the impact valve 6 closes and the liquid on the valve enters the NKB, and on the other hand, since the front of the cuts on the intake valve-cylinder is open, the well product enters the pump cylinder 1 from the well. At the end of the upward movement of the rods 11, the end of the rod 9 of the bore 3 of the cylinder 1 rests on the plunger from below (on the cover 8) and the bore 3 of the cylinder is lifted up by the plunger 2, the front of the cuts 4 opened in the cylinder is cut off and the liquid from the well enters the cylinder 2 is prevented.

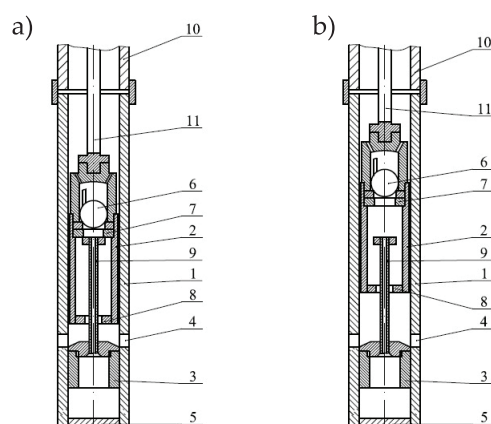


Fig. Pump with intake valve controlled by rod movement: a) end of downward movement of the plunger and upward movement; b) intermediate state during upward movement of the plunger

With the downward movement of the pump rods 11, the plunger valve 6 opens and the liquid enters the upper part of the plunger valve 6 from inside the cylinder. During the upward movement of the rod belt 11, the plunger valve 6 closes and the liquid enters the pump cylinder 1 from the well. When the pump rods 11 move down and up, the pump plunger 2 moves up and down in its cylinder 1 in a similar manner. At a certain stage of the downward movement of the rod belts 11, the intake valve groove 3 is also lowered and raised with it. As a result of the appropriate operation of the pump parts, the liquid enters the pump cylinder from the well in low-level wells.

Since the area of the holes on the cylinder of the developed pump design is 1.5÷2 times larger than the area of the suction valve hole in conventional pumps, the liquid easily enters the suction valve of the pump. At the end of the upward movement of the plunger, the end of the rod of the intake valve groove rests on the plunger cover and moves the groove up, closing the holes opened on the surface of the cylinder and stopping the flow of liquid into the pump cylinder. After the deformation of the rods ends during the downward movement of the rocker head, the plunger begins to move down, and at that moment the plunger valve opens and the liquid passes above the valve. After the deformation of the rods ends due to the up-down movement of the rocker head, the plunger begins to move up-down. During the upward movement of the plunger, the plunger valve is closed, the groove is below the holes on the cylinder, that is, the intake valve is open. During the downward movement of the plunger, the suction valve is closed, and the groove is at a level lower than the holes on the cylinder. Thanks to this constructive change, the pump cylinder is completely filled with liquid due to the forced opening and closing of the pump's intake valve, and since the liquid level in the cylinder is suf-

ficiently high during the downward movement of the plunger, the danger of a hydraulic shock between the plunger and the cylinder is eliminated.

The opening and closing of the pump's suction valve does not depend on the depth of the pump's immersion; the intake valve is forcibly closed and opened by the lifting and pushing of the plunger at the ends of the up-and-down movements.

Since the hole area in the intake valve is large, the liquid, regardless of viscosity, easily enters the suction valve and the space inside the pump cylinder, and the entire volume is completely filled with liquid. As a result, efficient operation of the pump is ensured.

Since the suction valve holes are on the lower side of the cylinder, the sandy-gas liquid changes its flow direction by 900 to enter the pump. Due to the separation mechanism, large-grained sands in the liquid are separated and settle to the bottom of the well. Accordingly, the wear of valves and other parts due to the influence of mechanical mixtures is reduced many times. Since the product changes its flow direction by 900, the associated gases contained in it are separated and collected in the inter-pipe space and come out to the surface of the earth.

When using a used pump in wells with low liquid levels, there is no need to replace surface and underground equipment, and a new pump structure is lowered into the well instead of the existing pump. Thanks to the use of a used pump structure in wells with low liquid levels, compared to mass-produced pumps, it is possible to increase the filling of the pump cylinder, prevent wear and tear of the intake valve parts, eliminate the impact of the plunger on the cylinder, and also increase the service life of the pump and well. It should be noted that since SOCAR has a large number of wells of the relevant category in its operational fund, the used pump struktura is of particular importance.

Conclusion

1. As a result of the introduction of the new pump, it is possible to improve the filling of the pump with liquid in wells with low liquid levels. Delays in opening and closing valves are eliminated.
2. The newly developed pump design prevents the pump's intake valves from quickly failing due to mechanical impurities.
3. By eliminating pump idling, the application of the new pump design in wells with low liquid levels results in increased well production.
4. As a result of the introduction of a new pump design, the service life of the pumps is increased and the TAM is increased.

References

1. Suleimanov, B. A., Abbasov, H. F., Ismayilov, Sh. Z. (2024). A comprehensive review on sand control in oil and gas wells. Part I. Mechanical techniques. *SOCAR Proceedings* 3, 9–23.
2. Safaei, A., Asefi, M., Ahmadi, M., et al. (2023). Chemical treatment for sand production control: A review of materials, methods, and field operations. *Petroleum Science* 20(3), 1640–1658.
3. Deng, F., Huang, B., Li, X., et al. (2022). Review of sand control and sand production in a gas hydrate reservoir. *Energy & Fuels* 36(19), 11712–11723.
4. Asadpour, R., Bataee, M., Moradi, B., Hamdi, Z. (2021). A short review of sand production control. *Journal of Review in Science and Engineering* 2021, JRSE-2107212112377.
5. Matanovic, D., Cikes, M., Moslavac, B. (2012). Sand control in well construction and operation. Berlin: Springer Science & Business Media.
6. Fang, X., Yang, D., Ning, F., et al. (2023). Experimental study on sand production and coupling response of silty hydrate reservoir with different contents of fine clay during depressurization. *Petroleum* 9(1), 72–82.
7. Ahad, N. A., Jami, M., Tyson, S. (2020). A review of experimental studies on sand screen selection for unconsolidated sandstone reservoirs. *Journal of Petroleum Exploration and Production Technology* 10, 1675–1688.
8. Hajikarimova, L. G., Azimova, E. Sh. (2023). An innovative approach to protect sucker rod pumps in sandy wells. *Scientific Petroleum* 1, 51–54.
9. Abdullaeva, E. S. (2023). Development of a foam composition for use in wells with potential risks of sanding. *Scientific Petroleum* 2, 30–34.
10. Khabibullin, M. Ya. (2019). Development of the design of the sucker-rod pump for sandy wells. *IOP Conference Series: Materials Science and Engineering* 560, 012065.
11. Stachowiak, J. (2015). New sucker rod pump technology with integral screen for sandy wells. SPE-173623-MS. In: *The SPE Production and Operations Symposium, Oklahoma City, Oklahoma, USA*, March 2015.
12. VanNatta, J., Logan, P., Stieg, A., et al. (2019). Improved rod-pump run time in sandy wells two stages filtration. SPE-195186-MS. In: *The SPE Oklahoma City Oil and Gas Symposium, Oklahoma City, Oklahoma, USA*, April 2019.
13. Myrzakhmetov, B. A., Nurkas, Zh. B., Toktamissova, S. M., Krupnik, L. A. (2020). Sand valves to protect downhole pumping equipment in the conditions of high sand production. *MIAB Mining Informational and Analytical Bulletin* 12, 125–136.
14. Gabibov, I. A., Aliyev, N. Sh. (2018). Rational exploitation of low-yield oil wells operated by sucker-rod pumps. *International Journal of Innovative Technologies in Economy* 2(14), 28–31.
15. Abdullaev, A. S., Abbasov, N. A., Ibragimova, M. O. (2008). On the methodology for determining the limits of profitability in the operation of low-flow oil wells. *Scientific works of the Institute "Neftgazproekt" SOFAZ* 24, 248–252.
16. Samedov, R. S. (2005). On the methodology for determining the economic efficiency of operating wells with low productivity. *Oil Industry of Azerbaijan* 25, 45–51.
17. Mutallimov, M. M., Mamedova, E. V., Shukyurova, G. D. (2019). Development of effective methods for operating low-yield oil wells. *Proceedings of IAM* 8(2), 167–186.
18. Ismailov, F. S., Kazimov, Sh. P., Hadjikerimova, L. G. (2021). Innovative developments of sucker rod pumps to improve the performance of sand producing wells. *SOCAR Proceedings* 4, 80–87.

SAND RISK IN WEAKLY CONSOLIDATED ROCKS AND THE APPLICATION OF CHEMICAL CONSOLIDATION TECHNOLOGIES: A RESEARCH REVIEW ON GARADAGH AND KALMAS UNDERGROUND GAS STORAGES

S. A. Isayeva

Azerbaijan State Oil and Industry University, Baku, Azerbaijan

ABSTRACT

Ensuring rock stability is of paramount importance for the efficient, safe, and long-term operation of underground gas storages. One of the most critical challenges affecting well integrity in unconsolidated or weakly cemented sandstone formations is sand manifestation, which includes sand production, influx, and migration. Such phenomena compromise the mechanical and technological stability of gas wells, leading to increased operational risks, equipment damage, and significant economic losses. In Azerbaijan, sand-related issues have been particularly observed in the Garadagh and Kalmas underground gas storage facilities, where uncontrolled sand migration poses a substantial threat to operational reliability and reservoir performance. This study presents a comprehensive geotechnical analysis of sand migration under unstable rock conditions, focusing on the mechanisms of sand mobilization and transport within poorly consolidated formations. The limitations of conventional mechanical sand control methods, such as gravel packs, sand screens, and other filtration systems, have been critically evaluated. Despite their widespread use, these techniques often fail to provide long-term stability under challenging subsurface conditions, necessitating alternative solutions. A location-specific, integrated approach has been scientifically substantiated for application in the Garadagh and Kalmas gas storages, combining selective chemical injection techniques with continuous monitoring programs to detect early signs of sand mobilization. The results demonstrate that managing sand risk in unconsolidated formations requires tailored technological strategies that account for reservoir heterogeneity, formation properties, and operational conditions. Chemical consolidation technologies, in particular, show high potential to significantly improve mechanical stability, reduce operational risks, and extend the productive life of gas wells in these storage facilities. In conclusion, this study underscores the importance of combining advanced geotechnical analysis, innovative chemical consolidation methods, and continuous monitoring to ensure safe, reliable, and economically efficient operation of underground gas storages in regions prone to sand-related challenges.

e-mail: sevil.isayeva@asoiu.edu.az

<https://doi.org/10.53404/Sci.Petro.20250200080>

Date submitted: 04.11.2025

Date accepted: 18.12.2025

KEYWORDS:

sand production;
chemical
consolidation;
underground
gas storages;
unconsolidated rocks;
nanotechnology;
MICP (Microbial-
Induced Carbonate
Precipitation);
Garadagh; Kalmas;
polymer systems;
gas well stability.

Introduction

Underground gas storages play a key role in ensuring energy security, balancing seasonal demand, and optimizing gas distribution. From this perspective, the technically safe and efficient operation, as well as the long-term stability of such facilities, is a priority issue. The Garadagh and Kalmas underground gas storages, which play a strategic role in the gas supply system of the Republic of Azerbaijan, are of special importance in this regard. However, one of the engineering and geotechnical challenges encountered during the operation of these facilities is sand manifestation (sand production, sand influx, sand migration) [1].

In unconsolidated formations (e.g., weakly cement-

ed sands, water-saturated sandstones, clay-interbedded layers), the migration of rock particles—primarily sand grains—into the wellbore is observed during operation. This process leads to erosion of the wellbore and equipment, loss of rock stability in the affected zone, flow obstruction, and consequently, adverse effects on the safety and economic efficiency of operations. Sand migration causes not only equipment-level problems but also structural damage in the rock-well interaction zone, directly threatening the operational lifespan and reliability of the storage.

Traditional mechanical sand control methods (e.g., gravel packs, slotted liners, sand screens) can manage this issue to a certain extent, but their effectiveness

depends significantly on formation conditions. High flow rates and pressure differentials in poorly cemented or water-saturated formations often result in the mobilization of sand particles, making these methods insufficient in certain cases.

In recent years, research in this field has focused on the application of chemical consolidation technologies. The aim of these technologies is to inject specific chemical agents—mainly polymer, gel, resin, and nano-particle-based solutions—into the near-wellbore zone to bond the rock particles together, thus preventing sand migration, enhancing the mechanical strength of the rock matrix, and restoring stability. These technologies offer key advantages in maintaining both rock stability and acceptable permeability levels.

However, there are several technical and technological challenges in applying chemical consolidation methods. These include the penetration depth of the injected solution, compatibility with the formation, temperature and pressure resistance, reaction kinetics and aging effects, and the ability to avoid blocking flow channels (selectivity). Therefore, comprehensive laboratory and field tests are necessary to select systems suitable for specific geological conditions.

Simultaneously, researchers and industry specialists are actively exploring new directions such as the use of nanotechnologies, emulsified epoxy systems, polymer-nanoparticle composites, and microbiological consolidation methods (MICP). However, many of these technologies are either in early development or not yet widely applied on an industrial scale.

Given the presence of unconsolidated formations and high-flow zones in storages like Garadagh and Kalmas, testing both modern chemical systems and hybrid approaches (mechanical + chemical) is highly relevant. The aim of this research is to perform a comparative analysis of promising technologies for managing sand manifestation under such formation conditions, evaluate their applicability, and develop practical recommendations.

Methodology

This research is based on a systematic review of the existing scientific literature regarding sand migration problems in unconsolidated rocks and their control methods. The main objective is to comparatively analyze the effectiveness of various technologies applied to manage sand risks in the specific geological and operational conditions of the Garadagh and Kalmas underground gas storages.

The main stages of the research include:

1. Systematic review of scientific literature: Recent studies in the field of sand migration and its mitigation, including mechanical, chemical, and hybrid consolidation methods,

have been reviewed through international journals and conference proceedings (SPE, Elsevier, ScienceDirect). Based on these sources, the advantages, limitations, and areas of application of existing technologies have been examined.

2. Analysis of operational and geological conditions of Garadagh and Kalmas gas storages: The rock structure, temperature and pressure regime, water content, and other engineering parameters of Azerbaijan's key underground gas storages—Garadagh and Kalmas—have been analyzed based on SOCAR's 2020 field reports and monitoring data. These data have been used to assess the compatibility of specific technologies with these reservoirs.
3. Comparative analysis of various consolidation methods: Differences in performance between mechanical (gravel packs, sand screens), chemical (polymer-based, gel, resin, and nanocomposite systems), and hybrid approaches (mechanical + chemical, chemical + microbiological) have been evaluated using laboratory results and field application experience. Special emphasis was placed on the potential of nanomaterials and microbiological consolidation methods.
4. Integration of collected data: Based on the collected and analyzed scientific and practical data, optimal technological approaches for managing sand migration in the Garadagh and Kalmas storages were identified, and their application possibilities and expected outcomes were assessed.

Scientific purpose and hypothesis

The main goal of this study is to comparatively evaluate the effectiveness of modern chemical consolidation technologies in preventing sand migration in unconsolidated formations, taking into account the geological and physical characteristics of the Garadagh and Kalmas underground gas storages. Special attention is focused on identifying optimal solutions through the use of polymer- and nanoparticle-based chemical systems. This approach aims to enhance rock stability and propose more sustainable and effective intervention technologies compared to traditional mechanical methods.

According to the presented hypothesis, the application of polymer and nanoparticle-based chemical consolidation systems can more effectively prevent sand migration in unconsolidated and weakly cemented formations, thereby providing higher rock stability than conventional mechanical methods. Chemical systems create molecular-level bonding within the rock matrix, increasing mechanical strength and limiting

the free movement of sand particles. The small size and high surface area of nanoparticles enable deeper penetration into the formation and more targeted consolidation effects.

This hypothesis is based on the search for ways to improve the efficiency and adaptability of chemical systems under the challenging operational conditions observed in the Garadagh and Kalmas storages, such as high temperature, pressure, and water content. At the same time, the broader implementation of such systems in the field holds significant potential for enhancing the safety of gas production processes and reducing operational costs.

Within the scope of this research, the mechanisms of chemical consolidation technologies, their interaction with the formation, and their compatibility with operational parameters (temperature, pressure, chemical reactivity) are also being evaluated. It should be noted that technical parameters such as the rheological properties of polymer-based systems and the dispersion stabilization methods of nanoparticles are central to this study.

As a result, this work lays the foundation for the development and application of new technological approaches to improve the geotechnical stability of gas storages and aims to provide scientifically grounded and practice-oriented recommendations tailored to local geological conditions.

Approaches to sand risk mitigation

When sand migration occurs in unconsolidated formations (e.g., weakly cemented sands, high-porosity or water-saturated layers), it significantly affects not only equipment but also the rock-well interaction environment. Sand control approaches have mainly evolved in three directions:

- mechanical methods (traditional);
- chemical consolidation methods (modern and innovative);
- hybrid systems (combined approaches).

Mechanical sand control approaches

Traditional sand control methods aim to create a physical barrier in the wellbore to prevent sand particles from entering the flow system. These include:

- Gravel Pack: A layer of coarse-grained sand or gravel is placed around the wellbore to prevent sand collapse under pressure;
- Sand Screens (Slotted Liners, Wire-Wrapped Screens): Perforated pipes or wire-wrapped filters installed inside the well;
- Expandable Sand Screens: Advanced systems designed for higher filtration precision [2, 3].
- While these methods offer certain advantages:
- simplicity of equipment;

- design based on field experience;
- ability to deliver immediate results.

Analysis shows that gravel packs and various filter systems (slotted liners, wire-wrapped screens, etc.) demonstrate limited effectiveness in sand control under specific geological conditions—particularly in complex formations like the Garadagh underground gas storage, where weakly cemented, water-saturated, and high-porosity sandstone formations dominate. Rock weakness, high flow velocities, and pressure differentials significantly limit the effectiveness of such systems.

Chemical consolidation systems

Studies have shown that chemical consolidation systems—especially those using acrylamide and epoxy-based polymer solutions—can deliver more effective results. These systems create strong binding interactions between rock particles, increasing compressive strength up to 3552 kPa, and can selectively reduce rock permeability by 40–60 %. This is considered a major advantage in maintaining wellbore stability without fully blocking fluid flow [4-8].

However, these systems also have technological limitations such as high sensitivity to temperature, difficulty in controlling curing kinetics, rheology issues, and limited penetration depth [9-11]. Therefore, the composition of chemical solutions must be adapted according to the specific geological conditions—mineralogical composition of the rock, water saturation, porosity level, and temperature regime—and must be verified through laboratory and field tests [7, 10-14] (table 1).

In this context, the integration of chemical consolidation with microbiological methods—particularly MICP (Microbial-Induced Carbonate Precipitation)—is considered a novel and promising approach. Through the MICP process, calcium carbonate crystals are precipitated within rock pores as a result of microbial activity, forming additional binding structures between rock grains. This process can create a more stable and durable consolidation effect, especially under moderate temperature conditions (60–80 °C) [2, 15].

This approach—i.e., the combination of chemical and biogenic consolidation methods—is regarded as one of the future development directions of hybrid technologies, aiming both to enhance mechanical strength and to maintain the rock's permeability balance [3].

Chemical consolidation approaches are focused on in-situ stabilization of sand particles in unconsolidated formations to prevent their migration. The main advantage of these methods is their ability to create stabilization directly within the rock matrix [12, 16-19].

Table 1

Characteristics of system types depending on their composition

System Type	Composition	Advantages	Limitations
Polymer-based	Acrylamide, polyacrylate, epoxy	Good penetration, moderate strength	Low thermal stability, sensitive to curing time
Gel systems	Cr(III)-acetate + polymer	Partial elasticity, selective barrier	Excessive gel formation → flow blockage
Resin or furan systems	Furan resin + catalyst	High strength and temperature resistance	Poor penetration ability, toxicity risk
Nanocomposite systems	Nano-silica + polymer	High compressive strength, micropore penetration	Expensive and complex mixing systems
Epoxy-based	Epoxy + hardener	Fast curing, high mechanical strength	Difficult to control curing time

Table 2

Comparison of the effectiveness of various chemical systems for sandstone stabilization

System Type	Composition	Advantages	Limitations
Polymer-based	Acrylamide, polyacrylate, epoxy	Good penetration, moderate strength	Low thermal stability, sensitive to setting time
Gel systems	Cr(III)-acetate + polymer	Partial elasticity, selective barrier formation	Excessive gel formation may block flow
Resin or furan systems	Furan resin + catalyst	High strength and temperature resistance	Poor penetration ability, toxicity risk
Nanocomposite systems	Nano-silica + polymer	High compressive strength, penetration into micropores	Expensive and complex mixing systems
Epoxy-based	Epoxy + hardener	Fast setting, high mechanical strength	Difficult to control curing time

This facilitates comparative analysis of data and enhances the reliability of the research results (table 2).

Microbial-Induced Carbonate Precipitation (MICP) technology facilitates the formation of calcium carbonate precipitates through microbial activity. These precipitates bind the rock grains together, creating a strengthening effect. Advantages:

- environmentally safe;
- high penetration potential.

Limitations:

- slow reaction rate;
- sensitive to temperature and pH changes.

The combination of several technologies yields successful results in high-risk and complex rock conditions. For example: Gravel Pack + Chemical Consolidation + Real-Time Monitoring:

- sand flow is initially reduced by a physical barrier;
- remaining loose particles are stabilized by chemical agents;
- continuous monitoring allows early detection of changes.

Sand control process with hybrid approach:

1. Gravel pack → 2. Chemical injection → 3. Monitoring → 4. Operational adaptation

Selection of chemical systems should be based on local rock conditions. In Garadagh and Kalmas reservoirs:

- medium grain-sized, weakly cemented sandstone;
- high-reactivity clay layers present;
- temperature ranges from 70 to 100°C;
- selective injection methods (diverter-based systems) should be applied only to problematic zones;
- both short- and long-term monitoring programs (sand sensors, fiber-optic systems) must be established.

The lack of experimental data on specific samples from Garadagh and Kalmas fields: The technological and chemical approaches used are mainly based on literature reviews and general laboratory experience. However, the absence of laboratory and field studies conducted on samples fully representing the specific geological and rock characteristics of the Garadagh and Kalmas underground gas reservoirs may limit the applicability of the study

results. This highlights the need for further research to optimize systems under local conditions and to test them in real operational environments.

Incomplete study of the behavior of chemical consolidation fluids under high temperatures: Some zones of underground gas reservoirs may experience temperatures between 70–100 °C or higher. However, existing studies have not extensively tested the long-term thermal stability and reactivity of all chemical systems – especially polymer- and epoxy-based fluids under such high-temperature conditions. This

introduces certain uncertainties in assessing system performance at elevated temperatures.

Early-stage industrial application of microbiological (biogenic) consolidation methods: Although biometods such as Microbial-Induced Carbonate Precipitation (MICP) are environmentally attractive and promising, their industrial-scale application is still limited. Issues such as efficiency, reaction speed, sensitivity to temperature and pH changes, and long-term stability under field conditions require additional research and optimization.

Conclusions

1. Sand production is a critical issue directly affecting rock stability in Garadagh and Kalmas gas reservoirs.
2. Chemical consolidation technologies, especially nanomaterial- and polymer-based systems, can offer effective and long-term solutions for unstable rocks [5, 9, 10, 20-24].
3. The choice and application of chemical agents should be adapted to local geological conditions – for example, temperature, pressure, water content, and rock mineralogical structure.
4. Microorganism-based methods (MICP) may emerge as alternative solutions in the future, but currently, technologies providing rapid and stable results (polymer/nano-based systems) have the advantage [5, 11,12].
5. The best results can be achieved through a composite approach: mechanical + chemical + continuous monitoring.

References

1. Suleimanov, B. A., Abbasov, H. F., Ismailov, Sh. Z. (2024). A comprehensive review on sand control in oil and gas wells. Part I. Mechanical techniques. *SOCAR Proceedings* 3, 9–23.
2. DeJong, J. T., Mortensen, B. M., Martinez, B. C., et al. (2010). Bio-mediated soil improvement. *Ecological Engineering* 36(2), 197–210.
3. Mokogwu, I., Tran, T., Gilmer, T. (2024). A wholistic approach for successful chemical sand consolidation treatments in high sand producing wells. SPE-217913-MS. In: *The SPE International Conference and Exhibition on Formation Damage Control, Lafayette, Louisiana, USA, February 2024*.
4. Nasr-El-Din, H. A., Al-Yami, A. S., Al-Qahtani, M. S. (2006). New epoxy-based system to control sand production. *SPE Drilling & Completion* 21(3), 176–183.
5. Nejati, H., Khamehchi, E., Derakhshan, A. A., et al. (2025). Near-wellbore laboratory simulation system to evaluate chemical sand consolidation with Epoxy/g-C₃N₄-NS nanofluid: an experimental and simulation study. *Journal of Petroleum Exploration and Production Technology* 15, 61–72.
6. Alanqari, K., Al-Yami, A., Wagle, V., et al. (2024). Assessing the viability of different bio-polymers and synthetic-copolymers with modified enzyme-induced carbonate precipitation solutions for sand consolidation applications. *Journal of Petroleum Exploration and Production Technology* 14, 3013–3029.
7. Tingting, W., Bo, S., Wang, L. (2020). A new filler for epoxy resin: study on the properties of graphite carbon nitride (g-C₃N₄) reinforced epoxy resin composites. *Polymers* 12, 76–87.
8. Yuhao, Q., Zhu, G., Zheng, J. (2020). Mechanical and thermal performances of epoxy resin/graphitic carbon nitride composites. *Journal of Applied Polymer Science* 137, 48598–48609.
9. Mao, X., Wang, Y., Zhang, Y., et al. (2021). Comprehensive research in chemical consolidator/stabilizer agents on sand production control. *Journal of Petroleum Science and Engineering* 196, 107733.
10. Mishra, S., Ojha, K. (2016). Nanoparticle induced chemical system for consolidating loosely bound sand formations in oil fields. *Journal of Petroleum Science and Engineering* 147, 15–23.

11. Nejati, H., Khamehchi, E., Derakhshan, A. A., et al. (2023). Synthesis and optimization of a novel epoxy-based nanofluid for sand consolidation in oil wells. *Geoenergy Science and Engineering* 10, 212–217.
12. Dargi, M., Khamehchi, E., Ghallath, F. (2024). Sandstone chemical consolidation and wettability improvement using furan polymer-based nanofluid. *Scientific Reports* 14, 5248–5258.
13. Shuiping, L., Wu, Q., Zhu, H., et al. (2017). Impact resistance enhancement by adding core-shell particle to epoxy resin modified with hyperbranched polymer. *Polymers* 9(12), 684–692.
14. Azadi Tabar, M., Ghazanfari, M. H. (2019). Experimental study of surfapore nanofluid effect on surface free energy of calcite rock. *Modares Mechanical Engineering* 1(3), 709–718.
15. Azadi Tabar, M., Bagherzadeh, H., Shahrabadi, A., et al. (2021). A comprehensive research in chemical consolidator/stabilizer agents on sand production control. *Journal of Petroleum Exploration and Production Technology* 11, 4305–4324.
16. Dargi, M., Khamehchi, E., Ghallath, F. (2024). Sandstone chemical consolidation and wettability improvement using furan polymer-based nanofluid. *Scientific Reports* 14, 5248–5258.
17. Fuxa, J., Di Giampaolo, P., Ferrara, G., et al. (2019). Shaped memory polymer: an innovative approach to sand control open hole completion in thin, multilayered, depleted low permeability gas reservoirs. IPTC-19160-MS. In: *The International Petroleum Technology Conference, Beijing, China, March 2019*.
18. Hadi, A. N., Setiadi, R., Agus, I., et al. (2019). Unlocking potential of Handil shallow oil reservoir by using resin sand consolidation technique. SPE-196250-MS. In: *The SPE/IATMI Asia Pacific Oil & Gas Conference and Exhibition, Bali, Indonesia, October 2019*.
19. Mishra, S., Chauhan, G., Ojha, K. (2024). An experimental study on optimizing parameters for sand consolidation with organic-inorganic silicate solutions. *Petroleum* 10(3), 483–493.
20. Miyagi, M., Nitta, S., Tsuboi, H., et al. (2019). Amide compound, catalyst for polyurethane production, and method for producing polyurethane resin (US11718704B2). *United States Patent and Trademark Office*.
21. Zivar, D., Shad, S., Foroozesh, J., et al. (2019). Experimental study of sand production and permeability enhancement of unconsolidated rocks under different stress conditions. *Journal of Petroleum Engineering* 10, 106–123.
22. Azadi Tabar, M., Ghazanfari, M. H., Dehghan Monfared, A. (2019). On the size-dependent behavior of drop contact angle in wettability alteration of reservoir rocks to preferentially gas wetting using nanofluid. *Journal of Petroleum Science and Engineering* 178, 1143–1154.
23. Azadi Tabar, M., Barzegar, F., Ghazanfari, M. H., Mohammadi, M. (2019). On the applicability range of Cassie–Baxter and Wenzel equation: a numerical study. *Journal of the Brazilian Society of Mechanical Sciences and Engineering* 41(10), 399–412.
24. Azadi Tabar, M., Ghazanfari, M. H., Dehghan Monfared, A. (2019). Compare numerical modeling and improved understanding of dynamic sessile drop contact angle analysis in liquid-solid-gas system. *Journal of Petroleum Science and Engineering* 178, 106552–106562.

ENHANCING OIL RECOVERY IN THE LATE STAGE OF FIELD DEVELOPMENT THROUGH BEHIND-THE-CASING FLOW ISOLATION

F. F. Ahmed^{*1}, S. I. Mansurova², M. A. Rzayeva²

¹«OilGasScientificResearchProject» Institute, SOCAR, Baku, Azerbaijan

²Azerbaijan State Oil and Industry University, Baku, Azerbaijan

ABSTRACT

Mature oil fields in Azerbaijan face significant production decline, high water cut, and operational challenges in late-stage development. A primary factor limiting oil recovery is the uncontrolled influx of water through behind-the-casing flows, often caused by deteriorated cement sheaths, casing defects, or intersecting natural fractures. These flows lead to premature water breakthrough, disrupt injectivity profiles, and reduce waterflooding efficiency, making effective isolation crucial for extending well life and maximizing hydrocarbon recovery. This study investigates the use of expanding cement slurry as an innovative solution for isolating behind-the-casing flows. The slurry is designed to expand volumetrically after setting, forming a tight bond with the casing and surrounding formation. This property allows it to fill micro-annuli, cracks, and channels in degraded cement sheaths, creating a durable hydraulic seal where conventional cement often fails. Laboratory experiments and field applications were conducted to evaluate the slurry under varying downhole conditions, including high water cut, temperature fluctuations, and differential pressures. Results demonstrate that expanding cement significantly reduces water inflow, stabilizes well pressure profiles, and enhances oil recovery efficiency during late-stage waterflooding. Implementation of this technology also decreases the frequency of remedial interventions, reduces operational costs, and improves overall reservoir management by promoting more uniform oil displacement. Practical guidelines for slurry design, deployment, and monitoring are provided, ensuring replicability across similar mature fields. In conclusion, expanding cement slurries represent a reliable and cost-effective method for mitigating water-related production issues, enhancing wellbore integrity, and improving economic recovery factors in late-stage reservoirs. This technology offers a scalable approach for mature field management, with broad implications for maximizing hydrocarbon recovery and sustaining production efficiency in aging oil fields worldwide.

*e-mail: fariz.ehmed@socar.az

<https://doi.org/10.53404/Sci.Petro.20250200081>

Date submitted: 22.10.2025

Date accepted: 10.12.2025

KEYWORDS:

Enhanced oil recovery; late-stage development; behind-the-casing flows; water cut; remedial cementing; expanding cement slurry; well cementing; water inflow isolation; oil fields of Azerbaijan; improved oil recovery factor (ORF).

Introduction

Enhancing oil recovery during the late stage of field development remains one of the key challenges for Azerbaijan's oil industry. Over time, productive formations become depleted, well flow rates decline, and the water cut of production increases, requiring the implementation of new technical solutions to maintain production efficiency. Most of the country's fields are currently in this late stage of exploitation [1-3].

The development of depleted formations is usually accompanied by a range of complicating factors: sand production, paraffin deposits, high water cut, and degradation of the behind-the-casing cement sheath [4-6]. One of the most significant complications that directly affects oil recovery is water ingress into production wells through behind-the-casing flows. These flows not only accelerate water breakthrough but also

reduce the efficiency of oil displacement by injected water, worsen the injectivity profile, and increase water production [7-9].

Timely and high-quality isolation of behind-the-casing flows can reduce the influx of formation and bottom water, thereby improving development efficiency and increasing the oil recovery factor (ORF). In this context, the use of an expanding cement slurry appears particularly promising, as it can effectively seal cracks and micro-channels in the degraded cement sheath due to its volumetric expansion after setting.

The expanding cement slurry not only ensures tight contact with the formation and casing, but also possesses high penetration ability, allowing for broader coverage of the isolation zone. All of this makes it one of the preferred materials for remedial cementing

aimed at improving oil recovery during the late stages of field development.

Based on the analysis of technological and geological conditions, as well as the results of implementing this technology at several fields, its effectiveness is substantiated as one of the key tools for enhancing oil recovery in the late stage of development.

Research methods

To evaluate the effectiveness of the developed expanding cement slurry designed for isolating behind-the-casing flows in late-stage oil field development, a series of laboratory and field tests was conducted. The aim of the research was to assess the rheological, physico-mechanical, and operational properties of the material, as well as to confirm its applicability under actual wellbore conditions [7, 9, 10].

The composition of the slurry included the following components:

- hydrochloric acid (HCl, 5%) – as a solvent and chemical reaction activator;
- class G oil well cement – the main binding component;
- calcium carbonate (CaCO_3) – used as a modifier, up to 15% by weight of dry cement;
- polycarboxylate superplasticizer – 0.3% by cement weight, for regulating fluid loss, flowability, and thickening time [9, 11, 12].

The slurry was thoroughly mixed under laboratory conditions in accordance with API Spec 10A and API RP 10B-2. Temperature, pressure, and conditioning time were carefully controlled to simulate wellbore conditions.

Viscosity and thixotropic properties were measured using a rotational viscometer at temperatures of 25 and 75 °C. The following parameters were evaluated: plastic viscosity; ability for self-compaction in a confined volume [13, 14].

Conducting the research

To simulate the conditions of behind-the-casing flows, an experimental setup was created, including a casing string, artificial fractures, and degraded cement sheath. The developed slurry was injected into the system, and its ability to:

- fill cracks up to 1 mm wide;
- form a dense isolation barrier;
- resist water penetration under pressure, was evaluated. After a 7-day curing period, the system was subjected to renewed water loading [7, 15, 16].

In the laboratory, test samples with varying component concentrations were prepared, and their filtration-mechanical characteristics were determined. The

process of slurry preparation and setting was carried out under conditions close to formation parameters.

To study the onset time of gas release in the expanding cement based on calcium carbonate (CaCO_3) expander at $T = 80^\circ\text{C}$ and $P = 20 \text{ MPa}$, rheological data (plastic viscosity) were analyzed as a function of time. The results of the study are shown in figure 1.

As shown in figure 1, minor changes are observed after 5 minutes; after 10 minutes, a gradual increase is noted; and at 15 minutes, viscosity begins to rise. Between the 17th and 19th minute, a sharp increase occurs – this marks the onset of intense gas evolution. This period is the reaction start point: at 17 minutes, a sudden increase in viscosity is observed (typical for the onset of gas release and the beginning of ettringite crystallization) [10, 11, 17-19].

At 20 minutes, an active phase of gas formation is observed. At 25 minutes, the reaction remains in its active phase. By 30 minutes, stabilization begins.

The onset of gas evolution in the cement system with CSA (calcium sulfoaluminate) at 80°C and 20 MPa occurs approximately at the 16–17th minute after mixing. This indicator can be adjusted depending on the composition of additives (retarders, dispersants) and mixing conditions.

For expanding cement based on a sulfoaluminate expander (CSA), the process of gas release (mainly hydrogen (H_2) or carbon dioxide (CO_2) depending on the chemical composition and present additives) may occur when gas-generating components (e.g., aluminum powder) are used. However, in this case, we are dealing with a swelling-type expanding cement, where the primary mechanism of expansion is ettringite formation, not gas evolution [10, 11, 20-22].

Next, we will analyze the volumetric expansion of the expanding cement. The research data are presented in table.

CSA causes expansion due to the formation of ettringite ($3\text{CaO} \cdot \text{Al}_2\text{O}_3 \cdot 3\text{CaSO}_4 \cdot 32\text{H}_2\text{O}$), whose crystals increase the volume.

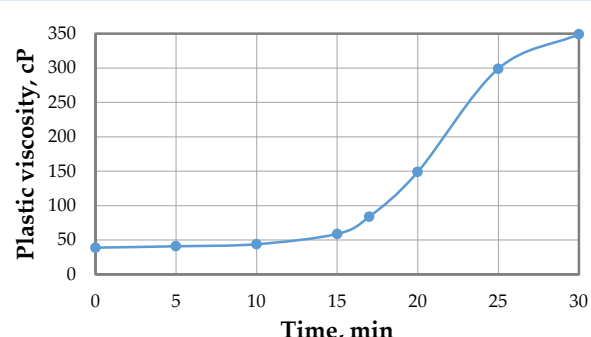


Fig. 1. Dependence of plastic viscosity on time

Table
Volumetric expansion of expanding cement

Cement slurry	Atmospheric expansion (24 hours), %	Autoclave expansion (24 hours), %
Control sample (0% CSA)	0.02%	0.05%
Experimental sample (10% CSA, without CaCO_3)	0.25%	0.45%
Experimental sample (10% CSA + 2% CaCO_3)	0.42%	0.5%

The addition of CaCO_3 can act as a microfiller and a reactive agent (in the presence of Al_2O_3), accelerating the growth of ettringite – therefore increasing the overall expansion. A 2% addition of CaCO_3 enhances the expansion effect due to synergy with CSA.

Next, we evaluate the strength of the cement stone for the base composition: Portland cement + CSA + additives; and a control mixture without CaCO_3 and HCl (likely, HCl is used in another composition for activation or as a reagent).

Samples: cubes $40 \times 40 \times 40$ mm; Curing conditions: 20 °C, humidity >90%; Molding: in forms without vibration (due to high fluidity); Testing: hydraulic press with ± 0.5 MPa accuracy.

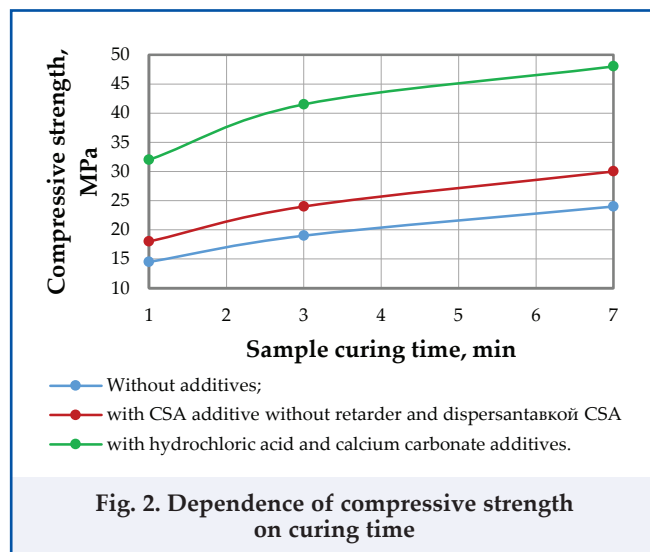


Fig. 2. Dependence of compressive strength on curing time

The compressive strength test data for 1, 3, and 7 days are presented and interpreted in figure 2.

CSA (calcium sulfoaluminate) significantly accelerates setting – 1-day strength is 30–65 % higher compared to ordinary cement.

CaCO_3 acts as a reactive microfiller: it strengthens the structure and promotes the formation of ettringite ($\text{Ca}_6\text{Al}_2(\text{SO}_4)_3(\text{OH})_{12} \cdot 26\text{H}_2\text{O}$).

A small amount of HCl (5%) can serve as an activator, acid-etching cement particles and enhancing the hydration reaction of CSA.

By day 7, all mixtures gain strength, but the difference remains: CSA compositions have 25–50 % higher strength.

CSA cements have rapid early strength, and the additives CaCO_3 and HCl further enhance these properties by accelerating hydration, improving cement stone structure, and increasing matrix density [9, 14, 17].

After curing (1, 3, and 7 days), samples underwent filtration and impermeability tests under excess pressure: water was passed at 3.5 MPa; filtration rate through the cement stone was measured; the cement showed minimal filtration (<0.1 ml/30 min), meeting high isolation standards [13, 16].

One of the key criteria for material suitability is its ability to volumetrically expand after setting. For this, the following tests were conducted: cement stone samples were placed in a water bath at 75 °C for 7 days. Volume change (%) was measured relative to the initial state. Adhesion to metal (casing pipe) and porous (rock formation) surfaces was simultaneously evaluated using a shear method. The average expansion was 1.2–1.5 % of the original volume, providing effective filling of microcracks in the degraded cement sheath.

Cement expansion can seal cracks and channels, preventing water ingress from the behind-the-casing space.

Ion leaching and secondary mineral precipitation can significantly reduce permeability of behind-the-casing cement and improve adhesion between the formation and cement. It is estimated that implementation can reduce water cut by 20–40 % and increase oil production by 15–25 % [9, 10, 14].

Conclusions

- Under the conditions of the late development stage of oil fields in Azerbaijan, the main factor reducing oil recovery is behind-the-casing cross-flows, which lead to intensive water cut in production wells and deterioration of oil production indicators.
- Timely isolation of behind-the-casing cross-flows is an effective means to reduce the volume of incoming water, which allows lowering costs for repair and isolation operations and increasing the oil recovery factor [7-9].

3. The use of expanding cement slurry for isolating water inflows provides a denser filling of cracks and micro-channels in the behind-the-casing cement sheath due to volumetric expansion after setting.
4. The high mobility and penetrating ability of the expanding cement slurry allow increasing the coverage zone and improving the sealing quality, contributing to stabilization of well operation and enhancement of oil recovery.
5. Implementation of this technology in the practice of late-stage field development will improve oil production efficiency, reduce operating costs, and extend the service life of wells [9-11].

References

1. Has, M. M. (2022). Various techniques for enhanced oil recovery: A review. *Iraqi Journal of Oil and Gas Research*, 2(1), 83–97.
2. Ying, Z. (2024). Research on the adjustment strategy and effect evaluation of oilfield in the late stage of water drive with ultra high water cut. In: *E3S Web of Conferences*, EDP Sciences, 554, 01006.
3. Khatib, Z. and Verbeek, P. (2002) Water to Value-Produced Water Management for Sustainable Field Development of Mature and Green Fields. In: *The SPE International Conference on Health, Safety and Environment in Oil and Gas Exploration and Production*, Kuala Lumpur, 20-22 March 2002.
4. Raikulov, S. Z. (2025). Methods for lost circulation control and water shutoff in oil and gas wells. *Journal of Petroleum Engineering*, 10(2), 101–115..
5. Duryagin, V., Nguyen Van, T., Onegov, N. (2023). Investigation of the selectivity of the water shutoff technology. *Energy*, 16(1), 366.
6. Ali, A., Alabdralnabi, M., Ramadan, M. A., Aljawad, M. S., Almohsin, A., Azad, M. (2024). A review of recent developments in nanomaterial agents for water shutoff in hydrocarbon wells. *ACS Omega*, 9, 14728–14746.
7. Kwatia, G., Al Ramadan, M., Salehi, S. (2019). Enhanced cement composition for preventing annular gas migration. In: *ASME 2019 38th International Conference on Ocean, Offshore and Arctic Engineering*.
8. Gu, C., Feng, Y., Li, X. (2023). Cement sheath integrity in oil and gas wells. *IntechOpen*, 1(1), 45–58.
9. Yun, J., Zhao, C., Li, X. (2023). Enhancement of mechanical properties of oil well cement by nano-SiO₂/h-BN. *Journal of Building Engineering*, 76(11), 107115.
10. Zhao, S., Qiu, K., Xu, Z. (2025). High-temperature mechanical and microstructural properties of well cement modified with ethylene-vinyl acetate polymer and polypropylene fibers for geothermal well applications. *Polymers*, 17(12), 1587.
11. Gomado, F. D., Khalifeh, M., Saasen, A. (2025). Effect of calcium expansive additives on the performance of granite based geopolymers for zonal isolation in oil and gas wells. *Journal of Petroleum Engineering Research*, 12(3), 210–225.
12. Baig, A. R., Alarifi, S. A., Murtaza, M. (2024). Assessing the viability of different bio-polymers and synthetic copolymers with modified enzyme-induced carbonate precipitation solutions for sand consolidation applications. *Journal of Petroleum Exploration and Production Technology*, 14, 3013–3029.
13. Velayati, A., Tokhmechi, B., Soltanian, H. (2015). Cement slurry optimization and assessment of additives according to a proposed plan. *Journal of Natural Gas Science and Engineering*, 23, 1–12.
14. Roy, A., Kabra, D., Pareek, G. (2023). A review of nanomaterials and their applications in oil and petroleum industries. *Petroleum Industries*, 5(2), 101–115.
15. Zheng, X., Song, W. (2025). A comprehensive evaluation method for cement slurry systems to enhance zonal isolation: A case study in shale oil well cementing. *Journal of Petroleum Engineering Research*, 17(3), 204–213.
16. Zheng, X., Song, W., Yang, X. (2024). Recent developments in oilwell cement formulations for enhanced zonal isolation. *Journal of Petroleum Engineering Research*, 16(4), 310–325.
17. Vissa, S. V. K., Massion, C., Lu, Y., et al. (2023). Zeolite enhanced Portland cement: Solution for durable wellbore sealing materials. *Journal of Petroleum Engineering Research*, 15(2), 145–158.
18. Ebied, A., Fakher, S., Kayed, H. (2025). Experimental investigation of inclusion of various nanocarbon black concentrations on mechanical characteristics of oil well cement slurries in high pressure high temperature conditions. *Journal of Petroleum Engineering Research*, 18(1), 102–115.

19. Nwaichi, P. I., Ridzuan, N., Nwaichi, E. O. (2025). Advances in oilwell cement retarders: A bibliometric and systematic review of mechanisms, challenges, emerging trends, and future directions. *Review*, 1, 8.
20. Alisheva, Z., Nadirov, K., Al-Dujaili, A. N. (2025). Integrated strategies for controlling water cut in mature oil fields in Kazakhstan. *Polymers*, 17(7), 829.
21. Olayiwola, O., Nguyen, V., Andres, R., et al. (2023). The application of nano silica gel in sealing well micro annuli and cement channeling. *Journal of Petroleum Engineering Research*, 17(3), 245–258.
22. Lu, H., Fu, B., Shi, P., et al. (2018). Late-Miocene thrust fault-related folding in the northern Tibetan Plateau: Insight from paleomagnetic and structural analyses of the Kumkol basin. *Journal of Asian Earth Sciences*, 156, 246–255.

THE EFFECT OF DIFFERENT HYDRAULIC FRACTURE LENGTHS ON WELL PRODUCTION

J. M. Eyvazov*, T. A. Aslanov

«Socar Upstream Management International LLC

ABSTRACT

Hydraulic fracturing is an engineering process in which specially formulated fluid and proppant agent are injected into the rock formation at high pressure to create new fractures or enlarge existing ones. These fractures significantly improve the flow pathways within the reservoir, enabling hydrocarbons to move more easily toward the wellbore and eventually to surface facilities. As one of the most widely used reservoir stimulation methods, hydraulic fracturing plays a crucial role in increasing production, particularly in formations with low permeability. The injected proppant agent prevents fracture closure by remaining within the fractures, thereby ensuring sustained conductivity over time. The fracturing fluid typically contains a range of chemical additives, each designed to enhance specific properties such as viscosity, suspension capacity, friction reduction, and compatibility with the formation. These additives may include friction reducers, gelling agents, corrosion inhibitors, biocides, and other specialized components. Proper fluid formulation directly influences the effectiveness of the operation, environmental considerations, and the overall safety of the procedure. Hydraulic fracturing is essential for the development of unconventional reservoirs, including shale gas, tight gas, and low-permeability oil formations. A comprehensive understanding of the reservoir's mechanical properties, porosity, natural fractures, and the chemical characteristics of formation fluids is necessary for designing an optimal fracturing operation. Important design parameters include fracture length, fracture width, fracture conductivity, fracture geometry, proppant size and concentration, pump rate, and surface pressure control.

*e-mail: jabrayil.eyvazov88@gmail.com

<https://doi.org/10.53404/Sci.Petro.20250200082>

Date submitted: 24.11.2025

Date accepted: 18.12.2025

KEYWORDS:

hydraulic fracturing;
proppant;
fracture conductivity;
fracture length;
fracture width.

Introduction

Hydraulic fracturing is a stimulation technique in which fluid, proppant, and additives are injected at high pressure into tight formations such as shale to create or enlarge fractures, enabling hydrocarbons to flow toward the wellbore and surface facilities [1].

Fracturing is commonly used today for hydrocarbon production. It prevents the immediate closure of induced fractures, allowing hydrocarbon flow from tight formations. Some key characteristics of hydraulic fracturing include [2]:

- It is used when near-wellbore formation damage occurs as a result of drilling and mud-filtrate invasion [3].
- It can bypass damaged zones and restore permeability.
- It can significantly improve flow capacity and reservoir drainage.
- According to Darcy's law, fracturing increases permeability, improves reservoir pressure support, and increases well productivity [4].

The goal of fracturing optimization is to maximize hydrocarbon production by maximizing the volume of stimulated reservoir rock. Modeling of fracture propagation includes input parameters such as reservoir properties, pumping pressure, and formation elasticity. Outputs include fracture geometry, width distribution, propagation rate, and productivity effects [5].

Optimizing fracture half-length relative to reservoir drainage area is crucial. The most likely drainage radius is obtained from geological studies. Once this value is defined, engineers can optimize fracture half-length [6].

Fracture conductivity and half-length are the two most critical parameters controlling fractured performance well.

Major factors reducing fracture conductivity include:

- Proppant type and strength.
- Fracturing fluid composition [7].

Two mechanisms reduce conductivity:

1. Reduced fracture width under closure stress.
2. Migration of fines, blocking pore spaces within the proppant pack [8].

One of the most critical design parameters in hydraulic fracturing is fracture length. Fracture length defines how far the induced fracture propagates into the reservoir from the wellbore. This parameter directly controls the contact area between the well and the productive formation [9].

Longer hydraulic fractures generally provide greater access to reservoir fluids. Increased reservoir contact reduces flow resistance and enhances productivity. Wells with longer fractures often demonstrate higher initial production rates [10].

Shorter fractures may only stimulate the near-wellbore region. Limited stimulation can restrict hydrocarbon flow and reduce production potential. Fracture length also influences the effective drainage area of the well [11].

A larger drainage area allows more reservoir volume to contribute to production. In tight and shale reservoirs, longer fractures are especially beneficial due to extremely low matrix permeability. Extended fractures help overcome near-wellbore damage and improve connectivity to natural fractures [12].

However, increasing fracture length requires higher injection rates and larger fluid volumes. These requirements increase operational complexity and treatment costs. Economic evaluation is therefore essential when selecting fracture length [13].

Excessively long fractures may intersect water zones or gas caps. Such intersections can lead to early water or gas breakthroughs. Early breakthrough negatively impacts hydrocarbon recovery and well performance [14].

Fracture length also affects pressure depletion behavior within the reservoir. Optimized fracture lengths can improve pressure support near the wellbore. Long fractures may contribute to more stable production over time. Production decline rates are often slower in wells with properly designed fracture lengths [15].

Proppant transport becomes more challenging as fracture length increases. Inadequate proppant placement can reduce fracture conductivity. Reduced conductivity may offset the benefits of longer fractures.

Reservoir heterogeneity plays a major role in fracture propagation. In layered formations, barriers can limit effective fracture growth [16].

Geomechanically properties influence achievable fracturing length. Numerical reservoir simulation is commonly used to study fracture length effects. Simulation helps predict production response under different fracture scenarios.

Field data generally confirms a positive correlation between fracture length and well production. However, the optimal fracture length varies across reservoirs. Operational constraints may limit maximum fracture extension [17].

Environmental and regulatory factors may also influence fracture design. Integrating geological, engineering, and economic factors leads to optimal fracture length selection. Therefore, proper hydraulic fracture length design is essential for maximizing well production and long-term reservoir performance [18].

Experimental section

This research was carried out in an unconventional reservoir. Permeability is in the range of 5–13 mD. The main objective of the study project is to determine the optimal hydraulic fracture length and fracture width for the specified well. Sensitivity analysis on hydraulic fracture length was conducted.

In the first case, the horizontal section length was 150 meters. Based on the hydraulic fracture length and total gas production results, several cases were compared. It was determined that a 125-meter hydraulic fracture length is the best result for this well [19] (fig. 1, table 1).

In the second case, the horizontal section length was 200 meters. Based on the hydraulic fracture length and total gas production results, several cases were compared. It was determined that a 125-meter hydraulic fracture length is also the best result for this well (fig. 2, table 2).

Then various fracture widths were applied to the hydraulic fracturing operation. The hydraulic fracture length is 125 meters. Based on this sensitivity analysis, it was determined that a fracture width of 0.045 meters is the most optimal case. At this point, oil production in the well reached the maximum gas production [20] (table 3).

Conclusion

According to the study, it was determined that the highest fracture length does not mean the highest production. In this research, the optimal fracture length for this well is 125 meters. Then, at a hydraulic fracture length of 125 meters, the reservoir model was simulated for this well at various hydraulic fracture widths. It was determined that a fracture width of 0.045 meters is the optimal end for this hydraulic fracturing operation.

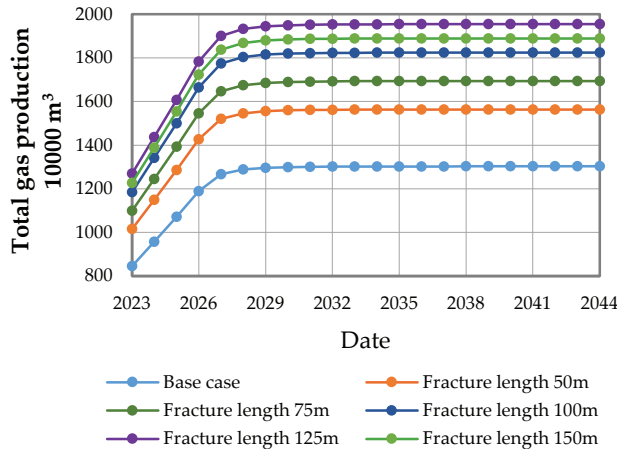


Fig. 1. Effect of fracture length (50-150m) on well production

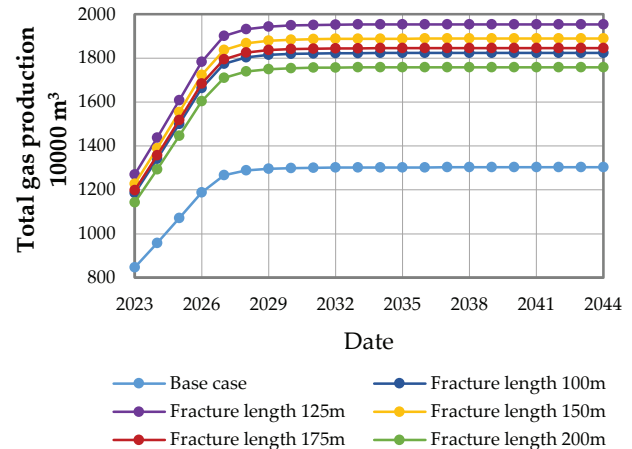


Fig. 2. Effect of fracture length (100-200m) on well production

Table 1
Effect of fracture length (50-150m)
on well production

Date	Base Case	Fracture length, m				
		100	125	150	175	200
2023	846.45	1185.03	1269.67	1227.35	1199.25	1142.7
2024	958.04	1341.25	1437.06	1389.15	1357.345	1293.35
2025	1071.78	1500.49	1607.67	1554.08	1518.496	1446.9
2026	1188.6	1664.04	1782.9	1723.47	1684.008	1604.61
2027	1267.11	1773.95	1900.67	1837.31	1795.237	1710.6
2028	1288.27	1803.58	1932.41	1867.99	1825.223	1739.16
2029	1296.25	1814.75	1944.38	1879.56	1836.527	1749.94
2030	1299.54	1819.36	1949.31	1884.33	1841.192	1754.38
2031	1301.09	1821.53	1951.64	1886.58	1843.388	1756.47
2032	1301.91	1822.67	1952.87	1887.77	1844.542	1757.58
2033	1302.34	1823.28	1953.51	1888.39	1845.159	1758.16
2034	1302.57	1823.6	1953.86	1888.73	1845.483	1758.47
2035	1302.69	1823.77	1954.04	1888.9	1845.655	1758.63
2036	1302.76	1823.86	1954.14	1889	1845.746	1758.73
2037	1302.8	1823.92	1954.2	1889.06	1845.807	1758.78
2038	1302.84	1823.98	1954.26	1889.12	1845.868	1758.83
2039	1302.87	1824.02	1954.31	1889.16	1845.908	1758.87
2040	1302.89	1824.05	1954.34	1889.19	1845.939	1758.9
2041	1302.9	1824.06	1954.35	1889.21	1845.949	1758.92
2042	1302.92	1824.09	1954.38	1889.23	1845.979	1758.94
2043	1302.93	1824.1	1954.4	1889.25	1845.989	1758.96
2044	1302.93	1824.1	1954.4	1889.25	1845.989	1758.96

Table 2
Effect of fracture length (100-200m)
on well Production

Date	Base Case	Fracture length, m				
		100	125	150	175	200
2023	846.45	1185.03	1269.67	1227.35	1199.25	1142.7
2024	958.04	1341.25	1437.06	1389.15	1357.345	1293.35
2025	1071.78	1500.49	1607.67	1554.08	1518.496	1446.9
2026	1188.6	1664.04	1782.9	1723.47	1684.008	1604.61
2027	1267.11	1773.95	1900.67	1837.31	1795.237	1710.6
2028	1288.27	1803.58	1932.41	1867.99	1825.223	1739.16
2029	1296.25	1814.75	1944.38	1879.56	1836.527	1749.94
2030	1299.54	1819.36	1949.31	1884.33	1841.192	1754.38
2031	1301.09	1821.53	1951.64	1886.58	1843.388	1756.47
2032	1301.91	1822.67	1952.87	1887.77	1844.542	1757.58
2033	1302.34	1823.28	1953.51	1888.39	1845.159	1758.16
2034	1302.57	1823.6	1953.86	1888.73	1845.483	1758.47
2035	1302.69	1823.77	1954.04	1888.9	1845.655	1758.63
2036	1302.76	1823.86	1954.14	1889	1845.746	1758.73
2037	1302.8	1823.92	1954.2	1889.06	1845.807	1758.78
2038	1302.84	1823.98	1954.26	1889.12	1845.868	1758.83
2039	1302.87	1824.02	1954.31	1889.16	1845.908	1758.87
2040	1302.89	1824.05	1954.34	1889.19	1845.939	1758.9
2041	1302.9	1824.06	1954.35	1889.21	1845.949	1758.92
2042	1302.92	1824.09	1954.38	1889.23	1845.979	1758.94
2043	1302.93	1824.1	1954.4	1889.25	1845.989	1758.96
2044	1302.93	1824.1	1954.4	1889.25	1845.989	1758.96

Table 3

Effect of fracture width on well production

Date	Fracture width, m								
	0.01	0.015	0.02	0.025	0.03	0.035	0.04	0.045	0.05
2023	1258.24	1258.88	1259.51	1260.15	1269.67	1274.12	1274.75	1275.39	1275.00
2024	1424.12	1424.84	1425.56	1426.28	1437.06	1442.09	1442.80	1443.52	1443.09
2025	1593.20	1594.00	1594.81	1595.61	1607.67	1613.30	1614.10	1614.90	1614.42
2026	1766.85	1767.75	1768.64	1769.53	1782.90	1789.14	1790.03	1790.92	1790.39
2027	1883.56	1884.51	1885.46	1886.41	1900.67	1907.32	1908.27	1909.22	1908.65
2028	1915.01	1915.98	1916.95	1917.91	1932.41	1939.17	1940.13	1941.10	1940.52
2029	1926.88	1927.85	1928.82	1929.79	1944.38	1951.18	1952.15	1953.12	1952.54
2030	1931.78	1932.76	1933.73	1934.71	1949.33	1956.15	1957.12	1958.10	1957.51
2031	1934.07	1935.05	1936.02	1937.00	1951.64	1958.47	1959.44	1960.42	1959.83
2032	1935.29	1936.27	1937.24	1938.22	1952.87	1959.70	1960.68	1961.65	1961.07
2033	1935.93	1936.91	1937.88	1938.86	1953.51	1960.35	1961.32	1962.30	1961.71
2034	1936.27	1937.25	1938.22	1939.20	1953.86	1960.69	1961.67	1962.65	1962.06
2035	1936.45	1937.43	1938.40	1939.38	1954.04	1960.87	1961.85	1962.83	1962.24
2036	1936.55	1937.53	1938.51	1939.48	1954.14	1960.98	1961.96	1962.93	1962.35
2037	1936.61	1937.59	1938.57	1939.54	1954.20	1961.04	1962.02	1962.99	1962.41
2038	1936.67	1937.65	1938.63	1939.60	1954.26	1961.10	1962.08	1963.05	1962.47
2039	1936.72	1937.69	1938.67	1939.65	1954.31	1961.15	1962.12	1963.10	1962.51
2040	1936.75	1937.72	1938.70	1939.68	1954.34	1961.18	1962.15	1963.13	1962.54
2041	1936.78	1937.75	1938.73	1939.71	1954.37	1961.21	1962.18	1963.16	1962.57
2042	1936.79	1937.77	1938.74	1939.72	1954.38	1961.22	1962.20	1963.17	1962.59
2043	1936.81	1937.78	1938.76	1939.74	1954.40	1961.24	1962.21	1963.19	1962.60
2044	1936.81	1937.78	1938.76	1939.74	1954.40	1961.24	1962.21	1963.19	1962.60

References

1. Boschee, P. (2012). Handling produced water from hydraulic fracturing. *Oil and Gas Facilities*, 5, 12–23.
2. Gandossi, L. (2013). An overview of hydraulic fracturing and other formation stimulation technologies for shale gas production. *Luxembourg: Publications Office of the European Union*.
3. Perkins, K. (1961). Widths of hydraulic fractures. *Journal of Petroleum Technology Transactions*, 222, 937–949.
4. Zhai, Z., Fonseca, E., Azad, A., Cox, B. (2015). A new tool for multi-cluster and multi-well hydraulic fracture modeling. SPE-173367-MS. In: *The SPE Hydraulic Fracturing Technology Conference, The Woodlands, Texas, USA, February 2015*.
5. Ahmed, U., Thompson, T. W., Kelkar, S. M., et al. (1984). Optimizing hydraulic fracture designs in formations with poor containment. SPE 13375. In: *Eastern Regional Meeting, Charleston, West Virginia, October 31–November 2*.
6. Economides, M., Nolte, K. G. (2000). Reservoir stimulation (3rd ed.). New York: John Wiley & Sons, Ltd.
7. King, G. E. (2010). Thirty years of hydraulic fracturing: What have we learned? *SPE Production and Operations*, 25(3), 323–331.
8. Warpinski, N. R., Mayerhofer, M., Vincent, M., et al. (2012). Hydraulic fracture diagnostics: Past, present, and future. SPE 152684. In: *The SPE Hydraulic Fracturing Technology Conference*.
9. Mayerhofer, M. J., Lolon, E. P., Warpinski, N. R. (2006). What is stimulated reservoir volume? *SPE Production and Operations*, 21(1), 89–98.
10. Cipolla, C. L., Warpinski, N. R., Mayerhofer, M. J. (2008). Hydraulic fracture complexity: Diagnosis, remediation, and exploitation. SPE 115769. In: *SPE Asia Pacific oil and gas conference and exhibition*.

11. Guo, B., Ghalambor, A. (2014). Hydraulic fracturing design and optimization: A practical approach. *Gulf Professional Publishing*.
12. Valkó, P., Economides, M. J. (1995). Hydraulic fracture mechanics. Wiley.
13. Barree, R. D., Conway, M. W. (2001). Stimulate to the limit: A new approach to hydraulic fracturing. SPE 71648. In: *The SPE Annual Technical Conference and Exhibition, New Orleans, LA, United States*.
14. Fisher, M. K., Warpinski, N. R. (2012). Hydraulic fracture-height growth: Real data. *SPE Production and Operations*, 27(1), 8–19.
15. Holditch, S. A. (1979). Factors affecting water blocking and gas flow from hydraulically fractured wells. SPE 7552. In: *The SPE Annual Technical Conference and Exhibition*.
16. Soliman, M. Y., El Rabaa, A. (1993). Fracture propagation in layered formations. SPE 25890. In: *The SPE Annual Technical Conference and Exhibition*.
17. Adachi, J., Siebrits, E., Peirce, A., et al. (2007). Computer simulation of hydraulic fractures. *International Journal of Rock Mechanics and Mining Sciences*, 44(5), 739–757.
18. Wu, R., Olson, J., Ribeiro, L. (2016). Modeling fracture interaction in multi-stage hydraulic fracturing treatments. SPE 181747. In: *The SPE Hydraulic Fracturing Technology Conference*.
19. Eyvazov, J., Hamidov, N. (2023). The effect of different hydraulic fracturing width on well production. *International Journal of Oil, Gas and Coal Engineering*, 11(4), 74–78.
20. Eyvazov, J., Hamidov, N. (2023). The effect of hydraulic fracturing length on well production. *Journal of Physics Conference Series*, 2594(1), 012022.

AN INTEGRATED DATA-DRIVEN INTELLIGENT AUTOMATION FRAMEWORK FOR PREDICTING AND CONTROLLING LIQUID LOADING IN GAS-CONDENSATE WELLS

K. F. Aliyev

Azerbaijan State Oil and Industry University, Baku, Azerbaijan

ABSTRACT

Liquid loading remains one of the most critical challenges in the operation of gas and gas-condensate wells, where the declining reservoir pressure and reduced gas velocity lead to the accumulation of condensate and water in the wellbore. This phenomenon increases backpressure, reduces gas deliverability, and often results in unstable slugging flow. The process is further complicated by retrograde condensation, where heavy hydrocarbons condense within the tubing even above the dewpoint pressure, altering the flow regime and accelerating instability. Traditional empirical models provide valuable theoretical understanding but are limited by their static assumptions and inability to capture transient, time-dependent effects observed in field operations. This study develops an intelligent, data-driven framework that integrates Artificial Neural Networks and Gated Recurrent Unit architectures with an automated choke-control system to enable real-time prediction and control of liquid loading. The Artificial Neural Network model demonstrated an 80% classification accuracy in distinguishing loaded and unloaded well conditions based on wellhead (bottomhole) pressure, gas rate, and tubing diameter. The Gated Recurrent Unit based forecasting model achieved a mean absolute percentage error of 3.98%, effectively capturing daily production fluctuations and early signs of instability. Integration of both models within an adaptive control system allows dynamic regulation of wellhead and bottomhole pressures through automated choke adjustments, maintaining stable flow regimes and preventing condensate buildup. The hybrid system thus establishes a novel, self-regulating approach for optimizing gas-condensate production. This research highlights the potential of combining machine learning and real-time automation to enhance flow assurance, extend well productivity, and advance the digital transformation of reservoir management.

e-mail: kananaliyev.kn@gmail.com

https://doi.org/10.53404/Sci.Petro.20250200083

Date submitted: 20.11.2025

Date accepted: 23.12.2025

KEYWORDS:

gas-condensate well;
retrograde
condensation;
liquid loading;
artificial neural
network;
automated choke-
control system.

1. Introduction

Liquid loading is a major flow assurance challenge in gas and gas-condensate wells, occurring when gas velocity becomes insufficient to lift accumulated liquids, mainly condensate and water, from the wellbore. As production continues and reservoir pressure declines, the gas loses its carrying capacity, leading to liquid buildup at the bottomhole and unstable flow conditions. In gas-condensate wells, this process is further complicated by retrograde condensation, where heavy hydrocarbon components condense within the wellbore even when reservoir pressure is above the dewpoint. As a result, the flowing fluid composition changes with depth, causing a transition from annular or mist flow to slug flow. This unstable regime produces intermittent liquid surges and gas spikes, marking the onset of liquid loading.

Liquid accumulation increases backpressure on

the formation, reduces effective gas permeability, and leads to significant production decline. Over time, condensate banking near the wellbore and rising condensate-to-gas ratio (CGR) can ultimately halt gas flow. Beyond productivity loss, liquid loading causes operational issues such as tubing corrosion, erosion, equipment wear, and measurement inaccuracy due to flow pulsations. Effective control and early detection of liquid loading are therefore critical for maintaining stable well operation and optimizing reservoir recovery. Predictive models and field-based indicators help identify the onset of loading, but their accuracy in gas-condensate systems requires detailed analysis of fluid and flow behavior. Operational challenges can also result from salt or wax deposition, along with sand and water inflow into the wellbore [1]. In essence, liquid loading and flow instability may stem from multiple contributing factors that must be thor-

oughly evaluated before selecting effective remedial actions. Therefore, beyond observing wellhead indicators, a detailed assessment of the fluid composition and flow characteristics is vital [2].

The main objective of this study is to design and implement an intelligent prediction and control system for gas-condensate wells that can accurately detect and prevent liquid loading using data-driven models. By integrating Artificial Neural Network (ANN) and Gated Recurrent Units (GRU) based predictive algorithms with an automated choke-control system, the study aims to achieve real-time, self-adjusting regulation of production parameters to ensure stable and efficient well performance.

2. Fundamental principles and mechanisms underlying liquid loading formation

2.1. Understanding of the liquid loading formation mechanism

Retrograde condensation in gas-condensate wells profoundly affects both reservoir and wellbore flow behavior. As the pressure drops below the dewpoint, part of the gas condenses into liquid hydrocarbons, forming a fine dispersed phase that accumulates near the bottomhole. This condensate, due to its higher density and surface tension, increases flow resistance and alters the gas-liquid distribution along the wellbore. According to recent studies, the hydrocarbon mixture often exists in a colloidal state, alternating between «liquid-in-gas» and «gas-in-liquid» dispersions depending on pressure and temperature [3]. Such colloidal transformations change the volumetric and rheological properties of the flowing mixture, weakening its ability to maintain stable flow regimes.

As a result, the flow becomes unstable, leading to intermittent slugging, liquid holdup, and eventually liquid loading. Fataliyev et al. [1] presented that even when reservoir pressure remains above dewpoint, local cooling and pressure drops along the well can push the fluid locally into two-phase behavior. As fluid ascends, flow regimes evolve as presented in fig. 1: initially, small droplets or mist are entrained in the gas; a thin film may form near the wall; with further condensation and drop-out, the flow transitions toward annular or annular-dispersed regimes; eventually, the disparity in velocities causes a piston-like or slug flow, with alternating slugs of liquid and pockets of gas.

2.2. Evolution of prediction models of liquid loading in gas-condensate wells

Two main mechanisms describe liquid loading in gas-condensate wells: droplet reversal and film reversal. In the droplet reversal model, liquid loading begins when gas velocity is too low to lift condensate

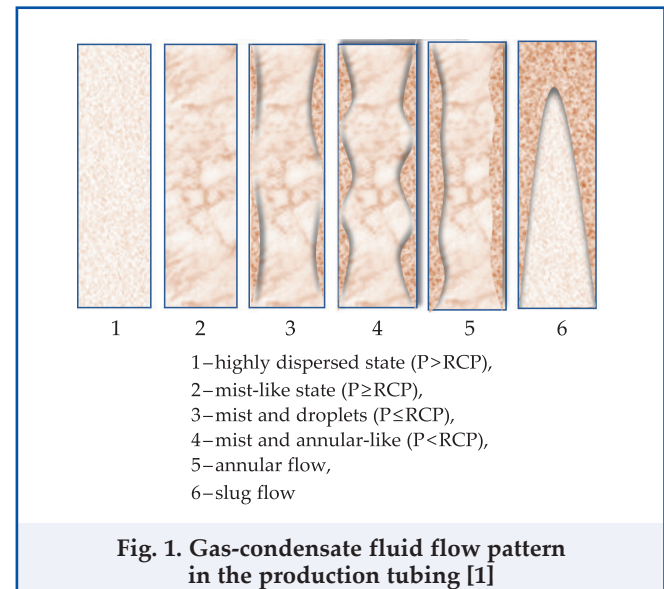


Fig. 1. Gas-condensate fluid flow pattern in the production tubing [1]

droplets. Turner's model, based on this idea, predicts a critical gas velocity for droplet fall-back [4, 5], though many wells remain unloaded even below that limit [6, 7] due to simplifying assumptions like rigid spherical droplets and air-based testing. It performs better in low-pressure wells (<3.45 MPa) [8], while later work emphasized the impact of droplet deformation [9]. Despite limitations, Turner's and Coleman's models are still widely applied, while Li's model is favored in China [6]. Building on Turner's concept, Guo et al. [10] proposed a kinetic-energy-based approach—later refined by Guo—to estimate the minimum energy needed to lift liquids and solids [5, 11], though time-dependent effects are excluded [12].

The film reversal mechanism instead attributes loading to the downward movement of a continuous liquid film. Barnea [13] first linked this to the transition from annular to intermittent flow as gas velocity declines, and Zhang et al. [14] later improved the model using momentum and continuity balances with interfacial friction correlations. Comparative studies [14] showed Turner's model gives the lowest critical velocity, Barnea's the most conservative, and Zhang's lies between. Overall, film-based models predict nearly twice the critical velocity of droplet models, emphasizing the complex, transient gas-liquid interactions governing liquid loading in gas-condensate wells.

Recent advancements leverage artificial intelligence for improved liquid loading prediction. Neural network systems imitate the structure and function of biological neural networks that exist in the human brain, enabling the transmission of information between interconnected nodes (neurons) [16]. Early neural network use in petroleum engineering began with Ali [17], who showed their potential for complex

modeling. Later, Nguyen et al. [18] and Chakra et al. [19] advanced forecasting and noise filtering, while Aizenberg et al. [20] introduced complex-valued neurons to better capture time-series dependencies. This new technology has demonstrated superior accuracy compared to empirical models [21, 22].

Deep learning architectures, particularly Long Short-Term Memory (LSTM) networks, marked a major step forward in modeling sequential and time-dependent petroleum data. Studies such as Sagheer and Kotb [23] demonstrated that LSTMs outperform traditional models in production forecasting. Ali and Guo [24] further advanced the field by integrating neuro-adaptive models to capture transient pressure and flow dynamics linked to liquid loading. However, existing models still fall short in identifying or predicting liquid loading events, motivating the present study's use of Gated Recurrent Units (GRUs) - a simpler, efficient alternative to LSTMs capable of real-time forecasting in data-limited environments.

Given these advantages, this study demonstrates how using neural network models inside automated control system can be effective in achieving smooth production of the gas-condensate wells encountering liquid loading phenomenon. This research is especially valuable as the petroleum sector moves toward data-driven automation for optimizing production. Reliable forecasting of production trends and the onset of liquid loading helps prevent unplanned shutdowns, reduce production losses, and enable timely implementation of lift and drainage measures.

3. Intelligent modeling and prediction of liquid loading in gas-condensate wells

3.1. Development of Artificial Neural Network (ANN) model for liquid loading prediction

Neural networks mimics the structure and operation of the human brain, where information passes between interconnected nodes, or neurons. Deep

Neural Networks (DNNs) are widely used for complex classification and regression tasks, as they can automatically learn patterns and relationships from data through iterative training [25]. Each neuron performs a computation by applying weights to inputs, adding a bias, and passing the result through an activation function to produce an output. The network, as presented in figure 2, typically consists of an input layer, one or more hidden layers, and an output layer that generates the final prediction.

During training, weights and biases are initialized - biases often set to zero and weights using methods like Xavier or He initialization for stable convergence. Data then passes through the network in forward propagation, where neurons compute a weighted sum and apply activation functions. Mathematically, this process is expressed as:

$$z^{(l)} = W^{(l)} a^{(l-1)} + b^{(l)}, \quad a^{(l)} = \varphi(z^{(l)}) \quad (1)$$

In these equations, $W^{(l)}$ represents the weight matrix that determines the strength of connections between neurons in consecutive layers, while $b^{(l)}$ is the bias vector that shifts the activation function to improve learning flexibility. The term $a^{(l-1)}$ denotes the activation (or output) from the previous layer, and $z^{(l)}$ is the linear combination of inputs before the activation function φ is applied. The activation function φ introduces non-linearity, producing the output $a^{(l)}$, which is then forwarded to the next layer for further computation. The Rectified Linear Unit (ReLU), defined as $\varphi(z) = \max(0, z)$, is commonly used due to its efficiency and ability to mitigate the vanishing gradient problem.

The network's performance is evaluated using a loss function that measures the difference between predicted and actual outputs. For binary classification, the binary cross-entropy loss is widely used. Learning occurs through backpropagation, where gradients of the loss are calculated and propagated backward to update weights:

$$W_{\text{new epoch}}^{(l)} = W_{\text{old epoch}}^{(l)} - \eta \frac{\partial L}{\partial W^{(l)}} \quad (2)$$

Here η is the learning rate. This iterative optimization minimizes the loss and improves predictive accuracy, though neural networks often remain «black-box» models due to their complex internal parameter interactions.

3.2. Application of Gated Recurrent Unit (GRU) model for time-series forecasting

The Gated Recurrent Unit (GRU) is a type of Recurrent Neural Network (RNN) designed to efficiently model sequential data and capture temporal dependencies while mitigating the vanishing gradient

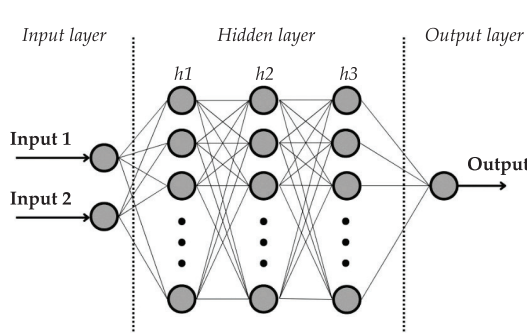


Fig. 2. Architecture of the neural network system [25]

problem common in traditional RNNs. Introduced as a simplified variant of the LSTM network, the GRU, as presented in figure 3, achieves comparable performance with fewer parameters by eliminating separate memory cells and integrating gating mechanisms that control information flow dynamically. Each GRU cell processes sequential inputs, learning both short- and long-term dependencies crucial for time-series prediction tasks.

A GRU cell maintains a hidden state h_t at time step t , which is updated using two key gates: the update gate z_t and the reset gate r_t . The update gate determines how much of the previous information should be retained:

$$z_t = \sigma(W_z x_t + U_z h_{t-1} + b_z) \quad (3)$$

How much of the past information should be forgotten is controlled by the reset gate:

$$r_t = \sigma(W_r x_t + U_r h_{t-1} + b_r) \quad (4)$$

Using these gates, the candidate hidden state \tilde{h}_t is computed as:

$$\tilde{h}_t = \tanh(W_h x_t + U_h (r_t \odot h_{t-1}) + b_h) \quad (5)$$

Finally, the updated hidden state is obtained by interpolating between the previous and candidate states:

$$\tilde{h}_t = ((1 - z_t) \odot h_{t-1} + z_t \odot \tilde{h}_t) \quad (6)$$

This mechanism enables GRUs to preserve relevant historical information while integrating new data efficiently.

During training, sequential data are divided into fixed-length windows, and the model predicts future values based on past observations. The Mean Squared Error (MSE) loss function measures prediction accuracy, while Backpropagation Through Time (BPTT) updates parameters across time steps using optimizers such as Adam. The hidden state is reset between sequences to ensure independent processing. Through multiple epochs, the GRU learns temporal dynamics effectively, making it a powerful yet computationally efficient model for time-series forecasting applications.

4. Data-driven modeling and intelligent control of gas-condensate well performance

4.1. Development and evaluation of ANN-based prediction model for liquid loading

A comprehensive dataset was compiled from multiple literature sources [7,15, 26-30], integrating key operational parameters such as wellhead pressure, gas production rate, tubing inner diameter (ID), and loading status. Despite data heterogeneity, the variables were standardized to create a consistent and

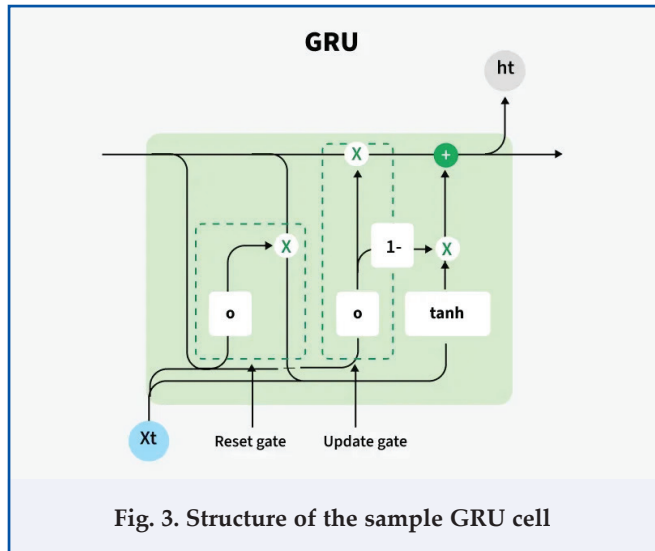


Fig. 3. Structure of the sample GRU cell

cohesive dataset consisting of 52% unloaded and 48% near-loaded wells, represented categorically (0 for unloaded and 1 for loaded). The dataset was divided into 85% for training and 15% for testing, ensuring proper validation for the artificial neural network (ANN) models. Data preprocessing and model development were carried out in Python using Pandas and TensorFlow. Several architectures were tested, and the optimal configuration was a five-layer sequential ANN comprising input layers with 1–3 neurons, hidden layers with 100, 40, and 10 neurons (using ReLU activation), and a single Sigmoid-activated output neuron for binary classification. The network was trained using the Adam optimizer for 150 epochs, ensuring stable convergence.

Three key parameters—wellhead pressure, gas rate, and tubing ID—were used to construct four models with identical architectures but different input combinations. Models 1 and 2 used pressure and gas rate individually, Model 3 combined both, and Model 4 included tubing ID. Testing on 15% of the data showed that Model 3 achieved the highest accuracy (80%), followed by Model 4 (66%), while Model 2 performed worst (57%). The limited variability in tubing ID (mainly 0.051 m and 0.062 m) constrained learning and slightly reduced model performance.

Although each model made minor misclassifications, none failed on the same data points simultaneously—suggesting that an ensemble of models could enhance diagnostic reliability. Overall, the results confirm the strong potential of ANN-based models for predicting liquid loading in gas-condensate wells, emphasizing the need for larger datasets and additional input features such as choke size, fluid properties, and temperature to further improve prediction accuracy and generalization.

4.2. GRU-based time-series forecasting for production trend and anomaly detection

In this study, daily gas production data from well X were analyzed using a GRU based deep learning model for short-term production forecasting. The dataset contained approximately 1500 days of production rates, normalized using the MinMaxScaler technique to improve convergence and model stability. The first 1200 days were used for training, and the remaining 300 days for testing, ensuring chronological integrity essential for time-series learning. To capture temporal dependencies, a sliding window of 10 consecutive days was used as input to predict the production rate of the following day. The GRU model architecture comprised four layers with 50, 30, 30, and 20 units, interspersed with dropout layers for regularization, and a final dense layer for output. The model was trained using the Adam optimizer with mean squared error (MSE) as the loss function and early stopping criteria to prevent overfitting.

After training, the predictions were inverse-transformed to their original scale, and the model achieved an MSE of 78.58, a Mean Absolute Error (MAE) of 3.35, and a Mean Absolute Percentage Error (MAPE) of 3.98% on the test set. These metrics reflect a high level of accuracy, as MAPE below 5% is typically considered excellent in forecasting tasks.

When applied to the test period shown in the figure 4, the GRU model accurately captured stable production trends and successfully identified sudden fluctuations in gas rates, with only a minor one-day lag—an inherent feature of sequential models dependent on prior temporal context. This responsiveness is particularly valuable for practical field applications, such as early detection of liquid loading. Since liquid loading develops gradually, the GRU model's sensitivity to early production anomalies can serve as a diagnostic indicator, alerting engineers to potential flow restrictions before severe productivity loss occurs.

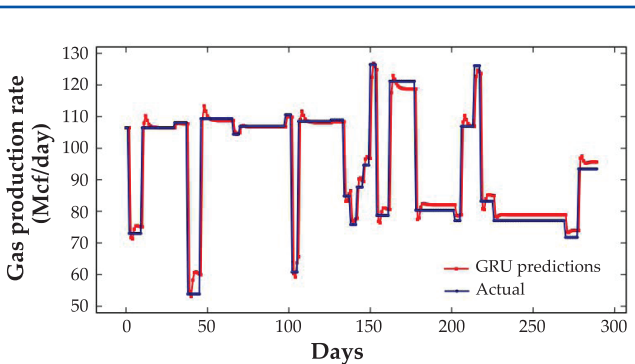


Fig. 4. GRU model predictions versus actual gas production rates for the test period

In conclusion, the GRU-based model demonstrated robust forecasting and anomaly-detection capabilities, offering an efficient, data-driven approach for real-time production monitoring. Its simplicity, accuracy, and adaptability make it a promising tool for intelligent well surveillance and proactive flow assurance management in gas-condensate operations.

4.3. Design and implementation of an intelligent automated control system for gas-condensate wells

Efficient management of gas-condensate well performance requires precise control of production parameters to maintain stable flow and prevent liquid loading. By adjusting the production parameters of a gas-condensate well, the gas flow rate and its kinetic energy can be effectively regulated through control of wellhead or bottomhole pressure using a choke valve. In addition, reducing the tubing diameter or using restriction adapters helps manage the flow characteristics within the production system. This technique is particularly effective for high-pressure wells during the early production stages, as it prevents liquid loading and stabilizes flow; however, in wells with low reservoir pressure, such interventions may lead to a decline in productivity due to increased flow resistance.

In this study, an automatic control system was developed to synchronize the choke valve with real-time changes in wellhead and bottomhole pressures, aiming to prevent condensate accumulation in the production tubing. The methodology and operation of the developed control system are shown in figure 5. The system operates differently from a conventional drawdown controller, as its actions are initiated only after confirming that liquid loading is occurring in the production tubing.

The system continuously measures the pressure differential ($\Delta P = P_{dh} - P_{wh}$) by receiving input from the downhole pressure gauge (DHPG) and the wellhead (WH) device, and automatically adjusts the choke opening to maintain an optimal flow regime. A pre-defined pressure difference (ΔP , U_n —nominal which is provided by Well control system) is input to the system, with a potentiometer connected to the microcontroller's channel. As the fluid density changes, the pressure difference varies, and the corresponding difference (U_r) is calculated. This helps to determine variation from the nominal value (M factor).

$$M = U_r - U_n \quad (7)$$

Based on these parameters and their variations, the Liquid Load Controller (LLC) confirms a stable reading from the sand detector (SD), identifies decreasing gas, water, and condensate flow rates (GF, WF, and CF), refers to the Well Control System (WCS) models

(ANN and GRU), and then activates the choke valve. The electrical actuator adjusts the choke position, or M factor, by opening or closing the valve. A hall sensor tracks rotation cycles and issues a stop command when needed. To prevent excessive tubing load, limits for bottomhole pressure and sample parameters affected by sand, water, or sediments are controlled.

The M-factor selection must not disrupt downstream equipment such as separators or gas-treatment units, after which the control block is fine-tuned for stable operation. In addition to this, the recommended system will be integrated with two predictive models - an artificial neural network that uses bottomhole pressure and gas rate as inputs, and a gated recurrent unit model that relies solely on gas rate time-series data to predict the loading status of the well. Integrating these models into the automated choke-control system (WCS and LLC) allows the well to be managed more intelligently and efficiently. The ANN model provides quick and accurate assessments of the current operating state, helping the system recognize when the well is approaching a loaded condition based on real-time pressure and flow data. Meanwhile, the GRU model analyzes gas-rate trends over time, learning the typical behavior of the well and detecting early signs of instability before liquid loading occurs. Considering that the LLC is linked to the WCS, it provides advanced assurance before taking action to adjust the choke valve.

By combining both models, the control system gains a powerful balance between instant reaction and forward prediction. The ANN supports immediate decisions on choke adjustments, while the GRU forecasts how the system will behave in the near future, allowing the controller to make preventive changes

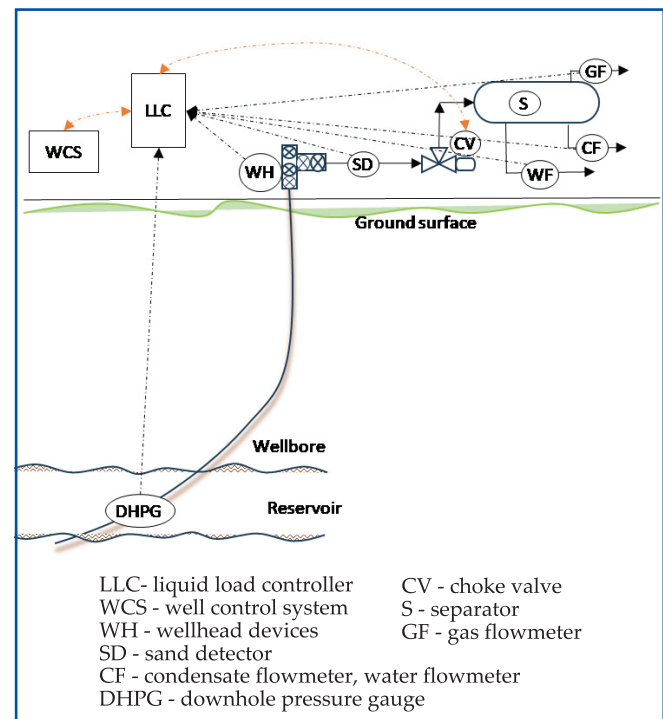


Fig. 5. Schematic representation of wellhead controller and possible flow regimes in a gas condensate well

rather than waiting for problems to appear. This predictive capability helps keep the flow stable, minimizes condensate buildup, and reduces the need for manual intervention. Overall, the integration of ANN and GRU models turns the automated control system into a smart, adaptive, and self-regulating solution, capable of maintaining optimal production conditions and improving long-term well performance.

Conclusions

- This study presents an integrated, intelligent framework for predicting and controlling liquid loading in gas-condensate wells, combining physical flow understanding with advanced data-driven methods. The analysis confirmed that retrograde condensation and multiphase flow transitions, particularly between annular, slug, and mist regimes, are key contributors to flow instability and condensate accumulation in the wellbore. Traditional mechanistic models, such as those by Turner, Barnea, and Guo, provide valuable physical insights but fail to fully capture the dynamic, time-dependent nature of liquid loading in gas-condensate systems.
- To overcome these limitations, artificial neural networks and gated recurrent units were implemented for real-time prediction and production forecasting. The ANN model effectively classified wells by loading status based on wellhead pressure, gas rate, and tubing diameter, while the GRU model accurately forecasted production trends and identified early anomalies with a mean absolute percentage error below 5%. Both models can be applied simultaneously to achieve higher accuracy and ensure smoother operation. These results highlight the strong potential of machine-learning-based systems for diagnosing and anticipating loading phenomena with high precision.

- Furthermore, by integrating the predictive models with an automated choke-control system, the study achieves a closed-loop, adaptive control mechanism capable of self-regulating production parameters. The intelligent controller continuously monitors pressure differentials and adjusts choke openings to sustain optimal flow regimes, thereby minimizing condensate buildup and ensuring stable operation.
- Overall, the proposed hybrid system represents a promising advancement in digitalized flow assurance by integrating predictive analytics, real-time automation, and physical modeling to develop a smarter drawdown controller, enhance production stability, minimize downtime, and extend the operational life of gas-condensate wells.

Acknowledgment

I would like to express my sincere gratitude to my supervisor, Fataliyev Vugar, D.Sc. (Tech) for his continuous support and guidance throughout this work. I also extend my appreciation to Hamidov Natig D.Sc. (Tech) and the Oil Gas Scientific Research Project Institute for their contribution to this research.

References

1. Fataliyev, V. M., Hamidov, N. N., Aliyev, K. F. (2025). Advances in understanding and controlling liquid loading in gas-condensate production well. *SOCAR Proceedings*, 2(2), 92–103.
2. Chi, U. I. (1992). Natural gas production engineering. *Malabar, Florida: Krieger Publishing Company*.
3. Fataliyev, V. M., Hamidov, N. N., Abbaszade, H. R., et al. (2024). On the transition of liquid dispersion states and their physical-thermodynamic nature in the development of gas-condensate reservoirs in depletion mode. *Azerbaijan Oil Industry*, 9(9), 32–39.
4. Turner, R. G., Hubbard, M. G., Dukler, A. E. (1969). Analysis and prediction of minimum flow rate for continuous removal of liquids from gas wells. *Journal of Petroleum Technology*, 21(11), 1475–1482.
5. Guo, B., Ghalambor, A. (2012). Natural gas engineering handbook (2nd ed.). *Gulf Publishing Company*.
6. Zhou, C., Wu, X., Li, H., et al. (2016). Optimization of methods for liquid loading prediction in deep condensate gas wells. *Journal of Petroleum Science and Engineering*, 146, 71–80.
7. Xiao, H., Li, X. P., Tan, X. H., et al. (2021). A novel model for calculating critical droplet entrainment rate of gas well considering droplet deformation and multiple parameters. *Energy Science and Engineering*, 9(6), 812–827.
8. Coleman, S. B., Clay, H. B., McCurdy, D. G., et al. (1991). A new look at predicting gas-well load-up. *Journal of Petroleum Technology*, 43(3), 329–333.
9. Li, M., Li, S. L., Sun, L. T. (2001). New view on continuous-removal liquids from gas wells. *Proceedings of the Permian Basin Oil and Gas Recovery Conference, Midland, Texas*.
10. Guo, B., Ghalambor, A., Xu, C. (2006). A systematic approach to predicting liquid loading in gas wells. *SPE Production and Operations*, 21(1), 81–88.
11. Jamalbayov, M. A., Hasanov, I. R., Dogan, M. O., et al. (2024). A hybrid modeling approach: Dynamic simulation of two-phase fluid flow in compacting gas condensate reservoirs using potential flow theory. *Scientific Petroleum*, 1(1), 29–35.
12. Fadairo, A., Olugbenga, F., Sylvia, N. C. (2015). A new model for predicting liquid loading in a gas well. *Journal of Natural Gas Science and Engineering*, 26, 1530–1541.
13. Barnea, D. (1986). Transition from annular flow and from dispersed bubble flow – unified models for the whole range of pipe inclinations. *International Journal of Multiphase Flow*, 12, 733–744.
14. Zhang, H. Q., Wang, Q., Sarica, C. (2003). Unified model for gas-liquid pipe flow via slug dynamics – Part 1: Model development. *Journal of Energy Resources Technology*, 125(4), 266–273.
15. Luo, S., Kelkar, M., Pereyra, E., et al. (2014). A new comprehensive model for predicting liquid loading in gas wells. *SPE Production and Operations*, 29(4), 337–349.
16. Aggarwal, C. C. (2018). Neural networks and deep learning. *Springer International Publishing*.

17. Ali, J. K. (1994). Neural networks: A new tool for the petroleum industry? *SPE European Petroleum Computer Conference Proceedings*.
18. Nguyen, H. H., Chan, C. W., Wilson, M. (2004). Prediction of oil well production: A multiple-neural-network approach. *Intelligent Data Analysis*, 8(2), 151–169.
19. Chakra, N. C., Song, K. Y., Gupta, M. M., Saraf, D. N. (2013). An innovative neural forecast of cumulative oil production from a petroleum reservoir employing higher-order neural networks (HONNs). *Journal of Petroleum Science and Engineering*, 106, 18–33.
20. Aizenberg, I., Sheremetov, L., Villa-Vargas, L. (2016). Multilayer neural network with multi-valued neurons in time series forecasting of oil production. *Neurocomputing*, 175, 980–989.
21. Ghadam, A., Kamali, V. (2015). Prediction of gas critical flow rate for continuous lifting of liquids from gas wells using comparative neural fuzzy inference system. *Journal of Applied Environmental and Biological Sciences*, 5(8S), 196–202.
22. Khamehchi, E., Yasrebi, S. V., Ebrahimi, A. (2014). Prediction of the influence of liquid loading on well-head parameters. *Petroleum Science and Technology*, 32(14), 1680–1689.
23. Sagheer, A., Kotb, M. (2019). Time series forecasting of petroleum production using deep LSTM recurrent networks. *Neurocomputing*, 323, 203–213.
24. Ali, A., Guo, L. (2019). Neuro-adaptive learning approach for predicting production performance and pressure dynamics of gas condensation reservoir. *IFAC-PapersOnLine*, 52(12), 396–401.
25. Fataliyev, V. M., Aliyev, K. F. (2025). Predictive modeling of liquid loading in gas condensate wells using deep neural networks. *Azerbaijan Oil Industry*, 9(9), 13–19.
26. Ikpeka, P., Okolo, M. (2018). Li and Turner modified model for predicting liquid loading in gas wells. *Journal of Petroleum Exploration and Production Technology*, 9(8), 1971–1993.
27. Ming, R., He, H. (2020). A new approach for predicting critical gas rate in condensate gas wells. *International Journal of Oil, Gas and Coal Technology*, 23(1), 76–91.
28. Zhou, D., Yuan, H. (2010). A new model for predicting gas-well liquid loading. *SPE Production and Operations*, 25(2), 172–181.
29. Abbasov, Z. Y. (1988). Gas-hydrodynamic bases of gas and gas-liquid systems of aero-disperse structure movement in wells (Doctoral thesis). *Baku*.
30. Abdullayev, V. J., Veliyev, R. G., Ryabov, S. S., et al. (2023). Application of gel systems for water shut-off in Uzbekistan oil fields. *SOCAR Proceedings*, 1(1), 68–73.



